UNIVERSITY OF SOUTHAMPTON

MECHANISM OF ACTION AND STRUCTURE-ACTIVITY STUDIES OF NORSPERMIDINE BASED PEPTIDIC INHIBITORS OF TRYPANOTHIONE REDUCTASE

Mark Joseph Dixon

A thesis submitted for the degree of DOCTOR OF PHILOSOPHY

School of Chemistry

Faculty of Science

July 2004

ABSTRACT

SCHOOL OF CHEMISTRY
FACULTY OF SCIENCE

Doctor of Philosophy

MECHANISM OF ACTION AND STRUCTURE-ACTIVITY STUDIES OF NORSPERMIDINE BASED PEPTIDIC INHIBITORS OF TRYPANOTHIONE REDUCTASE

By Mark Joseph Dixon

Infection by *Trypanosoma* and *Leishmania* parasites cause several diseases of major importance to third world health. These parasites are highly susceptible to oxidative stress, but help to maintain their intra-cellular redox balance by utilising the enzyme trypanothione reductase (TR) and the metabolite trypanothione disulfide, rather than the analogous glutathione reductase (GR) and glutathione found in mammalian cells. Despite sharing many similarities, TR and GR exhibit a high degree of selectivity for their respective substrates and thus TR has emerged as a highly promising target for the development of anti-parasitic drugs.

This thesis describes an investigation into the mechanism of action of a previously identified class of trypanothione reductase inhibitors by a variety of techniques including kinetic analysis, analytical ultracentrifugation, gel filtration chromatography and protein crystallography, leading to the identification of an allosteric mode of inhibition.

A library of simplified structural analogues of the lead compounds were screened and active compounds subjected to full kinetic analysis, to establish structure activity relationships (SAR) where subtle structural changes were found to cause changes in inhibition mechanism.

These findings give a better understanding of the enzymes mode of action and this class of inhibitors and will aid the development of more effective enzyme inhibitors in the future.

CONTENTS

ABBREVIATIONS

ADP	adeninediphosphate
Ala	alanine
ANS	8-anilino-1-naphthalene-sulfonic acid
Arg	arginine
Asn	asparagine
ATR	attenuated total reflectance
AUC	analytical ultracentrifugation
BME	β-mercaptoethanol
Boc	*tert*-butyloxycarbonyl
Boc_2O	di-*tert*-butyl dicarbonate
Cbz	benzyloxycarbonyl
cHex	cyclohexyl
Cys	cysteine
DCC	1,3-dicyclohexylcarbodiimide
DCM	dichloromethane
Dde	1-(4,4-dimethyl-2,6-dioxocyclohexylidene)ethyl
DEAE	diethylaminoethyl
DFMO	difluoromethylornithine
DIC	1,3-diisopropylcarbodiimide
DIPEA	*N,N*-diisopropylethylamine
DMAP	4-(dimethylamino)pyridine
DMF	*N,N*-dimethylformamide
DNA	deoxyribose nucleic acid
DVB	divinylbenzene
E. coli	*Eschericia coli*
EDTA	ethylenediaminetetraacetic acid
FAD	flavin adenine dinucleotide
Fmoc	9-fluorenylmethoxycarbonyl
FT-IR	fourier transform infrared

GDH	glutamate dehydrogenase
Glu	glutamic acid
Gly	glycine
GR	glutathione reductase
GSH	glutathione
GSSG	glutathione disulfide
HEPES	4-(2-hydroxyethyl)piperazine-1-ethanesulfonic acid
His	histidine
HIV	human immunodeficiency virus
HOBt	1-hydroxybenzotriazole
HPLC	high performance liquid chromatography
HRMS	high resolution mass spectrometry
IC_{50}	concentration required for 50% inhibition
IPTG	isopropyl-β-D-1-thiogalactopyranoside
IR	infrared
K_i	inhibition constant
K_m	Michaelis-Menten constant
Leu	leucine
LRMS	low resolution mass spectrometry
Met	methionine
Mpt	melting point
M_r	relative molecular weight
MS	mass spectrometry
MWCO	molecular weight cut off
NAD^+	nicotinamide adenine dinucleotide (oxidised form)
NADH	nicotinamide adenine dinucleotide (reduced form)
$NADP^+$	nicotinamide adenine dinucleotide phosphate (oxidised form)
NADPH	nicotinamide adenine dinucleotide phosphate (reduced form)
NHS	*N*-hydroxy succinimide
NMR	nuclear magnetic resonance
bs	broad singlet

d	doublet
m	multiplet
q	quartet
s	singlet
t	triplet
PAGE	polyacrylamide gel electrophoresis
PEI	polyethylenimine
Ph	phenyl
Phe	phenylalanine
PMC	2,2,5,7,8-pentamethylchroman-6-sulfonamide
ppm	parts per million
Pro	proline
PS	polystyrene
R_f	retention factor
RPM	revolutions per minute
rt	room temperature
R_t	retention time
SAR	structure activity relationship
semi-prep	semi-preparative
Ser	serine
SDS	sodium dodecyl sulfate
SOD	superoxide dismutase
Su	succinimide
TCA	tricarboxylic acid cycle
TEMED	*N,N,N',N'*-tetramethylethylenediamine
Tfa	trifluoroacetyl
TFA	trifluoroacetic acid
THF	tetrahydrofuran
Thr	threonine
T.l.c.	thin layer chromatography
TR	trypanothione reductase

Tris	tris(hydroxymethyl)aminomethane
Trp	tryptophan
Trt	trityl
TSH	trypanothione
TSST	trypanothione disulfide
Tyr	tyrosine
UV	ultraviolet
v	initial rate

ACKNOWLEDGMENTS

First of all, I would like to thank Professor Mark Bradley for all his advice, guidance, enthusiasm and support- it is greatly appreciated.

Thanks to Dr. Marco Kreick and Dr. Roberta Leonardi for help with protein preparation and purification; Professor Mike Gore for help with enzyme kinetic analysis; Dr. Andrew Leech for analytical utracentrifugation; Dr. Mark Montgomery for protein crystallography; Dr. Jonathan Essex for molecular modeling and Dr. Stifun Mittoo for extensive proof-reading and for answering my numerous questions on just about any chemistry related subject.

Thanks to all the members of staff that have helped me throughout my studies, especially Julie Herniman and Dr. John Langley for mass spectrometry; Joan Street and Dr. Neil Wells for NMR; Jill Queen and Sue Pipe in the departmental office and Ann, Carl and Phil in stores. Julia Quinn-Parsons deserves a special mention for maintaining group sanity, as does Pat for exceedingly good liquid refreshment.

Thanks to all the Bradley group past and present, unfortunately far too numerous to name! You've made my time in Southampton fun and enjoyable, its been a pleasure to work in the group.

Thanks to my housemates Neil, Ro, John, Cristina, Geoff, Monty, Foo and Michael, for providing such a rich, inspiring, intellectual enviroment. I'll miss you, my liver won't. Thanks also to Rich, Kelly, Chrissy and all at the Drummond Arms, my second home in Southampton.

Finally, I would like to thank all my family, especially mum and dad, for all their love and support. I couldn't have done it without you.

CHAPTER 1

INTRODUCTION

1.1 Kinetoplastida Derived Disease

The causative agents of several medically and veterinary important tropical diseases are parasitic protozoa of the Kinetoplastida order. These diseases almost exclusively affect the developing world, and as a result there is little financial incentive for the pharmaceutical industry to develop effective treatments.

1.1.1 African Trypanosomiasis

African trypanosomiasis (also known as African sleeping sickness) is widespread in sub-Saharan Africa and is caused by two parasites: *Trypanosoma brucei rhodesiense* (east and southern Africa) and *Trypanosoma. brucei gambiense* (west and central Africa).[1] A third sub-species, *Trypanosoma. brucei brucei*, is harmless to humans but causes the devastating disease, Nagana, in cattle. The decimation of cattle caused by Nagana is a major barrier to the development of otherwise fertile land where the disease is rife, with an estimated 3 million cattle deaths attributed to the disease each year.[2]

African trypanosomiasis is an old disease, having been known to the slave traders who would reject Africans bearing the swollen cervical glands that are characteristic of the disease. Infection occurs primarily through the bite of the infected tsetse fly, although today infection is also possible through transfusion of infected blood. Early symptoms include fever and enlarged lymph glands and spleen, and as the parasites invade the central nervous system, mental deterioration begins leading to coma and death. *T. b. rhodesiense* infection is severe and usually leads to death within days or weeks. *T. b. gambiense* infection is less aggressive and disease progression often lasts several years.

There have been three severe epidemics of the disease, the first occurred between 1896 and 1906; the second in 1920 and the third began in 1970. Over sixty million people are at risk from the disease and fifty thousand cases are reported each year, although the World Health Organization estimates that the true number of cases is 10 times greater.

1.1.2 Chagas' Disease

Chagas' disease (or South American trypanosomiasis) is found exclusively in Latin America and is named after Carlos Chagas, the Brazilian doctor who first described the disease in 1909.[3] The disease is widespread, spanning from Mexico in the north of the continent to the south of Argentina. At present, the disease is endemic in 21 countries; with sixteen to eighteen million people infected and over one hundred million people at risk, with approximately thirteen thousand deaths per year attributed to the disease. The causative agent is *Trypanosoma cruzi*, which is transmitted to humans by triatomine insects. A small sore usually develops at the site of infection and fever and swollen lymph glands can develop within a few days. This early, acute, stage of the disease can cause illness and death, particularly in young children, though more commonly patients enter a symptom-less phase that lasts for several months or years, during which time the parasite invades most of the organs of the body. Fatal damage to the heart and digestive tract occurs in 32% of patients during this chronic stage of the disease.

1.1.3 Leishmaniasis

Leishmaniasis, caused by parasites of the genus *Leishmania*, is widespread in 88 countries across 5 continents and an estimated twelve million people are currently infected with a further three hundred and fifty million at risk.[4] Periodic epidemics occur: an estimated hundred thousand mortalities occurred in Sudan in the 1990's and an estimated two hundred thousand people are currently afflicted in Afghanistan. Infections occur through the bite of infected sand flies and an estimated fifty-nine thousand deaths each year are attributed to the disease. Over 20 species and sub-species infect humans, and leishmaniases can be classified into 4 main categories:

1) Visceral leismaniasis: the most serious form, which is fatal if left untreated (e.g. Kala-azar caused by *L. donovani*).
2) Cutaneous leishmaniasis: the most common form, which causes skin lesions which heal without treatment within a few months but which leave unsightly scars (e.g. Baghdad ulcer, Delhi boil or Bouton d'Orient, due to infection with *L. major*).

3) Mucocutaneous leishmaniasis: initial skin ulcers spread to the soft tissue of the nose and mouth leading to large-scale tissue destruction. Caused by *L. braziliensis*.

4) Diffuse cutaneous leishmaniasis: leads to skin lesions that resemble leprosy. Caused by *L. aethiopica* and *L. mexicana mexicana*.

1.2 Current Treatments

1.2.1 Treatment of African Trypanosomiasis

If detected early, there are fairly effective drugs available for the treatment of African trypanosomiasis. Pentamidine **1** and berenil **2** (Figure 1) are both thought to inhibit *S*-adenosinylmethionine decarboxylase, an important enzyme in the parasitic polyamine biosynthetic pathway. However, in the late stage of the disease, following parasitic invasion of the central nervous system, treatment requires drugs capable of crossing the blood-brain barrier. Difluoromethylornithine (DFMO, **3**) is effective in the late stage treatment of *T. b. gambiense* infections but is ineffective against *T. b. rhodesiense* infections. DFMO inhibits another enzyme important in polyamine biosynthesis, ornithine decarboxylase.

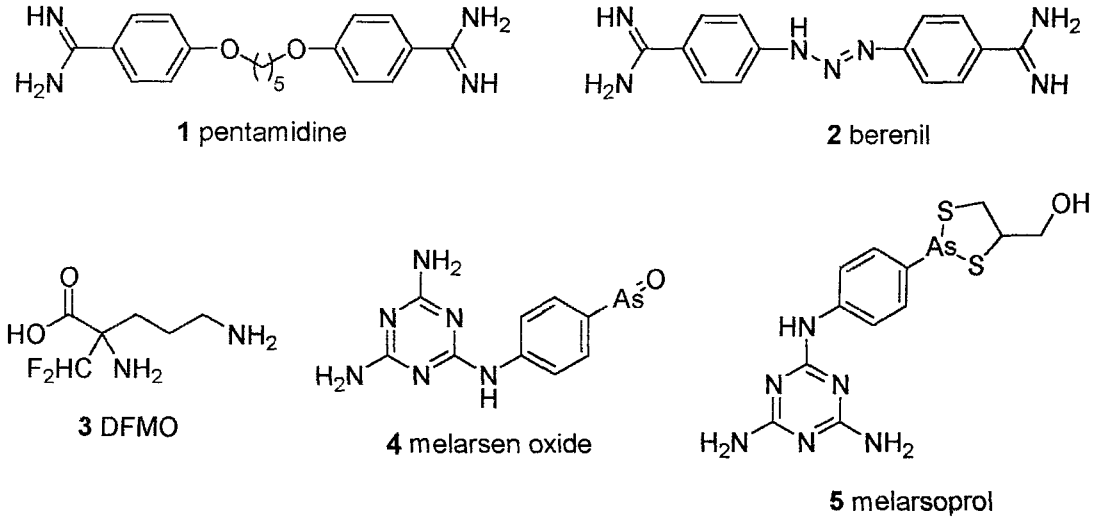

Figure 1: Drugs used against African trypanosomiasis derived disease.

The relatively high cost and poor availability of DFMO has led to the use of the trivalent arsenicals melarsen oxide **4** and melarsoprol **5**. Undesired effects with these drugs are severe, indeed fatal in as many as 10% of cases, and resistance to the drugs is also high. Early diagnosis, which would allow effective treatment of the disease, is rarely achieved due to the lack of effective screening regimes.

1.2.2 Treatment of Chagas' Disease

Nitroarenes such as nifurtimox **6** and benznidazol **7** (Figure 2) have been used against *T. cruzi* infection but their use is associated with severe side-effects. The severity of these side-effects led to the withdrawal of benznidazol from the market.

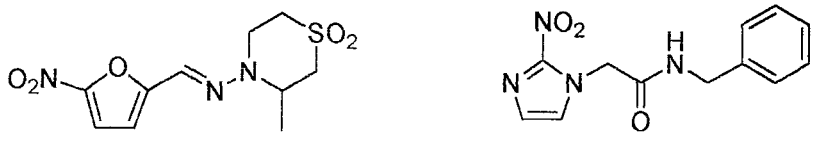

6 nifurtimox **7** benznidazol

Figure 2: Drugs used against *T. cruzi*.

1.2.3 Treatment of Leishmaniasis

Leishmaniasis is treated with the administration of moderately toxic and relatively expensive antimonial drugs such as pentostam **8** (Figure 3). In the increasingly frequent cases where antimonial drugs are found to be ineffective, other, highly toxic drugs such as amphotericin B **9** are used.

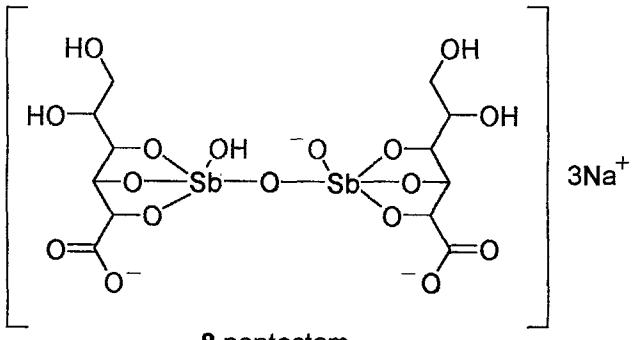

8 pentostam

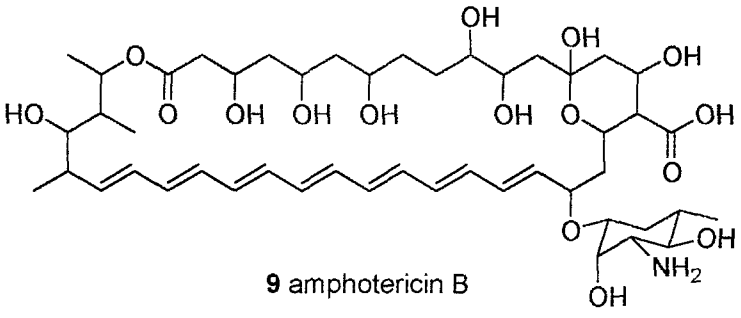

9 amphotericin B

Figure 3: Drugs used against Leishmaniasis derived disease.

In summary, currently available treatments have severe drawbacks, namely toxicity, efficacy and the reliance on the early detection of disease which is often impossible. The need for new effective treatments is clear.

1.3 Targeting Trypanosomes

The first step towards the rational design and discovery of new drugs is the identification of key, parasite-specific cellular components as potential drug targets. Several differences in the biochemistry of these organisms with their hosts have so far been identified. One of the most promising differences relates to the mechanism by which cytotoxic oxidants are removed from the cell.

1.3.1 Oxidative Stress Management

Oxidants, such as superoxide radical anions, hydrogen peroxide and hydroxyl radicals, all arise within cells from side reactions from aerobic respiration as well as from the host immune response to parasite infection. If these oxidants are not removed, several problems arise, including damage to DNA, proteins and membrane lipids. Both the sugar

and base moieties of DNA are susceptible to oxidation which causes base degradation, single strand breakage and cross-linking to proteins.[5] The high susceptibility of DNA to oxidative stress is one reason why eukaryotic organisms have compartmentalised DNA within the nucleus, away from sites of redox cycling. Oxidative attack on proteins results in site-specific amino acid modifications, fragmentation of the peptide chain, altered electrical charge and increased susceptibility to proteolysis. Oxidative attack on membrane lipids causes cell rupture and death.

The hydroxyl radical, a very reactive species, is generated by reaction of hydrogen peroxide and superoxide anion as well as by the Fe^{II} catalysed decomposition of hydrogen peroxide.[6] The level of hydroxyl radicals are minimized by the enzymatic removal of the precursor hydrogen peroxide and superoxide species. In both human cells and trypanosomatids, superoxide anion is removed by superoxide dismutase (SOD).[7,8] In humans, hydrogen peroxide is removed by a number of catalases and peroxidases including glutathione peroxidase. In general, trypanosomatids contain little or no catalase activity but evidence for a trypanothione-dependent peroxidase has been reported.[9] The last line of defence is the non-enzymatic scavenging of the oxidants by low molecular weight compounds. In humans and almost all organisms, the widely abundant cellular thiol, glutathione **10** (Figure 4), is utilized for this purpose.

1.3.2 Glutathione and Glutathione Reductase

Glutathione is a thiol-containing tripeptide that has numerous important metabolic and regulatory roles. As a result of its role in oxidative stress management, two molecules of glutathione are oxidized to glutathione disulfide **11**. Glutathione disulfide is reduced to glutathione by the enzyme glutathione reductase (GR), an NADPH-dependent flavoprotein (Figure 4), such that the ratio of glutathione to glutathione disulfide in most cells is usually greater than 300.[10] The enzyme has been widely studied and the crystal structure at high resolution has been reported.[11-14]

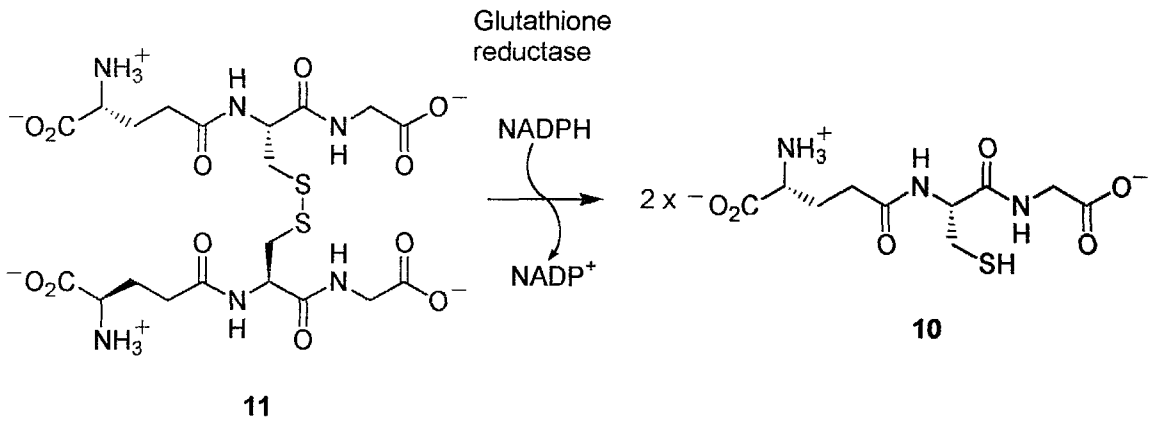

Figure 4: Action of glutathione reductase.

1.3.3 Trypanothione and Trypanothione Reductase

Trypanosomes and leishmania differ from most other organisms in that they maintain their intracellular redox balance by a different mechanism. Glutathione is not the most prominent thiol present in the trypanosomes, rather it is the structurally related N^1,N^8-*bis*(*L*-γ-glutamyl-*L*-cysteinyl-glycyl)spermidine (trypanothione, **12**), where the two glutathione residues are conjugated to the primary amines of the polyamine spermidine *via* the glycine carboxylates. It was first isolated and identified from *Crithidia fasciculata* in 1985,[15] and is probably chiefly responsible for the scavenging of cytotoxic oxidants in these organisms. GR is absent from trypanosomatids, its role performed by another enzyme, trypanothione reductase (TR). TR regenerates trypanothione from trypanothione disulfide **13** in an analogous manner to the regeneration of glutathione from glutathione disulfide by GR (Figure 5).

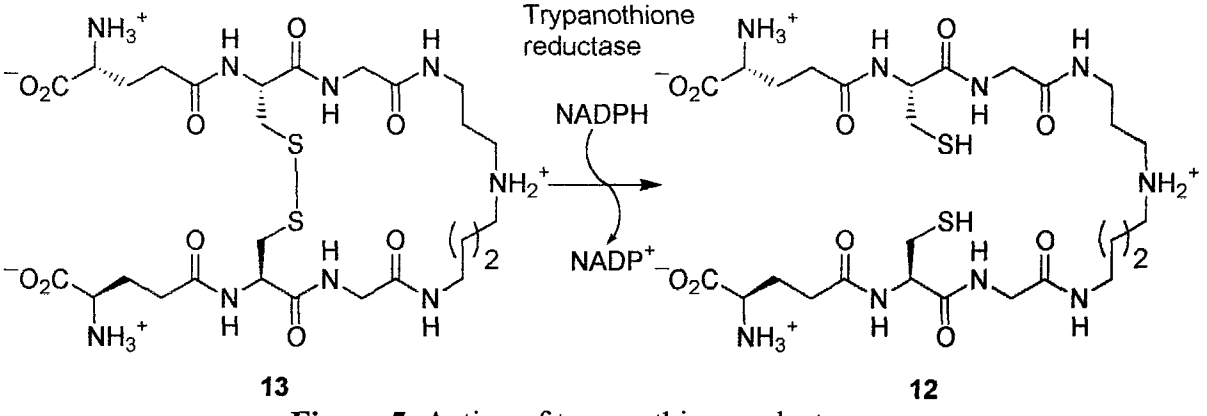

Figure 5: Action of trypanothione reductase.

TR has been found in all species of trypanosomatids investigated to date, was first isolated from *C. fasciculata*,[16] and since from *T. cruzi*[17], *T. brucei*[18] and *T. congolense*.[19] TR and GR are similar in that they contain a redox active disulfide bridge, are homodimeric proteins with a subunit molecular weight of approximately 52 kDa and catalyse the reduction of their respective substrates by the transfer of electrons from NADPH *via* a flavin, (FAD) prosthetic group.[20-23] Despite approximately 40% homology between the amino acid sequence of GR and TR, a high degree of specificity for their respective disulfide substrates is observed.[24] The substrate specificity (k_{cat}/K_m) for *T. congo* TR drops from 5.1 x 10^8 with trypanothione disulfide as a substrate to 0.84 with glutathione disulfide as a substrate. Similarly, k_{cat}/K_m for human GR drops from 1.2 x 10^8 with glutathione disulfide to 1.4 x 10^4 with trypanothione disulfide as a substrate.

The mechanism of action of TR is thought to be similar if not identical to GR, which has been extensively studied by a variety of means including X-ray crystallography.[25-30] The structure of the native enzyme with bound NADPH and glutathione disulfide, as well as two reaction intermediates, has been elucidated at a resolution of 0.3 nm, with the active site composed of residues from both sub units. The mechanism is outlined in Figure 6, where (A) represents the active site in the resting state with the disulfide bridge between Cys_{58} and Cys_{63} intact. Following binding of NADPH and protonation of the $His_{467'}$ residue (B), reduction of the active site disulfide occurs by electron transfer from the nicotinamide ring of NADPH *via* the isoalloxazine ring of FAD. Following release of $NADP^+$ and the binding of glutathione disulfide (C), a mixed disulfide is formed by attack of the sulfur of Cys_{58} on the disulfide of the substrate, releasing a molecule of glutathione that picks up a proton from $His_{467'}$. Regeneration of the active site disulfide by attack of the sulphur of Cys_{63} on the sulphur of Cys_{58} then releases the second molecule of glutathione, which again picks up a proton from $His_{467'}$ (D) and returns the active site to the resting state (A).

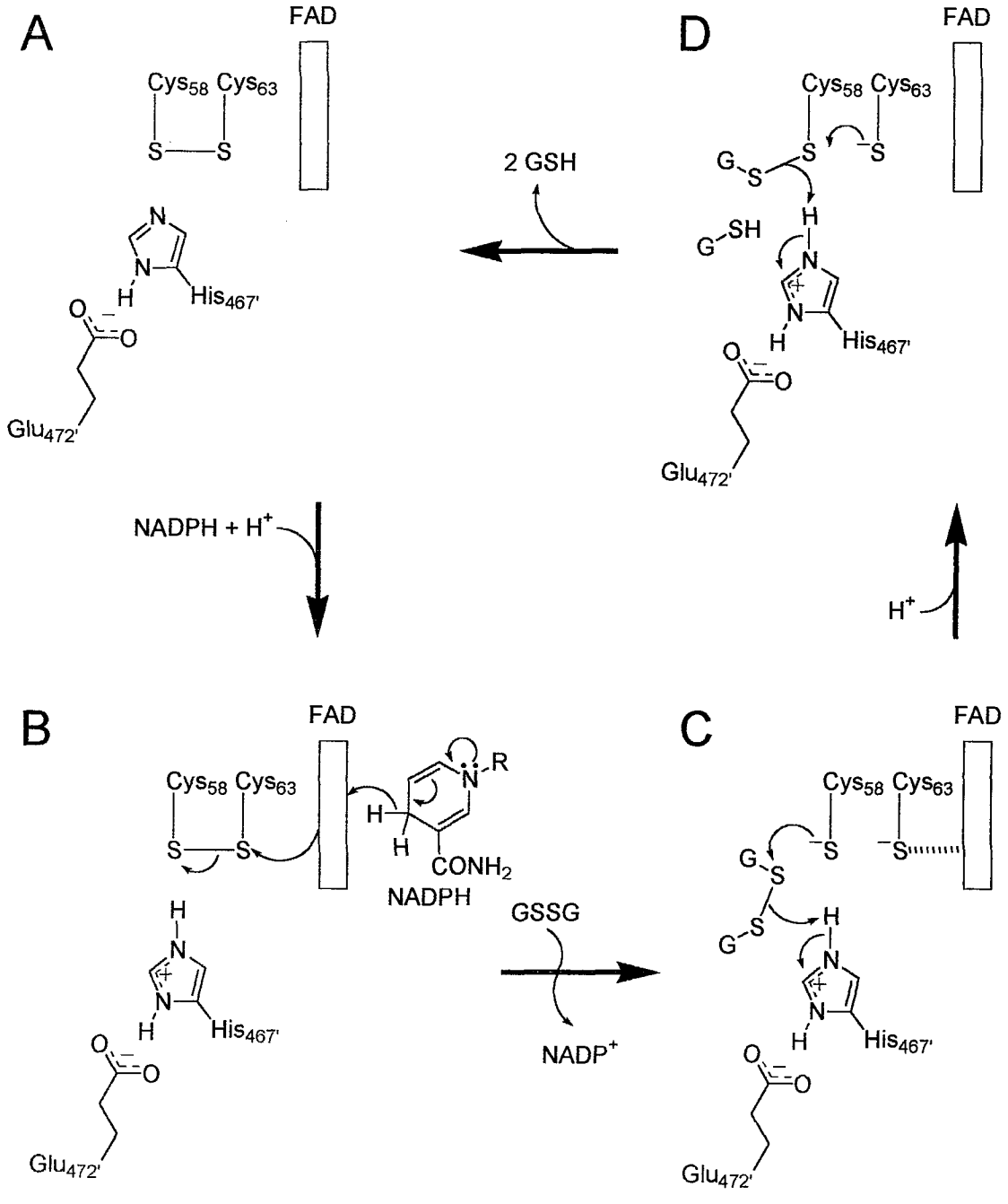

Figure 6: Mechanism of action of glutathione reductase. Residues marked ' refer to the second monomer unit of GR.

Evidence for a similar mechanism in TR includes the X-ray crystal structure of TR from *C. fasciculata* with bound substrate and NADPH at 2.4 Å resolution,[31] and alkylation studies using iodoacetamide, which indicate an essential catalytic role for the redox active cysteines.[16,17] The formation of a charge transfer complex on reduction of

the enzyme indicates the reaction proceeds *via* a two electron reduced intermediate.[16,17] Alignment of GR with all TRs so far sequenced indicates conservation of the redox active cysteines, the histidine base, the glutamic acid that holds the imidazolium ion in the correct orientation, and the tyrosine that stacks between the two glutathione moieties.[25,32-35]

The active site of GR and TR show a good deal of similarity, with 19 of the 27 residues common to both enzymes. This is perhaps surprising given the high degree of specificity observed for the enzymes with their respective substrates. Active site residues that interact directly with the γ-glutamylcysteinyl disulfide moiety common to both substrates show only minor, homologous substitutions (e.g. Ser for Thr), suggesting a very similar binding mode for this moiety in both enzymes. Not surprisingly, the major differences affect residues that interact with the glycyl carboxylate region of the substrates. In GR, in order to accomodate the negatively charged carboxylate groups of the substrate, this region is highly polar, containing the residues Arg_{37}, Tyr_{114}, and Asn_{117}. The corresponding region in TR contains a hydrophobic cleft, formed from the residues Leu_{17}, Trp_{21}, Tyr_{110}, Met_{113} and Phe_{114}, reflecting the lack of a negative charge and the greater hydrophobic nature of the spermidine chain of trypanothione disulfide. The importance of these residues has been investigated by site-directed mutagenesis in which substrate specificity was reversed, but the activity of the engineered enzyme was reduced in comparison to the native enzyme, suggesting the factors responsible for substrate specificity and turnover are more complex than simple side-chain substitutions.[36-38]

A second hydrophobic region within the TR active site, termed the Z site, has been identified, consisting of the residues $Phe_{396'}$, $Leu_{399'}$ and $Pro_{398'}$. The Z site is thought to be involved in the binding of the aromatic Cbz group of the alternative TR substrate *N,N'-bis*(benzyloxycarbonyl)-*L*-cysteinylglycine 3-dimethylaminopropylamide disulfide **14** (Figure 7).[39] This compound was proposed as a readily accessible alternative to trypanothione disulfide due to the expense and relatively difficult synthesis of the natural substrate.

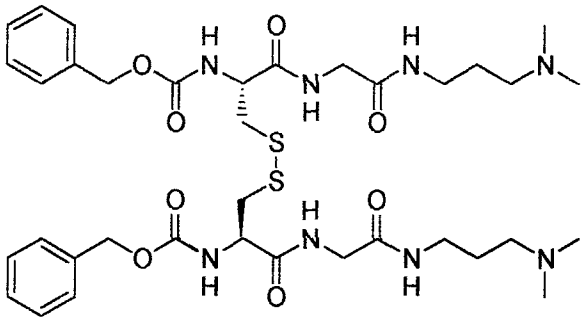

14

Figure 7: Alternative TR substrate **14**.

1.4 Trypanothione Reductase Inhibitors

1.4.1 Polycyclic Compounds

Molecular modelling has been utilised to probe the active site of TR in the search for new inhibitors, and one such study targeted the hydrophobic cleft region of the TR active site and suggested a number of known tricyclic antidepressants could be accommodated.[40] A subsequent assay of 30 such compounds against *T. Cruzi* TR confirmed this finding. Three compounds, namely clomipramine **15**, amitriptyline **16** and trifluoroperazine **17** (Figure 8), were studied in detail and found to be competitive inhibitors that showed no activity against human GR at a concentration of 1 mM (**15** and **16**) and 0.3 mM (**17**).

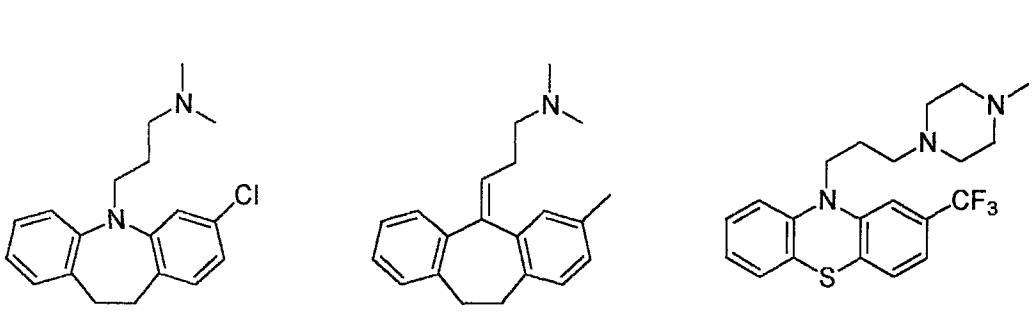

15 K_i = 6.5 μM **16** K_i = 93.6 μM **17** K_i = 21.9 μM

Figure 8: Tricyclic antidepressants clomipramine **15**, amitriptyline **16** and trifluoroperazine **17**.

Tricyclic compounds based on the saturated dibenzazepine nucleus of imipramine (**18**, Figure 9) have been reported as competitive inhibitors of *T. Cruzi* TR with K_i values in the micromolar range.[41] Inhibition studies provided evidence of multiple binding modes within the active site, consisting of an electrostatic interaction between the protonated dimethylamino group of the inhibitor with either the region comprised of $His_{461'}$, $Glu_{466'}$ and $Glu_{467'}$ (the "γ-Glu site") or Glu_{18} of the active site together with hydrophobic interactions between the tricyclic ring system and the hydrophobic cleft. The orientation and strength of binding of the tricyclic ring within the hydrophobic pocket was highly dependent on the exact substitution pattern of the dibenzazepine ring.

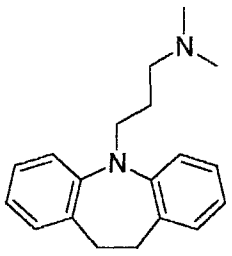

18

Figure 9: Imipramine **18**.

Following these findings, molecular modelling was used to design a large number of phenothiazine analogues to probe structure-activity relationships.[42] These compounds were found to be reversible inhibitors of *T. Cruzi* TR, competitive with trypanothione disulfide as substrate and non competitive with NADPH, with measured K_i values in the micromolar range. SAR were rationalized by considering several binding modes for the tricyclic compounds within the relatively large active site of TR, and interactions with not only the hydrophobic cleft, but also the Z-site were considered, as were interactions with polar regions such as the γ-Glu site and Glu_{18}.

A significant improvement in potency was achieved by the incorporation of a quaternary alkylammonium group onto phenothiazine chlorpromazine.[43] A series of such compounds was prepared and all were found to be competitive inhibitors of *T. Cruzi* TR (Figure 10). The most potent, **19**, had a measured K_i value of 0.12 μM, an improvement of 2 orders of magnitude over the parent compound chlorpromazine. The authors

postulated that the increase in potency resulted from both the stronger interaction between the ammonium ion of the side chain with the γ-Glu-site of TR and an additional hydrophobic interaction between the hydrophobic substituent of the ammonium ion and the Z-site.

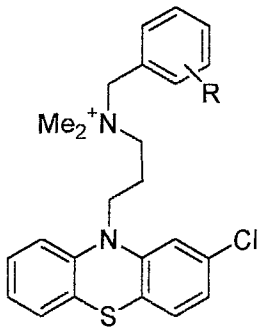

19 R = 3,4-dichloro K_i = 0.12 μM
20 R = 4-benzyloxy K_i = 0.47 μM
21 R = 3,4-dimethyl K_i = 0.47 μM
22 R = 4-*t*-butyl K_i = 0.68 μM
23 R = 3,5-dimethoxy K_i = 0.77 μM

Figure 10: Quaternary alkylammonium phenothiazines **19-23**.

A random screening strategy identified the structurally related 2-amino diphenylsulfides as inhibitors of TR.[44] 9 derivatives were studied and found to be selective, competitive inhibitors of *T. Cruzi* TR with measured K_i values in the micromolar range, the most potent inhibitor being **24** (Figure 11). The *in vitro* activity of several of the derivatives was also investigated and their activity confirmed. Although the 2-aminodiphenyl sulfides were found to be less potent than the tricyclic antidepressants discussed earlier, they have the advantage of not possessing the neuroleptic activity of the phenothiazine compounds.

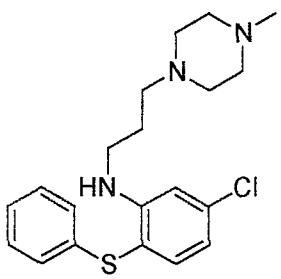

24 K_i = 27 μM

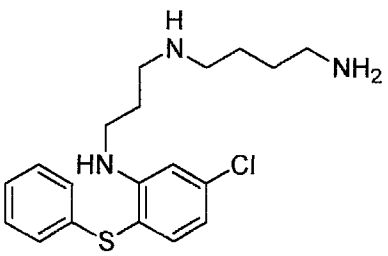

25 K_i = 24 μM

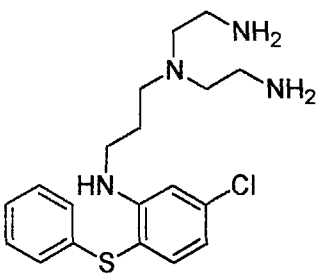

26 K_i = 12 μM

Figure 11: 2-Aminodiphenyl sulfide derivatives **24-26**.

The authors further extended their study using molecular modelling to dock **24** into the active site of TR.[45] The results showed a similar binding mode to the phenothiazines, with the aromatic moiety oriented towards the hydrophobic cleft region and the charged ammonium group within hydrogen bond distance of the γ-Glu site. Derivatives were investigated where the amino chain of **24** was altered in the hope of involving both $Glu_{466'}$ and $Glu_{467'}$ as well as other nearby acidic residues in the binding. The most active compounds identified were **25** and **26** (Figure 11), both of which contained additional amino groups capable of such interactions.

A further extensive study investigated a series of analogues incorporating two amino side chains, linked to either one or two aminodiphenyl sulfide moieties.[46] Previous molecular modelling studies suggested the TR active site was large enough to accommodate a second aromatic moiety. Additionally, the increased size of these compounds could assist the selectivity for TR over GR due to the fact that the active site in GR is significantly narrower than in TR. The most potent compound was found to be *bis*-derivative **27** (Figure 12), which has an IC_{50} of 0.55 μM. The mixed competitive inhibition displayed by these compounds was explained by their partial aggregation in solution, although this could be an example of non-specific inhibition caused by aggregation.[47]

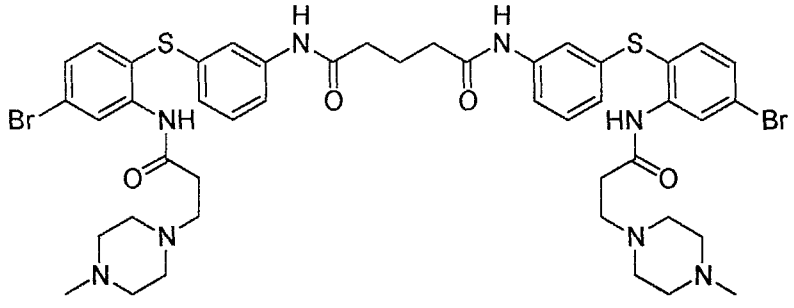

27 IC_{50} = 0.55 μM

Figure 12: *bis*(2-Aminodiphenyl sulphide) derivative **27**.

Subsequently, a slight improvement in potency was achieved by adding a third side chain to give derivatives **28-31** (Figure 13).[48]

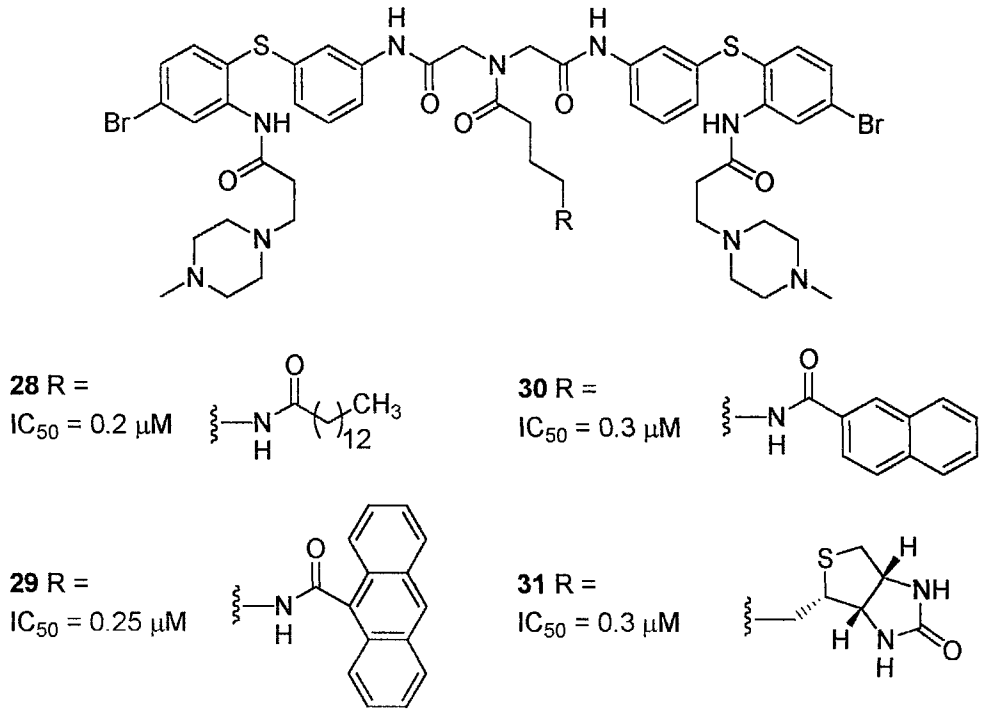

Figure 13: Aminodiphenyl sulfide derivatives **28-31**.

The crystal structure of the complex between *T. cruzi* TR and the antiparasitic drug mepacrine has been solved (Figure 14).[49] Mepacrine (**32**, Figure 15) is a competitive inhibitor of TR and was shown to bind in the active site with the acridine ring close to the hydrophobic cleft. Specific interactions were observed between the ring nitrogen and Met_{113}, the chlorine atom and Trp_{21} and the methoxy group with Ser_{109}. The alkylamino chain was found to point into the active site and form a solvent-mediated hydrogen bond with Glu_{18}.

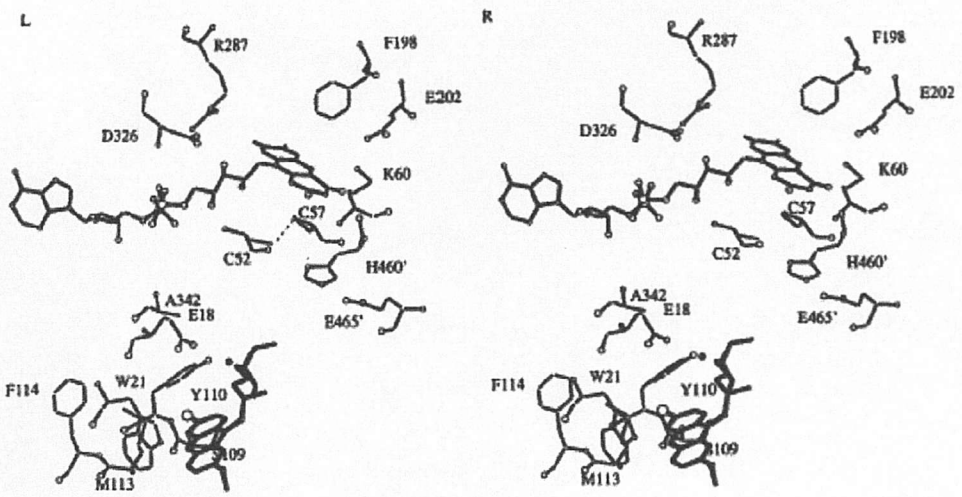

Figure 14: Stereoview of mepacrine binding in TR active-site from X-ray structure showing the position of the acridine ring in the hydrophobic cleft and the alkylamino chain orientated towards Glu_{18} (reproduced with permission).

Detailed kinetic analysis of a series of 9-aminoacridines based on mepacrine were found to competitively inhibit *T. Cruzi* TR with K_i values in the range 5 to 43 μM (Figure 15).[50] Again, evidence that subtle structural changes in the inhibitors could lead to significantly different binding modes was found, and it was shown that more than one inhibitor molecule could bind to the enzyme. Two 9-thioacridine compounds (**36** and **37**) were also found to inhibit TR and showed mixed-type kinetics. The K_i values were similar to those found for the aminoacridine derivatives whilst the K_{ii} values were somewhat higher, indicating a weaker binding of the inhibitor to the enzyme-substrate complex than to the free enzyme. The fact that relatively minor alterations to the inhibitor structure can lead to completely different inhibition modes highlights the difficulty of establishing meaningful structure-activity relationships with this class of compounds.

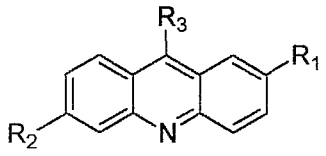

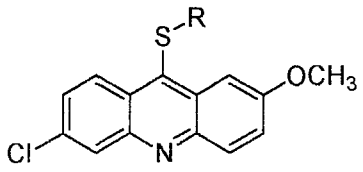

32 $R_1 = OCH_3$, $R_2 = Cl$,
$R_3 = NHCH(CH_3)(CH_2)_3N(Et)_2$, $K_i = 19$ μM
33 $R_1 = OCH_3$, $R_2 = Cl$,
$R_3 = NHCH(CH_3)(CH_2)_4N(Et)_2$, $K_i = 5.5$ μM
34 $R_1 = OCH_3$, $R_2 = Cl$,
$R_3 = NH_2$, $K_i = 7$ μM
35 $R_1 = H$, $R_2 = Cl$,
$R_3 = NHCH(CH_3)(CH_2)_3N(Et)_2$, $K_i = 10$ μM

36 $R = (CH_2)_2N(Et)_2$,
$K_i = 37$ μM, $K_{ii} = 83$ μM
37 $R = (CH_2)_4N(Et)_2$,
$K_i = 21$ μM, $K_{ii} = 67$ μM

Figure 15: 9-Aminoacridines **32-35** and 9-thioacridines **36** and **37**.

A series of 40 *bis*-acridine derivatives incorporating the 6-chloro, 2-methoxy substitution pattern of mepacrine were prepared and their antitrypanosomal properties investigated.[51] *In vitro* assays showed the series were particularly active against trypomastigote forms of *T. brucei* with three compounds causing total inhibition at a concentration of 1.56 μM. Reduced activity was observed against amastigote forms of *T. Cruzi*. Compound **38** (Figure 16) was assayed against *T. Cruzi* TR but found to inhibit with an IC_{50} of only 20 μM.

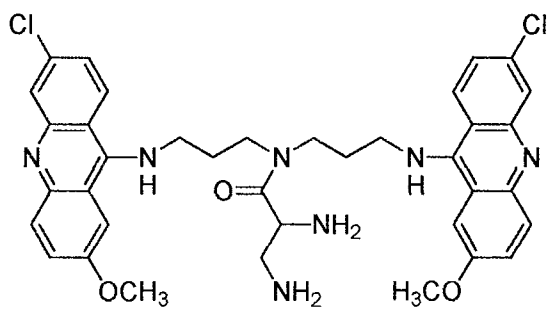

38

Figure 16: *bis*(9-Amino-6-chloro-2-methoxyacridine) derivative **38**.

Sulfonamide and urea analogues of mepacrine have also been examined.[52] Compounds **39-45** (Figure 17) were prepared and assayed against *T. Cruzi* TR and human GR. All compounds showed an increase in potency against TR compared to the parent

compound mepacrine (IC_{50} = 133 μM), although a significant loss in selectivity over GR was also observed. The authors suggested this loss in selectivity was due to the absence of the protonated tertiary amine group of mepacrine. It was also postulated that the generally better inhibition of the sulfonamide derivatives was due to the greater hydrophobic nature of the naphthalene moiety compared to the benzyl moiety of the urea analogues.

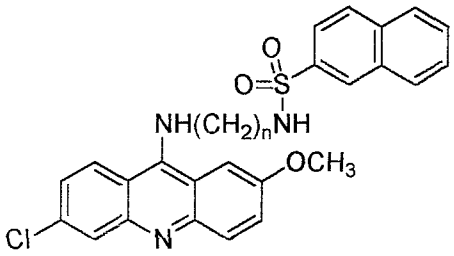

39 n = 2, IC_{50} = 5.9 μM
40 n = 3, IC_{50} = 3.3 μM
41 n = 4, IC_{50} = 5.0 μM

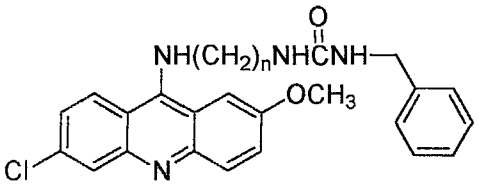

42 n = 2, IC_{50} = 19.3 μM
43 n = 3, IC_{50} = 13.1 μM
44 n = 4, IC_{50} = 15.5 μM
45 n = 6, IC_{50} = 11.4 μM

Figure 17: Sulfonamide and urea mepacrine analogues **39-45**.

9,9-Dimethylxanthene derivatives have been investigated as potential agents against TR, and in an initial study, derivatives **46-51** (Figure 18) were evaluated against *T. cruzi* TR and *in vitro*.[53] All compounds showed activity against TR and high *in vitro* antiparasitic activity was observed for **49**, **50** and **51**. There was however little correlation between *in vitro* antiparasitic activity and TR inhibition potency.

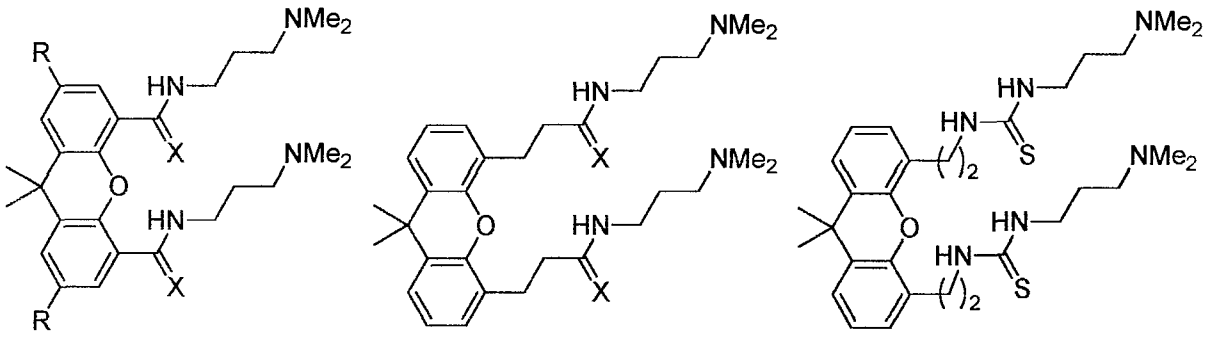

46 R = H, X = O
47 R = H, X = 2H
48 R = *t*-butyl, X = O

49 X = O
50 X = 2H

51

Compound	% Inhibition of TR ([I] = 100μM)	ED_{50} (μM) against *T. brucei*
46	40	9.66
47	14	7.58
48	28	0.02
49	58	8.24
50	63	0.14
51	52	0.10

Figure 18: Structure, inhibition of *T. cruzi* TR and activity against *T. brucei* macrophages of 9,9-Dimethylxanthene derivatives **46-51**.

Further xanthene derivatives have been reported as inhibitors of TR, the most potent being **52** (Figure 19), which was found to have a similar inhibitory potency to clomipramine **15**.[54] The authors postulated that, if bound in the correct orientation in the active site of the enzyme, the α,β-unsaturated moiety found in **52** may act as a Michael acceptor, reacting with the nucleophilic Cys_{53} residue of TR and thus irreversibly inhibiting the enzyme.

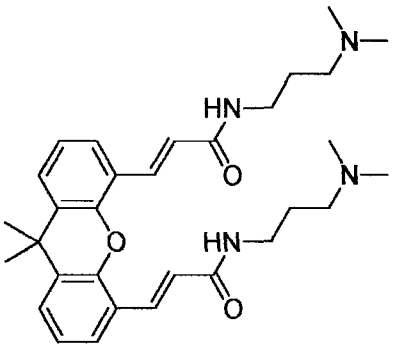

52

Figure 19: 9,9-Dimethylxanthene derivative **52**.

A study of chlorpromazine and analogues provided strong evidence of the importance of charge for specificity between TR and GR.[55] The inhibitory activity against human GR, *C. fasciculata* TR and *T. cruzi* TR of the four phenothiazines **53-56** was compared (Figure 20). Analogues **53-55**, which all contain a basic tertiary amine group in the side chain, were found to be selective for TR over GR. However, this selectivity was reversed for **56** which contained an acidic group in its side chain. These results, in agreement with mutagenic studies,[56,36] clearly imply that it is the charge of the side chain rather than the hydrophobic nature of the tricyclic nucleus that is responsible for the TR/GR selectivity.

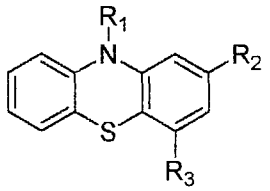

No.	R_1	R_2	R_3	K_i hGR (μM)	K_i *Cf*TR (μM)	K_i *Tc*TR (μM)
53	$(CH_2)_3N^+H(CH_3)_2$	Cl	H	762	14	10
54	$(CH_2)_3N^+H(CH_3)_2$	Cl	Cl	900	68	65
55	$(CH_2)_2N^+H(CH_3)_2$	Cl	H	440	24	17
56	$(CH_2)_2CO_2^-$	Cl	H	165	1400	nd

Figure 20: Structure and activity of chlorpromazine and analogues (*Cf*: *Crithidia fasciculata*, *Tc*: *Trypanosoma congolense*).

Bis-benzylisoquinoline compounds have been reported as moderate inhibitors of *T. Cruzi* TR, and eleven such compounds were screened for TR activity as well as for *in vitro* trypanocidal activity against trypomastigote forms of *T. cruzi*.[57] Several of the alkaloids were found to have significant *in vitro* activity with LC_{50} values lower than 100 μM. Cepharathine **57** (Figure 21) was found to be the most active against TR with a measured IC_{50} of 15 μM, although no direct relationship between TR activity and *in vitro* trypanocidal activity was observed.

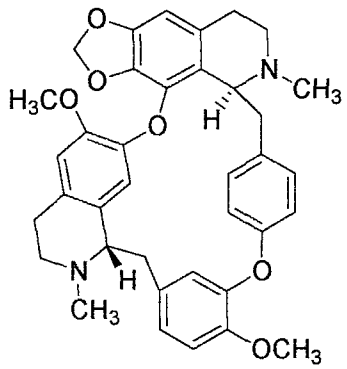

Figure 21: Cepharanthine **57**.

1.4.2 Polyamine Compounds

The polyamine backbone of trypanothione has been utilised as the basis for a number of inhibitors. Like the polycyclic compounds already discussed, polyamine based inhibitors typically contain both a positive charge and one or more hydrophobic groups.

The naturally occurring spermine derivative Kukoamine A (**58**, Figure 22) is a selective, mixed type inhibitor of TR with K_i = 1.8 μM and K_{ii} = 13 μM.[58] The authors suggested that the observed mixed-type inhibition might arise from a redox cycling process, as catechol ligands are known to switch between orthohydroquinone and orthoquinone oxidation states. However, other catechol containing compounds, including the spermidine analogue of Kukoamine A (**59**, Figure 22), showed purely competitive inhibition. The similar activity of **58** and **59** suggested that there was little discrimination between these two polyamines. Mono-acylated derivatives were found to be significantly weaker inhibitors, indicating the involvement of both hydrophobic groups in the binding.

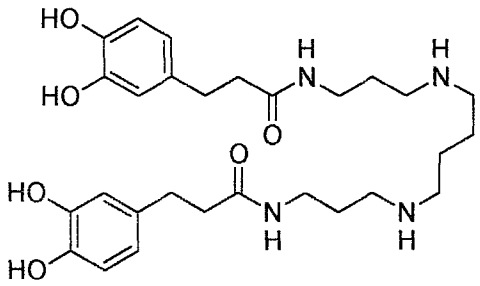

58 K_i = 1.8 μM, K_{ii} = 13 μM

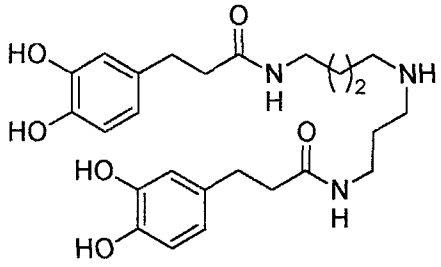

59 K_i = 7.5 μM

Figure 22: Kukoamine A **58** and the spermidine analogue **59**.

O'Sullivan reported numerous TR inhibitors based on spermine and spermidine, all of which were found to be competitive inhibitors of TR.[59-62] Initially, the spermine derivatives **60-62** (Figure 23) and spermidine derivatives **66** and **67** (Figure 24) were reported.[59,60] Of these, the compounds based upon the spermine backbone were generally more potent inhibitors. The *in vitro* trypanocidal activity of **60**, **61** and **66** was investigated against four *T. brucei* spp. strains. The compounds were found to be potent trypanocides with IC_{50} values ranging from 0.19 to 0.83 μM, although the lives of trypanosome infected mice were not prolonged by administration of the compounds. An order of magnitude increase in potency was achieved with the *N*-(3-phenylpropyl) substituted spermine compounds **63-65**.[62] Again, the related spermidine compounds **68** and **69** (Figure 24) were found to be slightly less potent inhibitors.

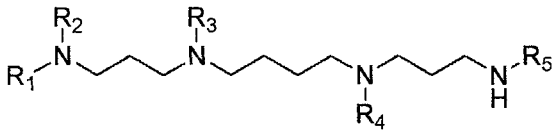

No.	R_1	R_2	R_3	R_4	R_5	K_i (μM)
60	H	H	$(CH_2)_3Ph$	$(CH_2)_3Ph$	H	3.5
61	H	H	CH_2-naphthyl	CH_2-naphthyl	H	5.5
62	H	H	CH_2Ph	CH_2Ph	H	19
63	$(CH_2)_3Ph$	$(CH_2)_3Ph$	$(CH_2)_3Ph$	$(CH_2)_3Ph$	$(CH_2)_3Ph$	0.15
64	$(CH_2)_3Ph$	H	$(CH_2)_3Ph$	$(CH_2)_3Ph$	$(CH_2)_3Ph$	0.61
65	$(CH_2)_3Ph$	H	$(CH_2)_3Ph$	$(CH_2)_3Ph$	H	1.38

Figure 23: Spermine derivaties **60-65**.

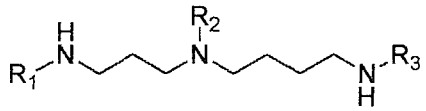

No.	R_1	R_2	R_3	K_i (μM)
66	CH_2-naphthyl	H	CH_2-naphthyl	9.5
67	H	CH_2-naphthyl	H	108
68	$(CH_2)_3Ph$	$(CH_2)_3Ph$	$(CH_2)_3Ph$	3.5
69	H	H	$(CH_2)_3Ph$	14.1

Figure 24: Spermidine derivatives **66-69**.

A small series of spermine and spermidine derivatives containing 2-amino diphenylsulfide moieties was prepared and assayed for activity against *T. cruzi* TR.[63] The most potent inhibitor (**70**, Figure 25) was found to inhibit competitively with a K_i of 0.4 μM. No activity against human GR at a concentration of 10 μM was observed.

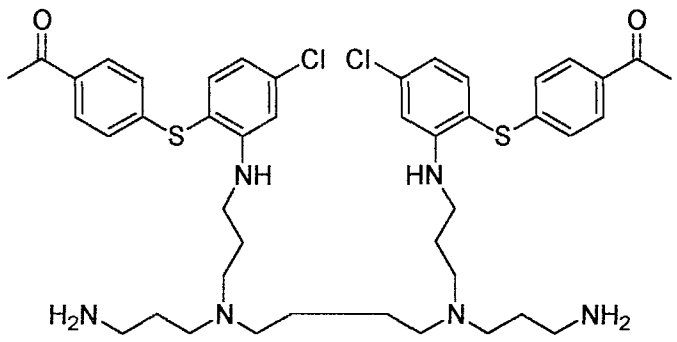

70

Figure 25: Spermine/2-amino diphenylsulfide conjugate **70**.

The trypanocidal activity and TR inhibition of compounds based on the polyamine 1,4-*bis*(3-aminopropyl)piperazine has been studied.[64] From a series of 25 compounds bearing aromatic and aliphatic substituents, the diphenylsulfides **71** and **72** (Figure 26) were found to be the most potent inhibitors of *T. cruzi* TR with IC_{50} values of 0.6 and 4 μM, respectively. When tested *in vitro* however, both compounds were found to be toxic towards the macrophages used in the test. Interestingly, **73** and **74**, the most active *in vitro* compounds, showed little activity towards TR and may therefore be useful in the search for new targets for anti-trypanosomal drugs.

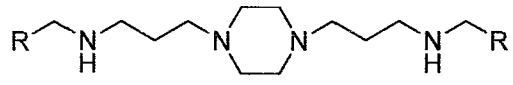

No.	R	IC_{50} on TR (μM)	% Inhibition *in vitro* at 3.1 μM
71	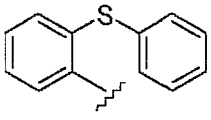	0.6	Toxic
72	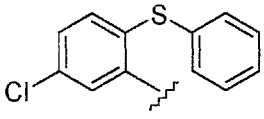	4	Toxic
73	Ph	>60	60
74	cHex	>60	80

Figure 26: 1,4-*bis*(3-Aminopropyl)piperazine derivatives **71-74**.

The Bradley group has used solid-phase chemistry in the synthesis of three libraries of compounds based on the polyamines spermine, spermidine and norspermidine.[65] The three polyamines were derivatised by capping the terminal amine groups with 24 aromatic carboxylic acids and the resulting libraries were assayed for activity against TR. Significant inhibition was observed for compounds based on all three of the polyamines. The most potent inhibitor found was **75** (Figure 27), where the aromatic moiety was an indole and the polyamine spermine. A further library was then prepared, consisting of spermine conjugated to 12 indole derivatives. The five most potent compounds in this series are shown in Figure 27. The 5-bromo-3-indole derivative **79** was the most potent with a K_i of 76 nM. Interestingly, these compounds were found to be non-competitive with trypanothione disulfide.

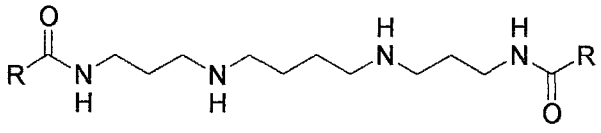

No.	R	K_i (μM)
75	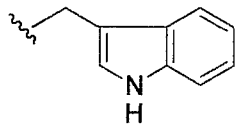	0.39
76	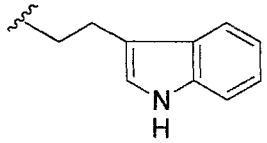	0.35
77	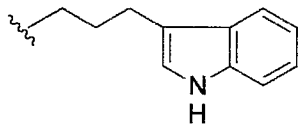	1.26
78	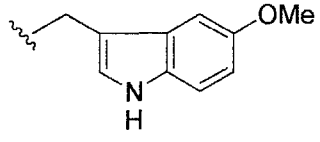	0.28
79	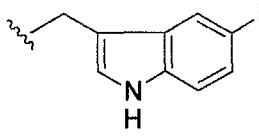	0.076

Figure 27: Indole-spermine conjugates **75-79**.

1.4.3 Substrate Analogues

A number of analogues of the alternative TR substrate **14** have been studied.[66] Compounds **80-82** (Figure 28), where the disulfide bridge of the alternative substrate is replaced with a sulfur containing, non-reducible bridge, were found to be competitive inhibitors of TR with K_i values ranging from 31 to 92 μM.

Similar inhibitors were prepared where the bridging group consisted entirely of carbon atoms (**83a**, **83b**, **84a** and **84b**, Figure 29).[67] These 4 compounds were found to be competitive inhibitors with respect to trypanothione disulfide and have similar K_i values to compounds **80-82**. Due to the known nucleophilic nature of Cys_{53} in the active site of TR, substrate analogues containing an electrophilic moiety have potential to irreversibly inhibit TR. Attempts to prepare the potential irreversible inhibitors **85a** and **85b** from the olefins **83a** and **83b** failed due to the instability of the epoxide ring. The authors attributed this instability to the intramolecular opening of the epoxide ring by the glycyl amide.

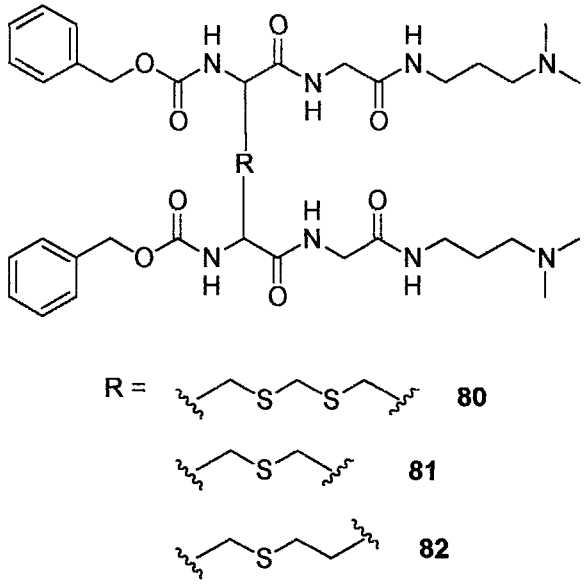

Figure 28: Non reducible substrate analogues **80-82**.

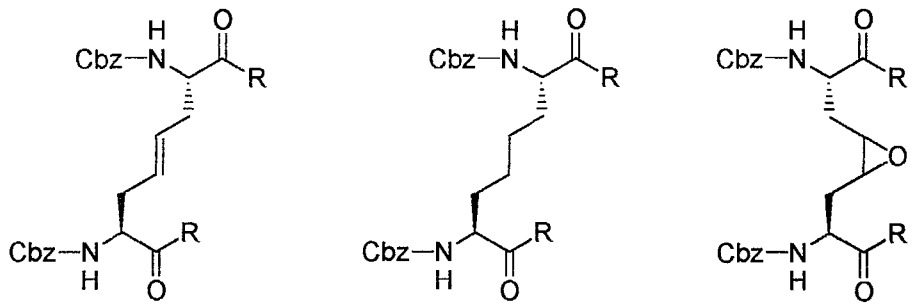

83a,b **84a,b** **85a,b**

(**a**) R = -Gly-NHCH$_2$CH$_2$CH$_2$N(CH$_3$)$_2$
(**b**) R = -Gly-NHCH$_2$CH$_2$CH$_2$NCH$_2$CH$_2$CH$_3$

Figure 29: Non reducible substrate analogues **83-85**.

1.4.4 Subversive Substrates

The anti-trypanocidal drugs nifurtimox **6** and benznidazol **7** are so-called subversive substrates that undergo a TR catalysed one-electron reduction to give a highly reactive anion radical. These species generate superoxide anions by reaction with molecular oxygen (Figure 30). Thus the normal anti-oxidative action of TR is reversed, or subverted.

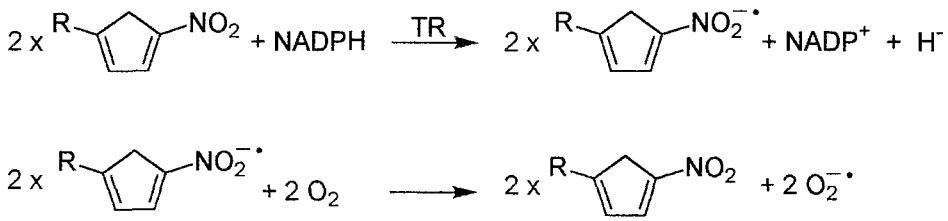

Figure 30: TR-catalysed reduction of nitroarenes.

A number of nitrofurans have been found to be noncompetitive or uncompetitive inhibitors against trypanothione disulfide and uncompetitive against NADPH.[68,69] Selectivity for TR over GR has been achieved by incorporating a positive charge, as with Chinifur **86** (Figure 31), a non-competitive inhibitor of TR (K_i = 4.5 μM) with good selectivity over GR (K_i = 100 μM).[68] A number of naphthoquinone derivatives also have trypanocidal activity again attributed to their redox-cycling properties.[70-72] **87** was found to inhibit *T. cruzi* TR uncompetitively with a K_i of 0.5 μM.[72]

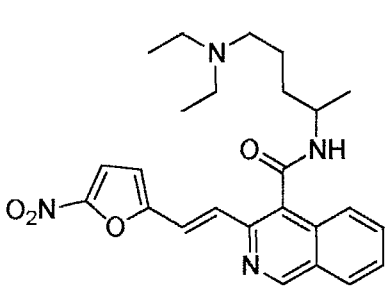

86

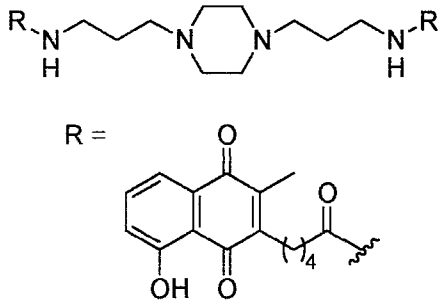

87

Figure 31: Subversive TR substrates **86** and **87**.

The garlic-derived natural product ajoene (**88**, Figure 32) is a covalent inhibitor and subversive substrate of both GR and TR.[73] X-ray crystallography was utilised to probe its mechanism of action, and evidence for the existence of a mixed disulfide between ajoene and Cys_{58} of the GR active site was obtained.

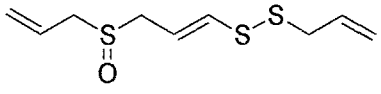

88

Figure 32: Ajoene **88**.

1.4.5 Other Inhibitors

A series of (2,2':6',2"-terpyridine)platinum(II) complexes was found to irreversibly inhibit *T. cruzi* TR, apparently by modification of the active site Cys_{53} residue.[74] In contrast, the compounds were found to be weak, reversible inhibitors of human GR. Platinum complexes have also been conjugated to an acridine moiety to generate mixed type inhibitors of *T. cruzi* TR.[75] The authors postulated that the reversible nature of the conjugate might result from the binding mode of the acridine ring, holding the platinum portion away from the Cys_{53} residue in the active site.

Peptide based inhibitors have been rationally designed based on the active site of TR. In an initial study, benzoyl-Leu-Arg-Arg-β-naphthylamide was identified as a competitive inhibitor of *T. cruzi* TR with a K_i of 13.8 μM. A further series of rationally

designed peptide inhibitors was investigated and the most active compound, Cbz-Ala-Arg-Arg-4-methoxy-β-naphthylamide, was found to be a reversible, competitive inhibitor with a K_i of 2.4 μM and a selectivity for TR over GR of 3 orders of magnitude.[76] A peptoid derivative of this lead compound has since been reported,[77] which was also a competitive inhibitor of TR, but a significant drop in potency was observed (K_i = 179 μM).

In the Bradley group, combinatorial chemistry has been used to generate a series of both solution and resin-based peptide libraries based on the polyamine spermidine.[78] Subsequent screening of these libraries for activity against *T. cruzi* TR led to the discovery of compounds **89-91** (Figure 33), the most active compound being **90**, a potent inhibitor with a K_i of 100 nM. The presence of the Pmc group was crucial for activity, as the fully deprotected compound **89** showed greatly reduced inhibiton (K_i = 16 μM), the presence of 2 Pmc groups (**91**) slightly reduced activity (K_i = 190 nM). Interestingly, all these compounds were found to be non-competitive with trypanothione disulfide as substrate. This finding was surprising given the structure of the compounds, which contain similarities to both the substrate and competitive inhibitors, namely hydrophobic groups (the indole rings and Pmc group) and a positive charge.

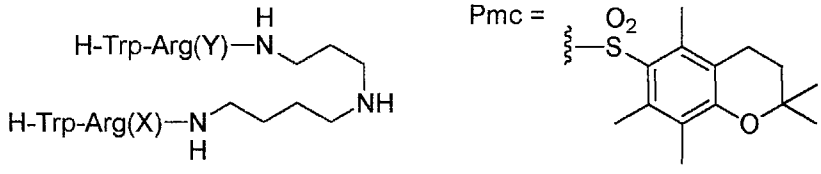

89 X = Y = H, K_i = 16 μM
90 X = H, Y = Pmc/X = Pmc, Y = H, K_i = 100 nM
91 X = Y = Pmc, K_i = 190 nM

Figure 33: Spermidine based peptidic inhibitors **89-91**.

It may also be noted that many groups use 4-(2-hydroxyethyl)piperazine-1-ethanesulfonic acid (HEPES) buffer when assaying TR. HEPES contains structural features (tertiary amino, hydroxyl and sulfonic acid groups) which could bind to the active site and interfere with the assay, and therefore the Bradley group has always avoided using this buffer, preferring either phosphate or acetate buffer systems.

1.5. Aims of this Project

The diseases caused by the *trypanosoma* and *leishmania* parasites are widespread and devastating, and currently available drugs fall a long way short of providing an effective weapon against such infection. The need for new treatments is unequivocal. The discovery of TR, its importance to parasitic oxidative stress management and the high substrate specificty of TR and GR has made the enzyme a highly promising therapeutic target. Numerous inhibitors of TR have been reported and **90**, being one of the most potent, is an interesting lead compound. The aim of this project was to investigate inhibitors of the type **89-91** in the hope that a better understanding of their mechanism of action would aid the rational design of more potent inhibitors, with the ultimate aim of developing an effective treatment for these devastating diseases.

CHAPTER 2

INVESTIGATING THE MECHANISM OF ACTION

In order to investigate the mechanism of action of the inhibitors identified from the library screening, it was first necessary to prepare the inhibitors, substrate and enzyme. In order to avoid the use of a mixture of regioisomers, as generated with the spermidine based inhibitor **90**, the norspermidine analogues of **89-91** were prepared. It was envisioned that this minor structural modification, whilst simplifying purification, would have little effect on the inhibitory properties of the compounds, but this of course had to be proved experimentally.

2.1 Preparation of Immobilised Polyamines

The inhibitors and substrate were prepared from suitably protected polyamine scaffolds using solid phase chemistry *via* a modified procedure to that reported in the literature.[78] Previously, the spermidine-linker conjugate was prepared from spermidine by initial protection of the primary amino groups with trifluoroacetyl (Tfa) groups to give **92**, followed by reaction with carbonate **93** to give **94**. Hydrolysis of both the ethyl ester and Tfa groups of **94** was followed by Fmoc-protection of the resulting primary amino groups to furnish carboxylic acid **95** ready for attachment to the solid-phase (Scheme 1). This allowed inhibitor synthesis to be completed by standard solid phase peptide chemistry.

In the modified procedure, the 1-(4,4-dimethyl-2,6-dioxocyclohexylidene)ethyl (Dde) protecting-group was utilised to protect the primary amino groups prior to attachment of the linker to the secondary amine. This avoided the necessity of "switching" the protecting groups during the synthesis. The Dde group, first descibed in 1993,[79] has found increasing use as an amine protecting group in solid-phase synthesis due to its facile introduction and removal under mild conditions.[80-85] The Dde group is introduced by reaction of an amine with 2-acetyldimedone, a reaction which is specific for primary over secondary amine groups.[80] Cleavage is usually achieved by brief treatment with a dilute solution of hydrazine in DMF.[79]

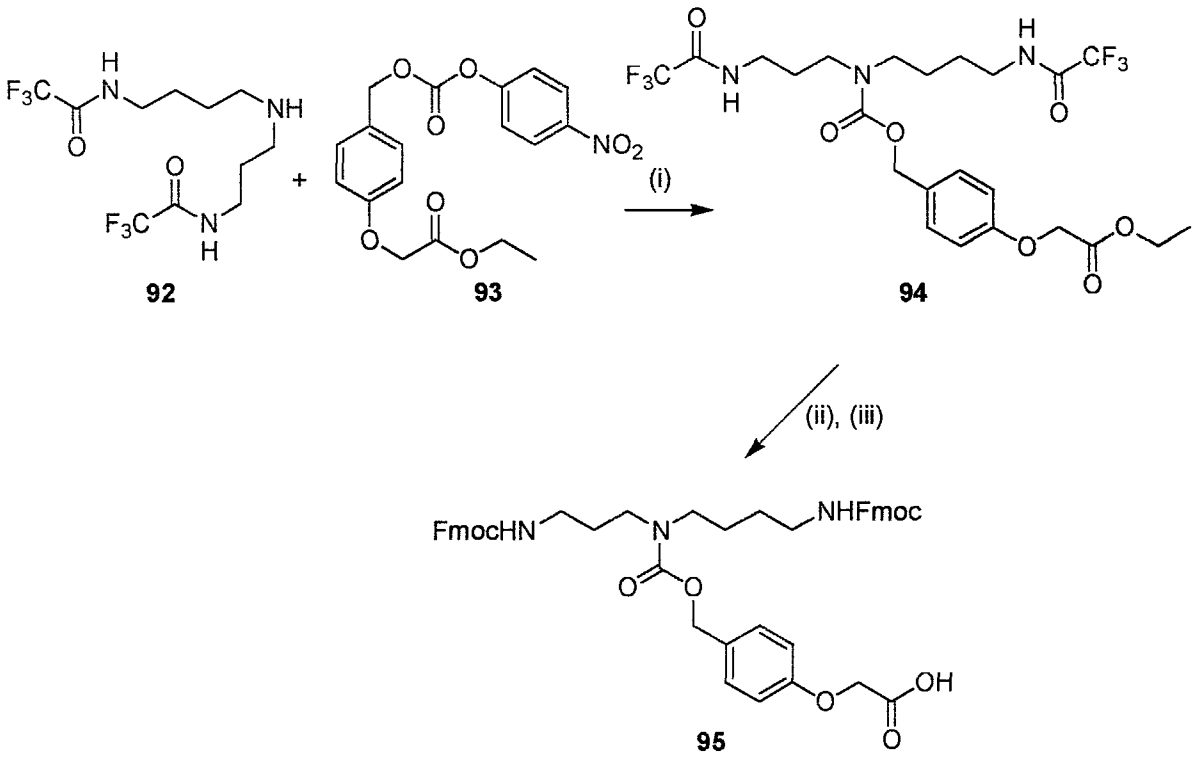

Scheme 1: Reported preparation of *bis*-Fmoc-spermidine linker conjugate **95**.[78]
***Reagents and conditions*:** (i) NEt_3, DMF, 61%. (ii) 2M NaOH. (iii) FmocOSu, 10% $NaHCO_3$, 97% (2 steps).

It was necessary to prepare both polymer-supported norspermidine **96** and spermidine **97** for the synthesis of the inhibitors and the natural substrate trypanothione disulfide **13**. The primary amino groups of **96** and **97** were Dde protected in near-quantitative yield by treatment with two equivalents of 2-acetyldimedone in refluxing EtOH for 2 hours (Scheme 2).[82]

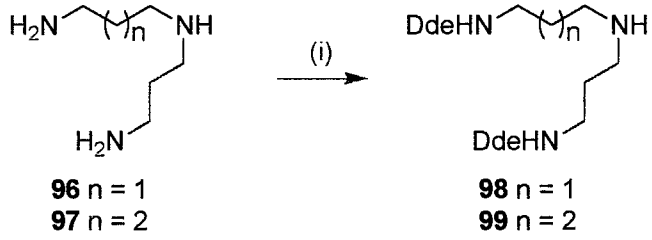

96 n = 1
97 n = 2

98 n = 1
99 n = 2

Scheme 2: Preparation of *bis*-Dde-protected norspermidine **98** and spermidine **99**.
***Reagents and conditions*:** (i) 2-acetyldimedone, EtOH, reflux, 2 hr, **98** (99%), **99** (98%).

Attachment of the *bis*-Dde protected polyamines to the solid-support *via* the secondary amino group was accomplished with a variation of the acid-labile urethane linker **93** used previously. The linker was attached to the polyamines with the carboxylic acid masked as the allyl- rather than the ethyl-ester.

The allyl-protected carbonate **103** was prepared in good yield from 4-hydroxybenzaldehyde **100** in three steps (Scheme 3).[86] **100** was alkylated with allylchloroacetate in near quantitative yield and the resulting aldehyde **101** reduced with $NaBH_3CN$ to give alcohol **102**. Reaction of **102** with 4-nitrophenylchloroformate furnished the carbonate **103**, ready for reaction with protected amines **98** and **99**.

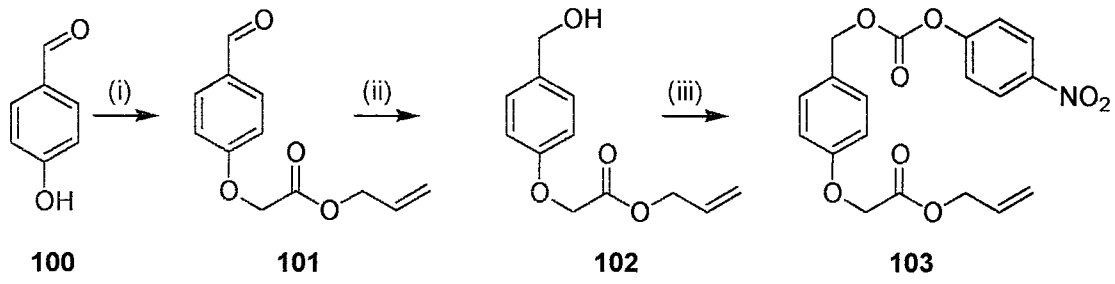

100 **101** **102** **103**

Scheme 3: Preparation of activated linker **103**.

***Reagents and conditions*:** (i) allylchloroacetate, KI, K_2CO_3, MeCN, reflux, 6 hr, 97%. (ii) $NaBH_3CN$, HCl, water/THF (1:1), 0 °C, 2 hr, 91%. (iii) 4-nitrophenylchloroformate, pyridine, DCM, 16 hr, 82%.

Reaction of **98** and **99** with **103** proceeded smoothly to furnish the desired allyl esters **104** and **105** in good yield. The allyl esters were cleaved upon treatment with $Pd(PPh_3)_4$ and thiosalicylic acid to give the carboxylic acids **106** and **107**, which were coupled to aminomethyl polystyrene resin (1% DVB crosslinked) using standard HOBt/DIC activation to give the desired immobilised scaffolds **108** and **109** (Scheme 4). The loading of the resins, determined by a quantitative ninhydrin test, were 0.66 (**108**) and 0.62 (**109**) mmol/g.

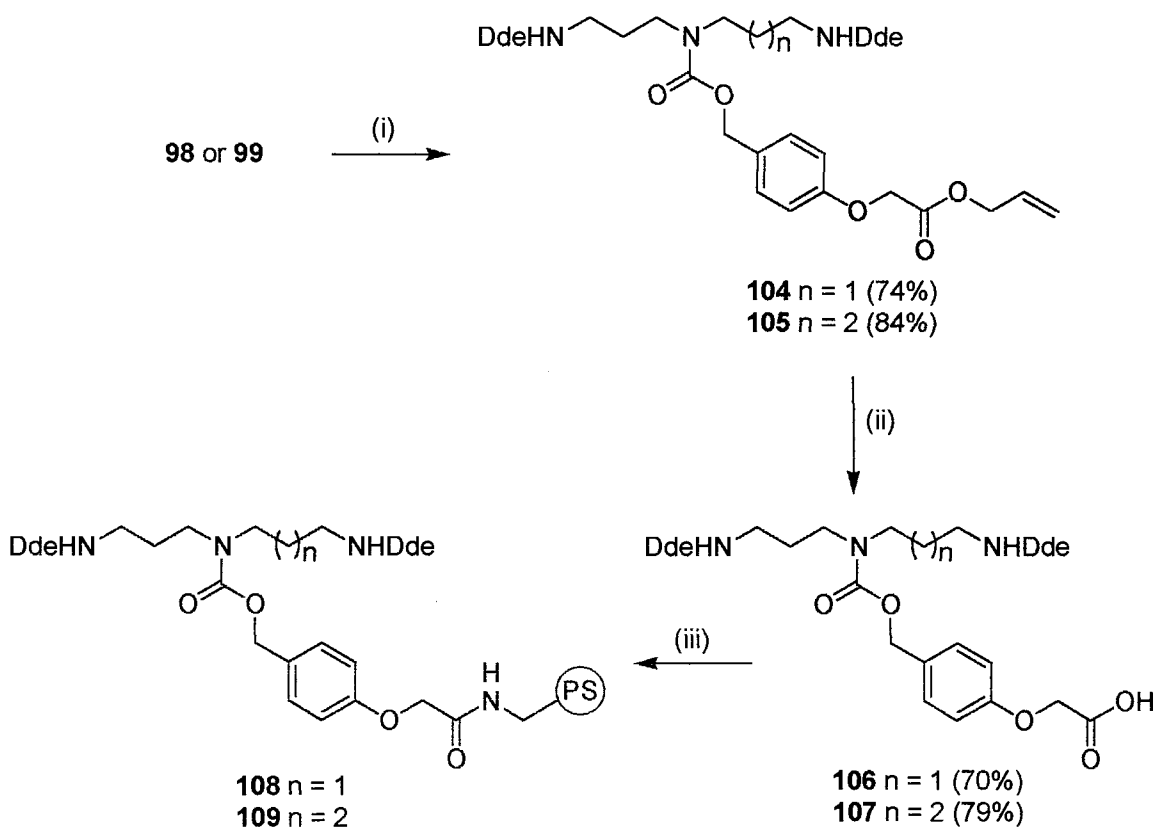

Scheme 4: Preparation of polymer-supported Dde-protected norspermidine **108** and spermidine **109**.

***Reagents and conditions*:** (i) **103**, DMF, 16 hrs. (ii) $Pd(PPh_3)_4$, thiosalicylic acid, DCM/ THF (1:1), 2 hrs. (iii) aminomethyl polystyrene resin, HOBt, DIC, DCM/ DMF (4:1), 16 hrs.

2.2 Inhibitor Synthesis

Synthesis of the inhibitors started from resin **108**, with removal of the Dde groups accomplished by treatment of the resin with 5% hydrazine in DMF for 30 minutes. Cleavage of the Dde groups was monitored by observation of the loss of the characteristic C=O signal at 1573 cm^{-1} in the FT-IR spectrum of the resin (Figure 34).

Following Dde deprotection, inhibitor synthesis was completed using standard HOBt/DIC activation for peptide bond formation and treatment with piperidine in DMF for Fmoc deprotection. Cleavage from the resin was achieved using a modification of the reported procedure, which utilised 10 x 1 hour treatments with 7.5% TFA in DCM.[78] This procedure was necessary to effect cleavage from the resin without total deprotection of

the Pmc group. As this procedure was inefficient, a more convenient procedure was sought *via* which the cleavage conditions would give a mixture of the three desired compounds in similar quantities in as short a time as possible.

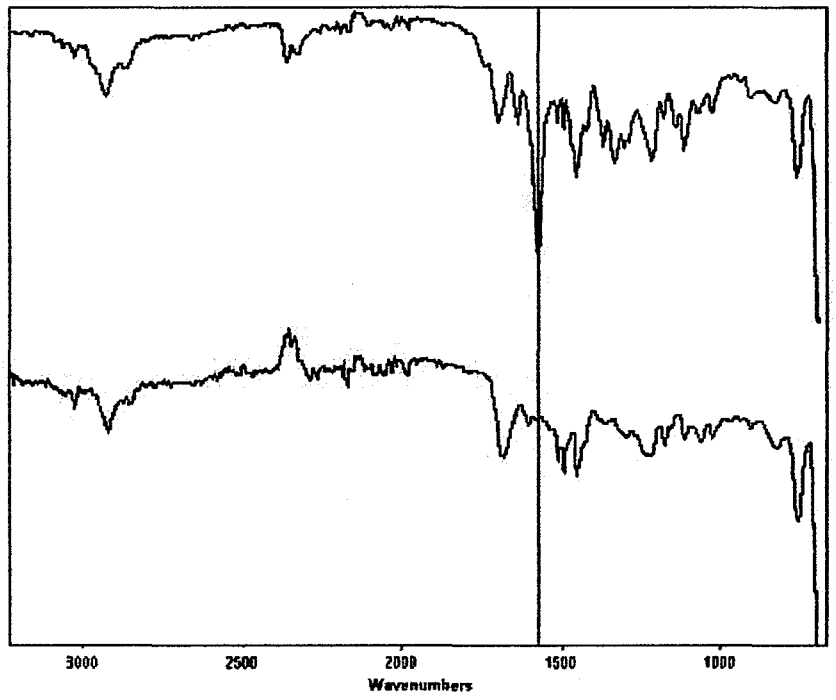

Figure 34: FT-IR spectra of Dde protected (top) and deprotected (bottom) **108**, showing loss of Dde group C=O signal at 1573 cm^{-1} (highlighted with red line).

The modified procedure utilized treatment with a cleavage cocktail consisting of TFA/thioanisole/ DCM/water (10:2:7:1) for 4 x 15 minutes, which furnished a mixture of the desired compounds **110**, **111** and **112** (Scheme 5). To ensure that cleavage from the resin was complete, a small portion of the resin was treated with the cleavage cocktail for a further hour. No further product cleavage was observed, indicating that the conditions were sufficient to effect total cleavage from the resin. The resin was washed with a large volume of MeOH after each treatment with the cleavage cocktail, to dilute the TFA and prevent further deprotection of the Pmc group as well as to maximise recovery from the resin. MeOH was used due to the poor solubility of the highly polar product **110** in organic solvents such as DCM. Due to the poor swelling properties of polystyrene resins in protic solvents, the resin was swollen in DCM after each wash cycle and prior to the

subsequent cleavage cycle. The combined washes were then concentrated *in vacuo*, the residue dissolved in a minimum amount of TFA and immediately precipitated with ice-cold ether. The resulting precipitate was collected by centrifugation and lyophilized.

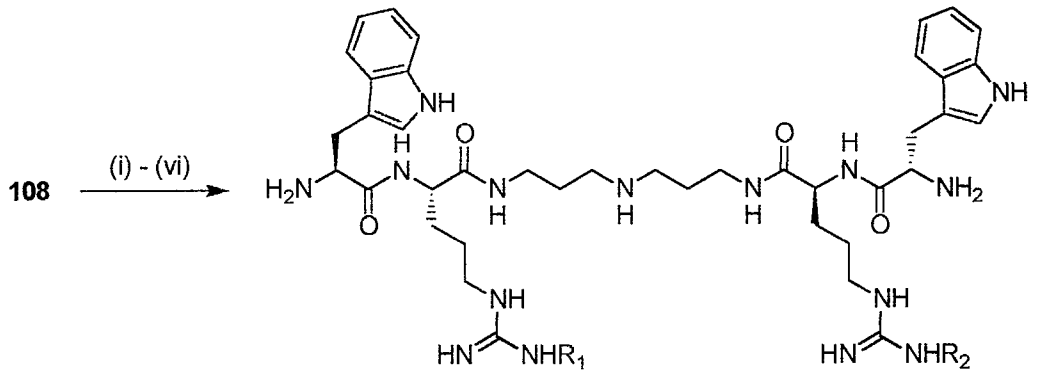

110 $R_1 = R_2 = H$ (7%)
111 R_1 = Pmc, $R_2 = H$ (5%)
112 $R_1 = R_2$ = Pmc (5%)

Scheme 5: Preparation of inhibitors **110-112**.

***Reagents and conditions*:** (i) 5% H_2NNH_2/DMF, 30 min. (ii) Fmoc-Arg(Pmc)-OH, HOBt, DIC, DCM/DMF (4:1), 2 hrs. (iii) 20% piperidine/DMF, 2 x 10 min. (iv) Boc-Trp(Boc)-OH, HOBt, DIC, DCM/ DMF (4:1), 2 hrs. (v) TFA/thioanisole/DCM/water (10:2:7:1), 4 x 15 min. (vi) semi-prep HPLC purification.

The modified cleavage conditions gave a mixture of the three desired compounds in similar quantities, as shown by analytical HPLC of the crude cleavage mixture (Figure 35), but in a fraction of the time of the reported procedure.

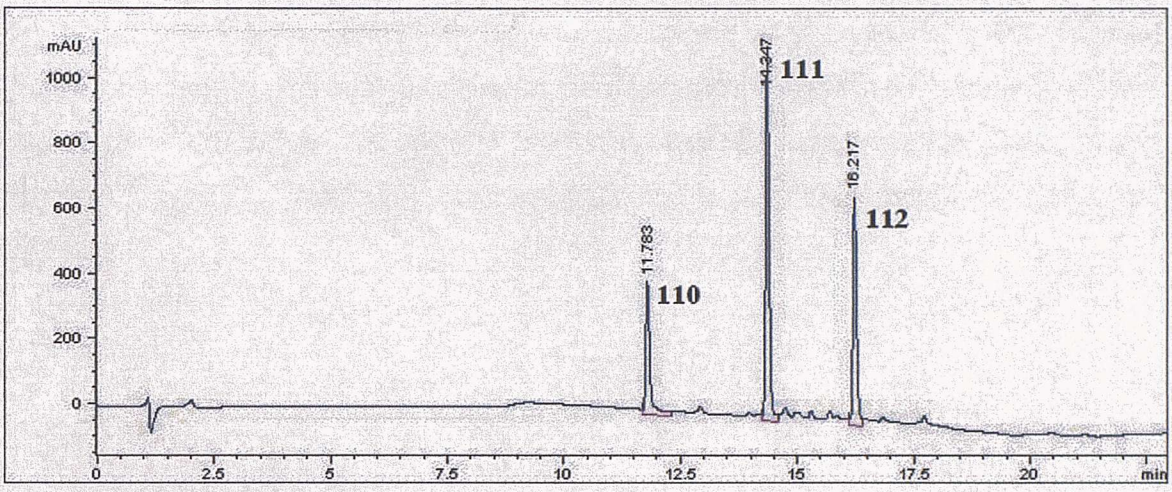

Figure 35: HPLC trace following cleavage from the resin to give the 3 desired products **110-112**.

The low yields of the three compounds resulted from poor recovery from semi-prep HPLC, a problem which was encountered with all compounds that were purified in this way.

2.3 Substrate Synthesis

Synthesis of the TR natural substrate trypanothione disulfide **13** and the norspermidine analogue nortrypanothione disulfide **115** was accomplished from resins **108** and **109** using the same procedure (Scheme 6). **115** is reported to be as good a substrate for TR as **13**,[87] and thus the use of **115** as a replacement for **13** was investigated as its use would allow the preparation of substrate and inhibitor from the same polyamine and eliminate the need to prepare both immobilised spermidine and norspermidine. Following Dde deprotection, standard solid-phase peptide chemistry was used to couple Fmoc-Gly-OH, Fmoc-Cys(Trt)-OH and Boc-Glu-O^{t}Bu to each arm of the polyamines to give resin-bound, fully protected nortrypanothione **113** and trypanothione **114**. Removal of the trityl group from the cysteine side chain and disulfide bond formation was achieved in one step upon treatment with a solution of iodine in DMF. Cleavage from the resin was accomplished by treatment with a cleavage cocktail consisting of TFA/thioanisole/DCM/water (16:2:1:1) for 2 hours.

HPLC analysis showed more than one species in the crude cleavage products (Figures 36 and 37). MS analysis showed the major species from each synthesis to have a mass corresponding to the desired disulfide, and the impurities to have masses corresponding to the dimer (and additionally in the case of trypanothione disulfide, the trimer).

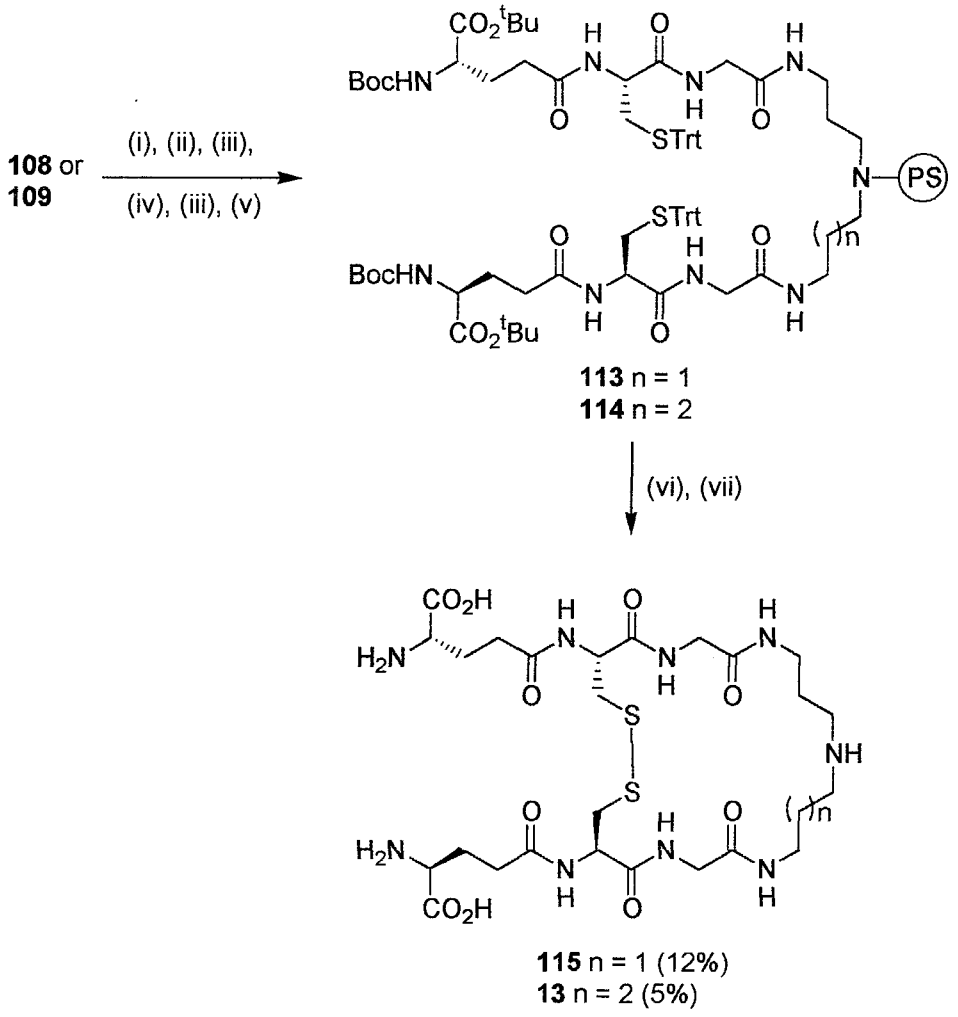

Scheme 6: Preparation of nortrypanothione disulfide **115** and trypanothione disulfide **13**.

***Reagents and conditions*:** (i) 5% H_2NNH_2/DMF, 30 min. (ii) Fmoc-Gly-OH, HOBt, DIC, DMF, 2 hrs. (iii) 20% piperidine/DMF, 2 x 10 min. (iv) Fmoc-Cys(Trt)-OH, HOBt, DIC, DCM/DMF (4:1), 2 hrs. (v) Boc-Glu-O^{t}Bu, HOBt, DIC, DCM/DMF (4:1), 2 hrs. (vi) I_2, DMF, 2 hr. (vii) TFA/thioanisole/DCM/water (16:2:1:1), 2 hrs. (viii) semi-prep HPLC purification.

It would appear that during disulfide bond formation, the resin bound compounds were of sufficient length to reach neighbouring sites on the resin and thus both inter- and intra-molecular disulfides were formed.

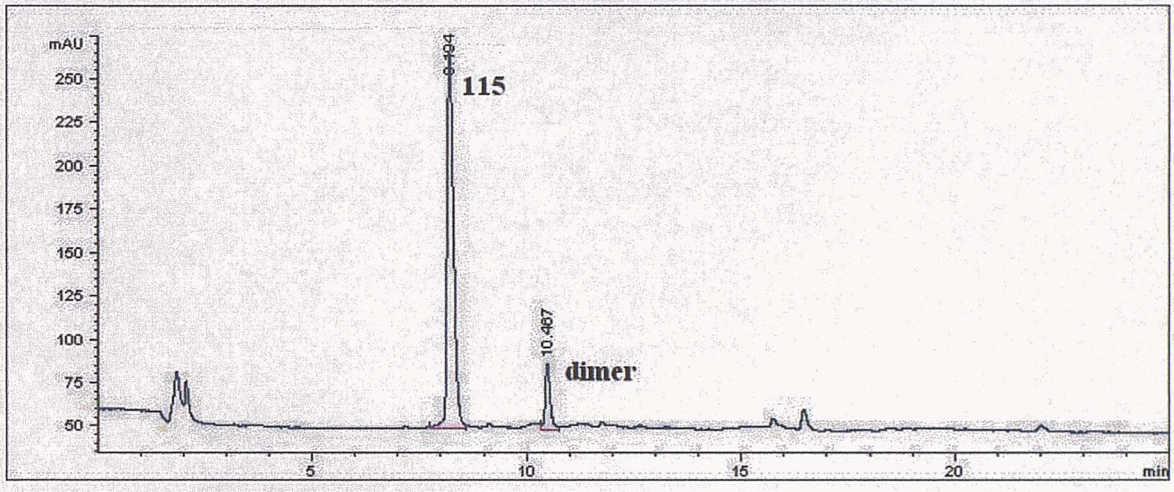

Figure 36: HPLC trace of crude nortrypanothione disulfide **115**.

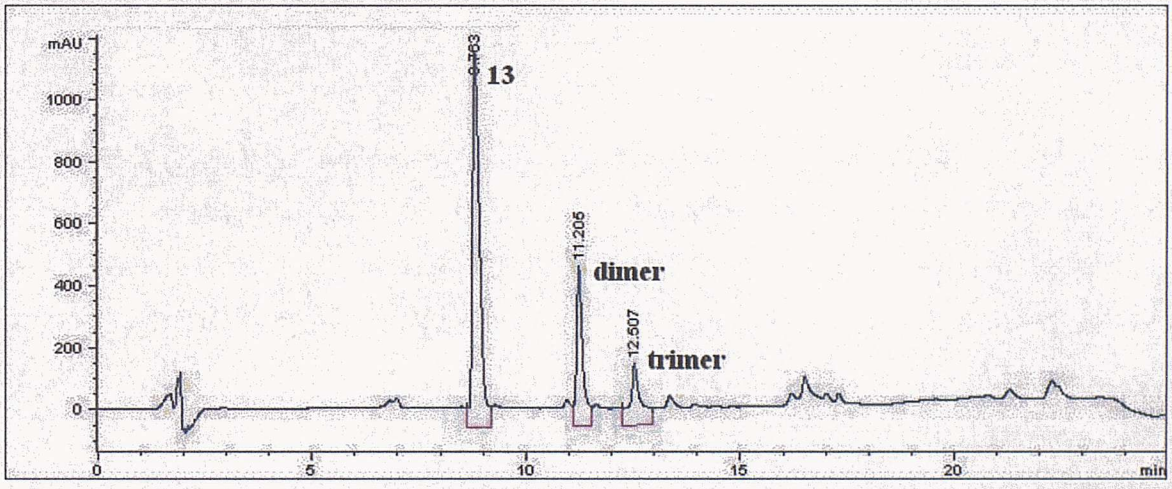

Figure 37: HPLC trace of crude trypanothione disulfide **13**.

Due to the poor recovery of **13** and **115** by HPLC, the more readily accesible alternative substrate **14** was also prepared. In a slight modification of the published procedure,[39] dimethylaminopropylamine was reacted with the symmetrical anhydride of Cbz-Gly-OH to give **117**, prior to removal of the Cbz group by hydrogenation and coupling to Cbz-Cys-OH disulfide using HOBt/DCC activation (Scheme 7).

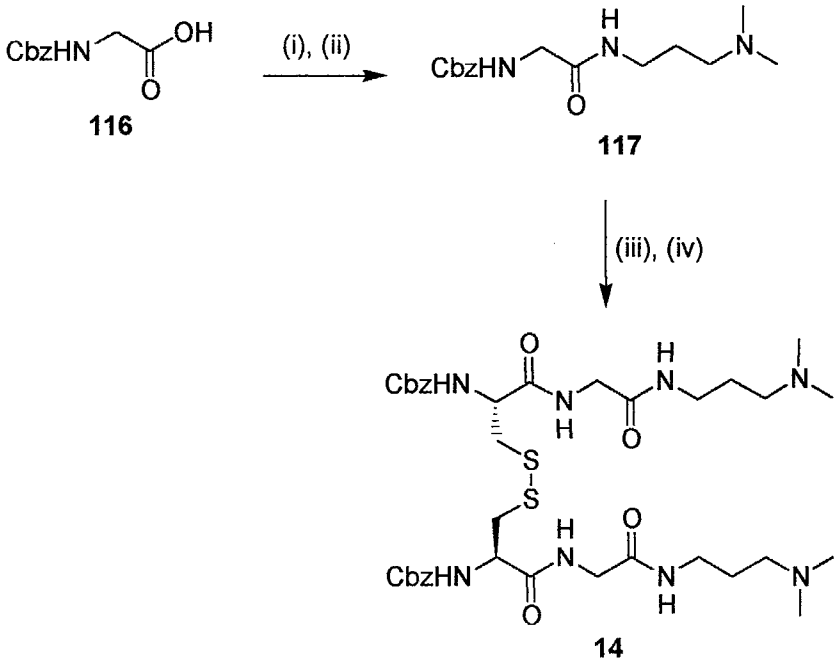

Scheme 7: Preparation of alternative substrate **14**.

***Reagents and conditions*:** (i) DCC, THF, 1 hr. (ii) Dimethylaminopropylamine, THF, 16 hrs, 67%. (iii) H_2, Pd-C, EtOH, 16 hrs, 95%. (iv) Cbz-Cys-OH disulfide, HOBt, DCC, DMF, 16 hrs, 38%.

2.4 Preparation and Purification of *T. Cruzi* Trypanothione Reductase

Over-expression of recombinant TR was achieved using BL21 DE3 *E. coli* bacteria that had been transformed with pIBITczTR.[34] The plasmid contained the *T. Cruzi* TR gene with a T7-RNA polymerase specific transcription promoter and a gene for ampicillin resistance. The bacteria contain a chromosomal copy of the T7-RNA polymerase gene under the control of the *lac* promoter. This polymerase transcribes the TR gene starting at a specific promoter and is induced by IPTG. The ampicillin resistance gene allows the bacteria to survive in the presence of the antibiotic ampicillin that kills contaminant bacteria.

The transformed cells were grown on a 5 L scale and yielded approximately 21 g of cells. Following sonication to lyse the cells, initial purification of the desired protein was achieved by ammonium sulfate precipitation. The protein was further purified by affinity chromatography using an adenine-2,5-diphosphate (ADP) agarose column. The ADP ligands have an affinity for the NADPH binding sites within TR and hence retain

the desired protein. Once unbound components had been washed from the column, bound components were eluted with a salt gradient. SDS-PAGE analysis of the protein at this stage revealed the presence of several small impurities, probably other NADPH dependent enzymes that were retained by the affinity column (Figure 38). These were separated from the desired protein by ion-exchange chromatography to give 10 mg of the pure enzyme (Figure 39).

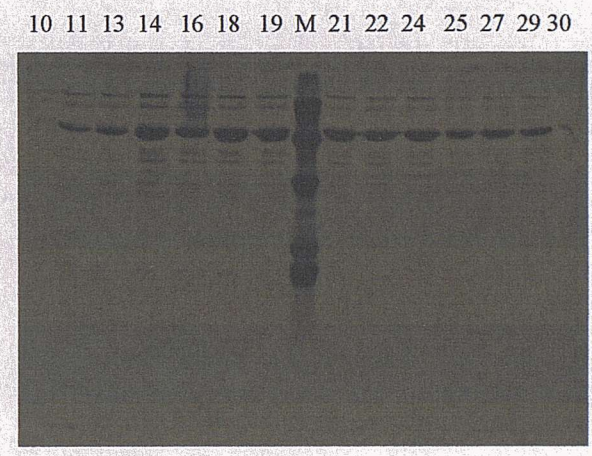

Figure 38: 15% SDS-PAGE gel of fractions 10-30 from affinity column and salt elution purification, with molecular weight markers (M).

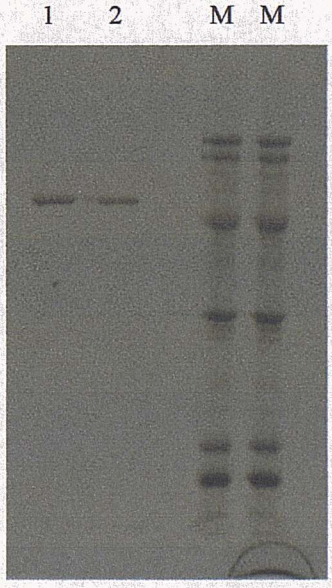

Figure 39: 12 % SDS-PAGE gel of purified TR (1 and 2) from ion-exchange chromatography with molecular weight markers (M).

With the inhibitors, substrates and enzyme in hand, investigation of the mechanism of inhibition began. Initial investigations focussed on the kinetic analysis of inhibition.

2.5 Introduction to Enzyme Kinetic Analysis

Enzyme kinetic analysis is the study of the factors influencing the rate of enzymatic reactions. These factors include enzyme concentration, ligand (substrates, products, inhibitors and activators) concentration, temperature, pH and ionic strength, and allow a great deal of information regarding the enzyme-catalysed reaction to be determined. For example, the effect of pH can reveal information about the amino-acid residues present in the active site, and the kinetic mechanism (the order in which substrates bind and products leave) can be deduced by varying the substrate and product concentrations. Of particular interest to this project, the effect of an inhibitor on enzyme kinetics can provide information regarding the binding sites of the inhibitor on the enzyme.

Enzyme kinetic analysis is performed under conditions where the concentration of enzyme is negliable in comparison with that of the substrate and the initial rate of reaction, involving only the first few percent of product formation, is measured. This ensures the concentration of substrate and product are not appreciably altered during the experiment. In most cases it is found that the initial rate of reaction is directly proportional to enzyme concentration but displays saturation kinetics with respect to the substrate concentration. This means that at low concentrations of substrate, the initial rate increases linearly with substrate concentration. However, at higher substrate concentrations, this relationship breaks down and the initial rate increases less rapidly than the substrate concentration. At sufficiently high (or saturating) substrate concentrations, the initial rate approaches a limiting value termed V_{max}. The substrate concentration that produces a rate equal to $0.5V_{max}$ is designated the Michaelis-Menten constant (K_m) and is an inverse measure of the affinity of the enzyme for the substrate (i.e. the lower the K_m, the greater the affinity between substrate and enzyme and the lower the [S] needed to achieve a given v).

In the case of competitive inhibition, the inhibitor and substrate bind at the same site on the enzyme. In the prescence of such an inhibitor, a higher [S] is required to achieve the same velocities as in the absence of inhibitor, so while V_{max} is unchanged, $0.5V_{max}$ requires a higher [S] than before and hence the effective K_m is larger. In the case of non-competitive inhibition, inhibitor and substrate bind at different sites and hence the effect of inhibitor cannot be overcome by increasing the [S]. V_{max} is therefore reduced but K_m is unchanged as the active site of the enzyme molecules are not full of inhibitor.

There are many different diagnostic plots available for displaying kinetic data, but two of the most commonly used are the double recipricol, Lineweaver-Burke or Eadie-Hofstee plot. These plots give a characteristic appearance depending on the type of inhibition exhibited (Figure 40 and 41). The Lineweaver-Burke plot has the disadvantage of compressing data points at high [S] and overemphasizes the data points at low [S], as well as magnifying small errors in the measurement of v. These errors tend to be most significant at low [S] values, where one or two "bad" points can markedly change the slope of the plot. The Eadie-Hofstee plot does not compress the higher values and is generally considered superior. Both plots were utilised for all the kinetic analyses in this project.

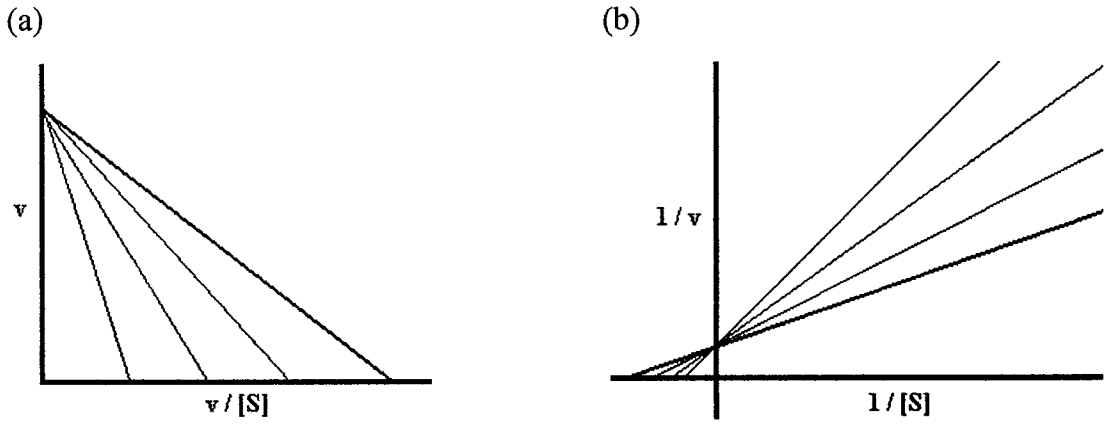

Figure 40: (a) Eadie-Hofstee plot and (b) Lineweaver-Burke plot of typical competitive inhibition (reaction in absence of inhibitor shown in bold).

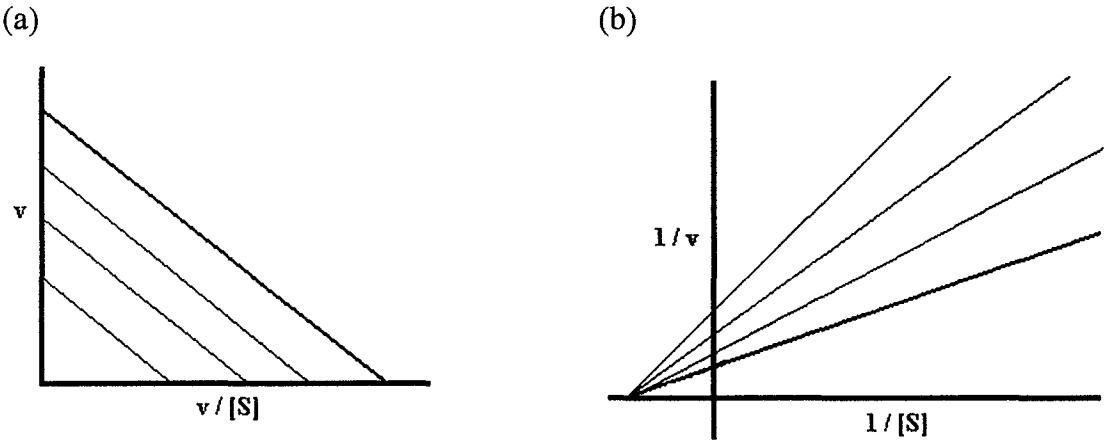

Figure 41: (a) Eadie-Hofstee plot and (b) Lineweaver-Burke plot of typical non-competitive inhibition (reaction in absence of inhibitor shown in bold).

2.6 Determination of Kinetic Parameters of Substrates and Trypanothione Reductase

The K_m was determined for each of the three substrates by measurement of the initial rate of reaction at various concentrations of substrate. NADPH has a characteristic UV absorbance (λ_{max} = 340 nm) that provides a convenient method for monitoring NADPH-dependent enzymatic reactions. The assays were performed in triplicate and analysed using non-linear regression with the aid of the program Grafit (Erithacus Software Ltd). The resulting graphs are shown in Figures 42-44. The respective K_m values obtained were 17 +/- 1 μM (nortrypanothione disulfide, literature value = 28 μM),[87] 55 +/- 5 μM (trypanothione disulfide, literature value = 50 μM)[39] and 27 +/- 3 μM (CbZ-Cys-Gly-DMAPA disulfide, literature value = 24 μM).[39]

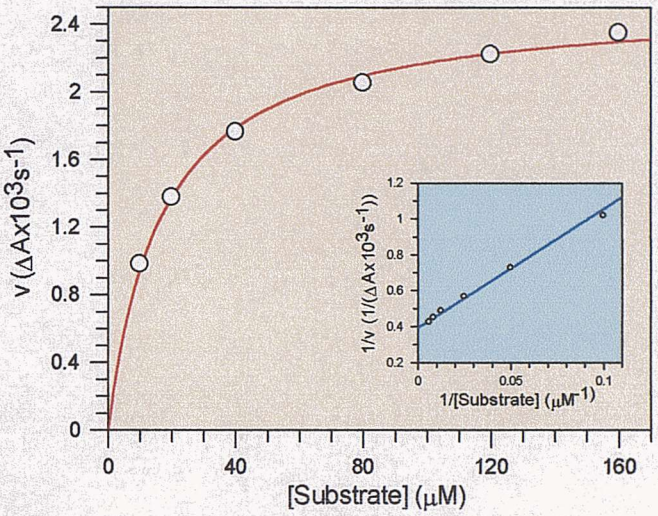

Figure 42: Plot of initial rate versus nortrypanothione disulfide **115** concentration and resulting Lineweaver-Burke plot (inset). K_m = 17 +/- 1 μM.

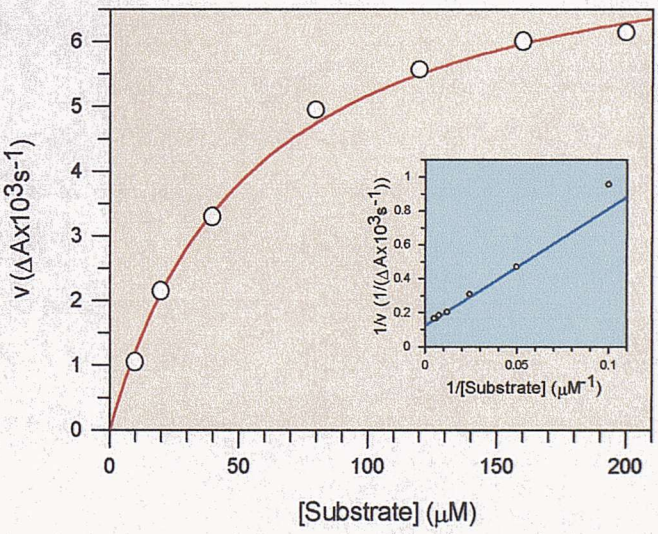

Figure 43: Plot of initial rate versus trypanothione disulfide **13** concentration and resulting Lineweaver-Burke plot (inset). K_m = 55 +/- 5 μM.

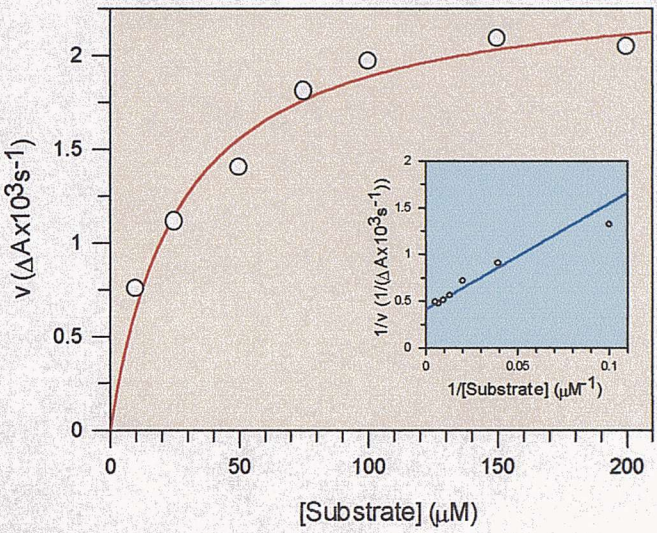

Figure 44: Plot of initial rate versus alternative substrate **14** concentration and resulting Lineweaver-Burke plot (inset). K_m = 27 +/- 3 μM.

2.7 Kinetic Analysis of Inhibition

Enzyme kinetic analysis of **110-112** was performed to determine the inhibition constants K_i and the nature of inhibition with respect to the disulfide substrate. Initial rates were recorded using various concentrations of nortrypanothione as substrate, in the absence of inhibitor and at three concentrations of inhibitor (estimated to be 0.5, 1 and 2 x K_i). The nature of inhibition was deduced from the resulting Lineweaver-Burke and Eadie-Hofstee plots (Figures 45-47) and the K_i values determined by non-linear regression with the aid of the program Grafit.

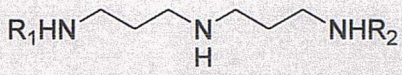

110 $R_1 = R_2$ = Trp-Arg

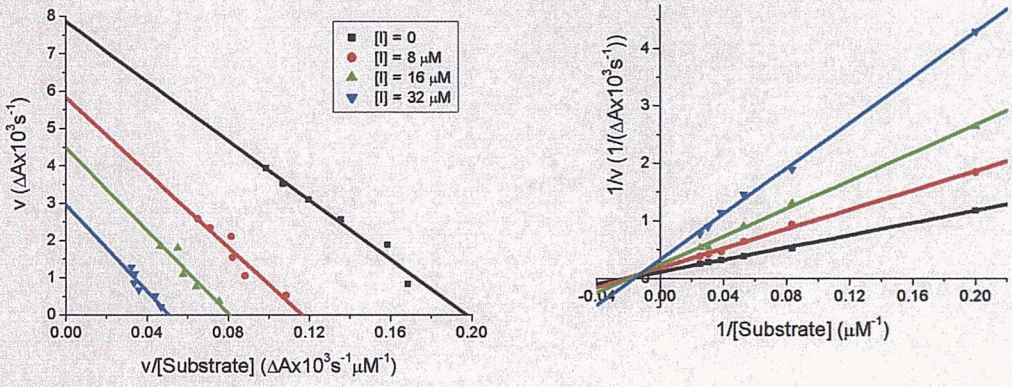

Figure 45: Inhibitor **110** - non-competitive behaviour (K_i = 14.3 +/- 0.5 μM).

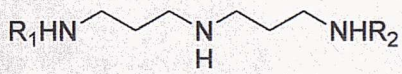

111 R_1 = Trp-Arg
R_2 = Trp-Arg(Pmc)

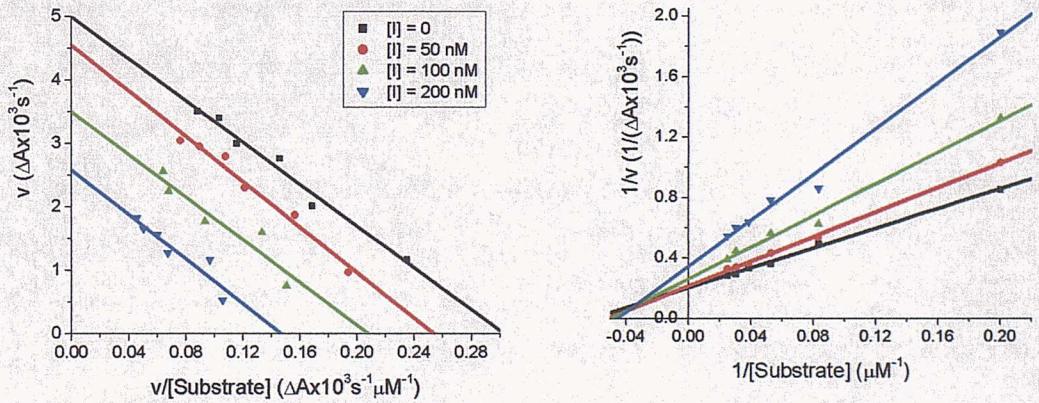

Figure 46: Inhibitor **111** - non-competitive behaviour (K_i = 220 +/- 15 nM).

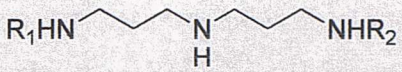

112 $R_1 = R_2$ = Trp-Arg(Pmc)

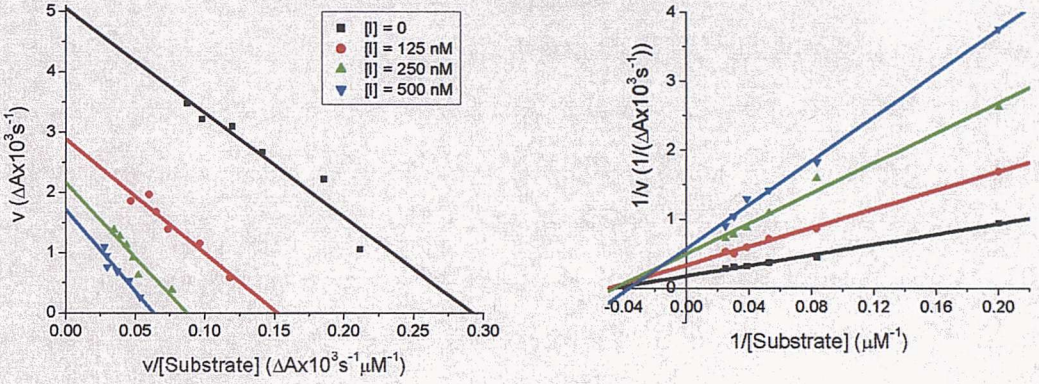

Figure 47: Inhibitor **112** - non-competitive behaviour (K_i = 160 +/- 8 nM).

As with the spermidine compounds **89-91**, all three compounds exhibited non-competitive inhibition with respect to the disulfide substrate. The K_i values obtained were also in close agreement with those reported for **89-91**, with the Pmc-containing compounds **111** and **112** having significantly greater activity than the fully deprotected compound **110**. The measured K_i of **110** was 14.3 +/- 0.5 μM (compared with 16 μM for the spermidine analogue, **89**), **111** was 220 nM +/– 15 (100 nM for **90**) and **112** was 160 +/-8 nM (190 nM for **91**). These results confirmed that changing the polyamine backbone from spermidine to norspermidine had little effect on the biological properties of the inhibitors. These assays were also performed with trypanothione disulfide as substrate, from which near identical results were obtained. Satisfied that **115** was therefore a suitable substitute for **13**, it was used for all subsequent analyses.

The nature of inhibition with respect to NADPH was also investigated, but this proved far more challenging than with the disulfide substrate due to problems with the sensitivity of the assay. Substrate concentrations in the region of the K_m are necessary for these assays, and the K_m for NADPH is low (reported to be 5 μM).[88] An unacceptably low signal to noise ratio resulted from assays at the lower NADPH concentrations, making determination of initial rate impossible. In an attempt to improve the signal to

noise ratio, a UV cell with an increased path length of 4 cm was used in the experiments. Unfortunately, the four-fold increase in sensitivity this provided proved to be not enough to overcome the problem, and the increased volume of the assay had the added drawback of increasing the consumption of inhibitor and substrate.

The problem was overcome by monitoring the consumption of NADPH by fluorescence rather than UV absorbance, as NADPH has fluorescent properties with λ_{ex} at 340 nm and λ_{em} at 460 nm. The increase in sensitivity this provided was sufficient for the kinetic assay to be performed. It is important that the concentration of the disulfide substrate changes as little as possible during the assay and therefore a large excess was required for this experiment. Due to this, the alternative substrate **14** was used rather than the more precious substrates trypanothione disulfide **13** or nortrypanothione disulfide **115**. As the assay was investigating the relationship of the inhibitor with NADPH, the nature of the disulfide substrate should have little effect on the outcome of the experiment.

The results of the kinetic analysis of **111** showed non-competitive behaviour with respect to NADPH with a measured K_i of 88.1 +/- 3.3 nM (Figure 48). This result is perhaps not surprising if the structures of NADPH and the inhibitor are considered. Although there are some structural similarities (both contain aromatic moieties, for example), NADPH has a net negative charge and its binding pocket within TR has a corresponding positive charge. The inhibitors are positively charged at physiological pH and therefore are unlikely to bind within the positively charged NADPH pocket. Due to the difficult nature of performing the NADPH kinetics, only **111** was analysed in this way.

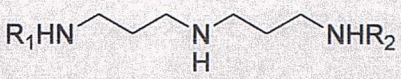

111 R_1 = Trp-Arg
R_2 = Trp-Arg(Pmc)

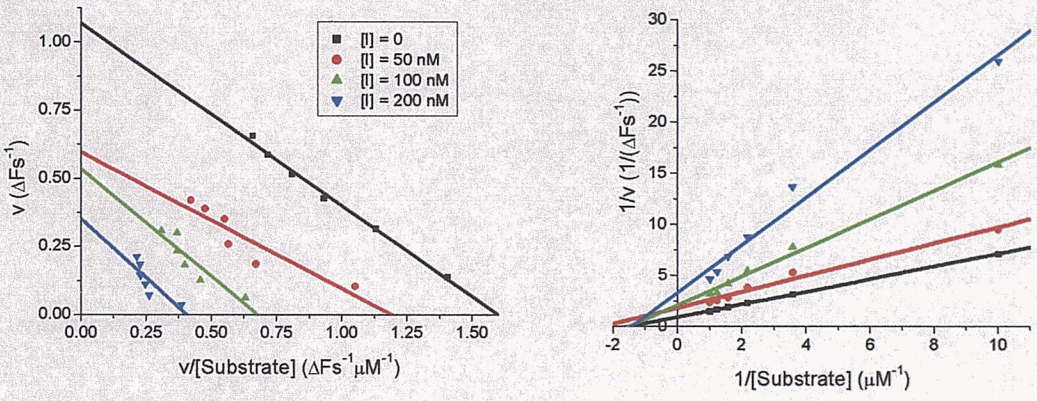

Figure 48: Inhibitor **111** - non-competitive behaviour with NADPH as variable substrate (K_i = 88.1 +/- 3.3 nM).

2.8 Assay against Glutamate Dehydrogenase

As an alternative assay for binding in the NADPH pocket and to confirm the findings of the NADPH kinetics, **110-112** were screened for activity against glutamate dehydrogenase. Glutamate dehydrogenase is an NADPH dependent enzyme that links amino acid metabolism and tricarboxylic acid (TCA) cycle activity, catalysing the interconversion of α-ketoglutarate, ammonium ions and glutamate (Figure 49).[89]

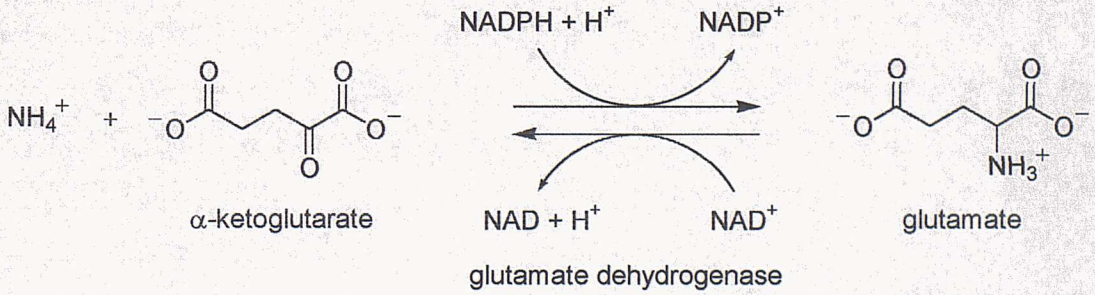

Figure 49: Action of glutamate dehydrogenase.

The forward reaction is important for converting free ammonia and α-ketoglutarate into glutamate, one of the 20 naturally occurring α-amino acids used in protein synthesis and a principal amino donor in the biosynthesis of other amino-acids. The reverse reaction is involved in energy metabolism, as α-ketoglutarate is a key intermediate in the TCA cycle.

Although TR and GDH are unrelated enzymes, the NADPH binding sites are similar in both and it is reasonable to expect a nanomolar inhibitor that binds in the NADPH active site of one enzyme might also bind in the NADPH active site of the other.

The three inhibitors were screened against GDH at a concentration of 100 μM, but no activity was observed, supporting the findings of the NADPH kinetic analysis with **111**.

2.9 Aggregation Inhibitors

The use of high-throughput screening is common in the search for novel lead compounds.[90-92] Such screens have identified a number of "hits" which upon closer inspection show unusual, undesirable behaviour such as non-competitive inhibition with little relationship between structure and activity and poor target selectivity.[93,94] A recent study looking at the mechanism of action of 45 such compounds produced some startling results.[47] Of the 45 compounds investigated, 35 showed activity against enzymes unrelated to their original target. These 35 compounds also exhibited reversible, time dependent inhibition which was greatly attenuated by albumin, guanidium or urea. Additionaly, it was found that a 10-fold increase in enzyme concentration largely eliminated inhibition despite a 1000-fold excess of inhibitor.

This behaviour was explained by the formation of aggregates comprised of many individual inhibitor molecules. Such aggregates were observed by light scattering and electron microscopy experiments and were found to be between 30 and 400 nm in diameter. Electron microscope images of tetraiodophenolphthalein and Congo Red, two of the inhibitors investigated, show this aggregation behaviour (images A-D, Figure 50) whereas the competitive, well behaved inhibitor 8-anilino-1-naphthalene-sulfonic acid (ANS) showed no such aggregates (image E, Figure 50).

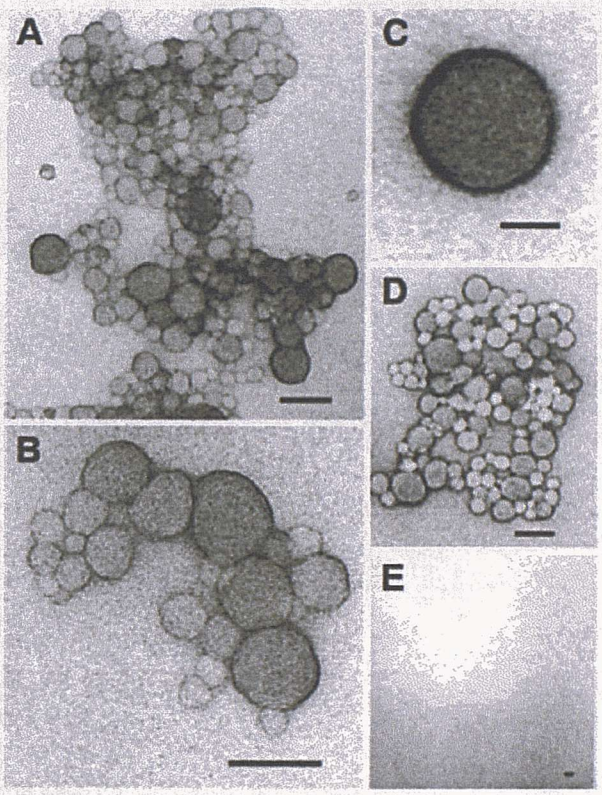

Figure 50: "Aggregation inhibitors" visualised by transmission electron microscopy: A-C: 100 μM tetraiodophenolphthalein in 20 mM Tris; D: 50 μM Congo Red in 20 mM Tris; E: 625 μM ANS (negative control) in 20 mM Tris. Bar = 100 nm (reproduced with permission).

Given the non-competitive nature of inhibition by **110-112**, the possibilty that this was the mechanism of action was investigated. Characteristically, and in contrast to well-behaved inhibitors, aggregation inhibitors exhibited a significant reduction in activity upon a moderate increase in the concentration of target enzyme. Of the reported aggregation inhibitors, an increase in IC_{50} of between 4- and 50-fold was observed when the concentration of β-lactamase was increased 10-fold from 1 to 10 nM, whereas a competitive, reversible inhibitor was unaffected by this change in enzyme concentration, as expected for Michaelis-Menten kinetics. The extreme sensitivity of aggregation inhibitors to enzyme concentration could be explained by the fact that, due to the number of inhibitor molecules involved in each aggregate, the aggregates are saturated with enzyme.

The effect of enzyme concentration on the inhibition of TR by **111** was measured at three concentrations of inhibitor (125, 250 and 500 nM) at an enzyme concentration of 1.1 and 11 nM (Table 1). A slight decrease in inhibition was observed at the higher enzyme concentration with all three inhibitor concentrations (approx. 10%), but this was a fraction of the change reported with the aggregation inhibitors.

[TR] (nM)	% Inhibition at specified [**111**] (nM)		
	125	250	500
1.1	29	44	52
11	41	54	66

Table 1: Efffect of TR concentration on inhibition with **111**.

The reported aggregation inhibitors also showed activity with a number of different enzymes. The lack of activity displayed by **110-112** against glutamate dehydrogenase was further evidence that a different mechanism of action was at work with these compounds.

2.10 Dimerisation Inhibitors

TR exists as a homo-dimer, the disulfide active site contains residues from both enzyme sub-units and the monomer form is therefore inactive. An alternative mechanism of action involves the disruption of the TR dimer, possibly by binding of the inhibitor in the interface region between the two enzyme sub-units leading to inactivation of the enzyme. This type of inhibition, termed dimerisation inhibition, has been reported for HIV-1 protease and nitric oxide synthase.[95-99] Analytical ultracentrifugation (AUC) and gel filtration chromatography analysis of trypanothione reductase in the presence and absence of the inhibitor was undertaken to investigate this possibility. If indeed this was the mechanism of action, a shift in the equilibrium towards the monomer should be apparent in the presence of the inhibitor.

2.10.1 Ultracentrifugation Analysis of Inhibition

Analytical ultracentrifugation is a technique used in the study of the behaviour of macromolecules in solution when exposed to centrifugal forces. The technique was first developed in the 1920's and allows the thermodynamic and hydrodynamic characterisation of macromolecules in solution without interaction with any surface or matrix, as is the case with techniques such as gel filtration chromatography or electrophoresis. The instrument consists of a centrifuge coupled to a detection system to measure the concentration distribution of the sample, usually by measurement of the UV absorbance or Rayleigh scattering.

Two types of experiment can be performed using the technique. In sedimentation velocity experiments, the sample is exposed to very high centrifugal forces that cause sedimentation of the solute towards the bottom of the cell. The rate of this sedimentation gives the sedimentation coefficient and the experiment is useful for determining mass, density and shape of the macromolecule. In equilibrium sedimentation experiments, the sample is exposed to a lower centrifugal force. Equilibrium between sedimentation and diffusion of the solute is established and a concentration gradient across the cell is formed. Analysis of this gradient provides information on the mass of the species independent of its shape and is particularly useful for the determination of stoichiometry of a macro-molecular complex. Trypanothione reductase was therefore analysed using equilibrium sedimentation in the presence and absence of **110-112** to see if there was any change in the relative amounts of monomer and dimer. These experiments were performed by Dr. Andrew Leech at the University of York.

A wavelength of 280 nm was chosen for the experiments, as this corresponds to the λ_{max} for TR and required the least amount of the enzyme. A TR concentration of 0.4 mg/mL (7.4 μM) gave the optimum absorbance of 0.4, and an inhibitor concentration of 5 x K_i was chosen to ensure that in the case of dimerisation inhibition, the equilibrium would lie on the monomer side and the effect would therefore be easily observable. As 5 x K_i for **111** and **112** would be sub-stoichiometric with respect to TR, a concentration of 15 μM (2 x [TR]) was chosen for these samples. The absorbance of the inhibitors at their experimental concentration was found to be negligible. The samples were run against blanks which were identical in composition except they did not contain any enzyme. The

run was performed twice, initially with a rotor speed of 8 K RPM and then at 12 K RPM, over 24 hours to allow equilibrium prior to data accumulation, to give the results summarised in Table 2.

Sample (conc.)	Observed mass (KDa)	Species	% error from lit value (107.8 kDa)
TR	104.3	Dimer	-3.2
TR + **110** (70 μM)	110.3	Dimer	+2.4
TR + **111** (15 μM)	111.8	Dimer	+3.7
TR + **112** (15 μM)	101.5	Dimer	-5.8

Table 2: Results from AUC analysis of TR.

In the absence of inhibitor, the molecular mass of enzyme was determined to be 104.3 kDa, which is in good agreement with the reported molecular mass of TR dimer (107.8 kDa).[100] No significant change in the mass of the enzyme was observed in the presence of either **110**, **111** or **112**, and the values obtained were all in good agreement with the reported molecular mass of the TR dimer. The results clearly show that **110-112** do not cause a change in the stoichiometry of the enzyme.

2.10.2 Gel Filtration Chromatography Analysis of Inhibition

Gel filtration is a simple, reliable technique that has found widespread use in the purification and analysis of enzymes, polysaccharides, nucleic acids and other biological macromolecules, and provides a means of determining the molecular weight of proteins.[101] This technique was used to analyse the inhibitor:enzyme complexes to confirm the findings of the AUC experiments.

In gel filtration, molecules in solution are separated according to differences in their size as they pass through a column packed with a chromatographic gel. The gel contains pores of a carefully controlled size made from an inert matrix that is chemically and physically stable so as to minimise interactions between the sample and the matrix, and are formed by crosslinking polymers (such as dextran or agarose) to form a three-

dimensional network. The properties of the gel are dependent on the degree of cross-linking as well as the nature of the polymer.

The pores in the gel matrix are of a similar size to the molecules in the sample. Molecules that are small relative to the pores can diffuse inside the gel matrix whereas molecules that are relatively large are restricted from diffusing into the gel to the same degree. Therefore, when a sample containing a mixture of molecules of different sizes is passed through a gel filtration column, the smaller molecules that diffuse inside the gel matrix are delayed in their passage through the column relative to larger molecules that cannot diffuse so freely inside the matrix. The largest molecules thus elute from the column first followed by the smaller molecules, in order of decreasing size.

The technique can be used to determine the molecular weight of proteins by first calibrating the column with a number of standard proteins of varying mass. The mass of an unknown sample can then be determined from its retention time on the column.

A column packed with Sephadex G-200, a polymer consisting of dextran chains cross-linked with epichlorohydrin, was used for the analysis of TR in the presence and absence of inhibitor. The column was calibrated by analysing six protein standards of molecular weight ranging from 17 to 2000 KDa. A plot of retention time against Log_{10}Mwt gave good correlation (Figure 51).

TR was then analysed under the same conditions and was found to have a retention time of 25.0 minutes, equating to a molecular weight of 103.0 KDa, which was in broad agreement with the literature value for the dimer (107.8 KDa).[100] The column was then equilibrated with buffer containing the inhibitor (10 μM) and the calibration repeated. The protein standards gave almost identical retention times in the presence of inhibitor as with buffer alone. Analysis of a sample of TR that had been incubated with inhibitor for 30 minutes found it to have a retention time of 24.7 minutes, almost identical to the value in the absence of inhibitor (Figure 52).

(a) (b)

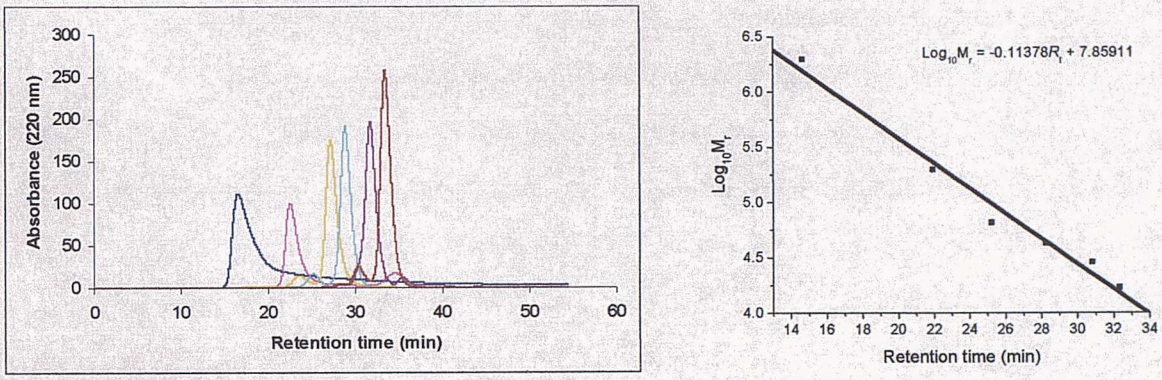

Figure 51: (a) Gel filtration analysis of protein standards for (b) column calibration.

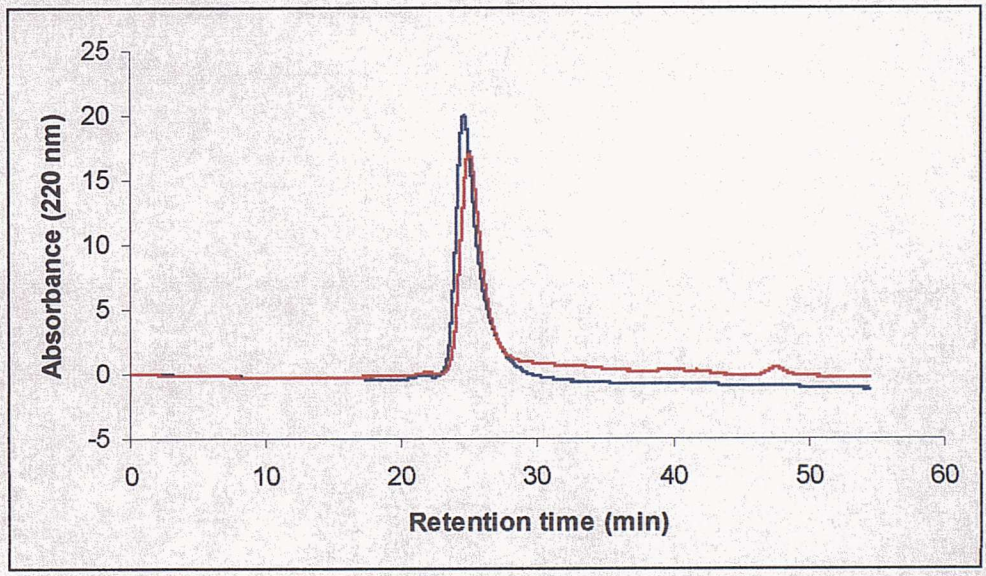

Figure 52: Gel Filtration analysis of TR in absence (red) and presence (blue) of inhibitor **111**.

The findings of the gel filtration studies were in agreement with the AUC results and showed that inhibition was not caused by binding in the interface region leading to disruption of the dimer. The results of both the AUC and gel filtration studies are also further evidence that no aggregation of the enzyme is taking place as no high mass species were observed by either technique.

2.11 Protein X-Ray Crystallography Studies

X-ray crystallography was utilised to probe the enzyme-inhibitor complex in collaboration with Dr. Mark Montgomery working in the laboratory of Professor Steve Wood. Co-crystallisation of TR with **111** was attempted using crystal screening kits (Molecular Dimensions Inc, Soham, UK) to obtain suitable crystallisation conditions. Each co-crystal was grown by the hanging drop vapour diffusion method at room temperature. The best crystals were obtained with 0.1 M HEPES pH 7.5 and 20% w/v PEG 10000 (Figure 53). Data to 3.1 Å were collected at 100 K on beamline ID14-2 (λ = 0.933Å) at the European Synchrotron Radiation Facility (Grenoble, France) with an ADSC CCD detector. The space group was determined to be tetragonal $P4_3$ with unit cell dimensions a = b = 87.624 and c = 153.510. The asymmetric unit contains two TR monomers and the solvent content of the crystals was estimated at 56%.[102] However, owing to the low resolution of the structure, electron density for the ligand remained uninterpretable.

(a) (b)

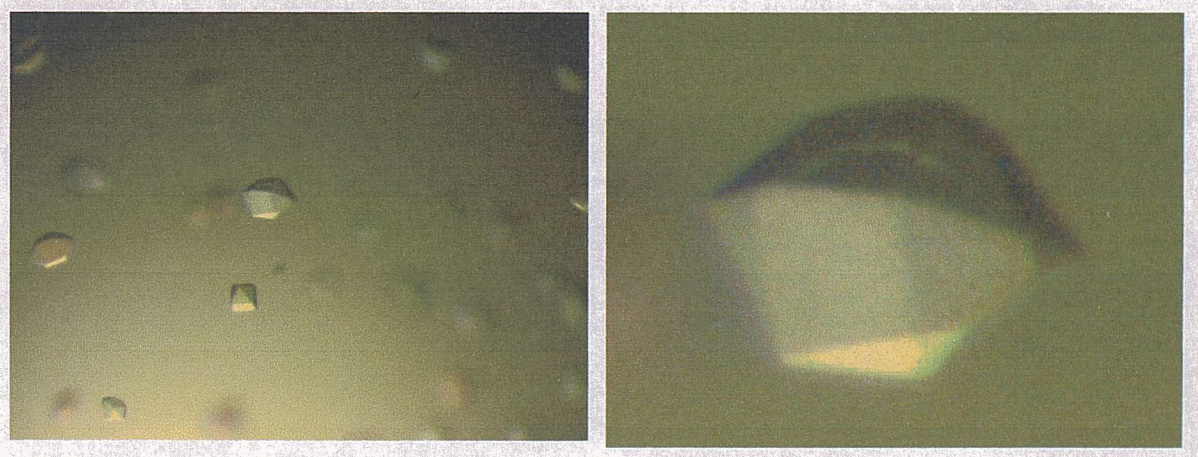

Figure 53: (a) TR crystal shower. (b) Close up of a single TR crystal.

The structure of the homodimer from the acquired data is shown in Figure 54, where the residues depicted as ball and stick structures are the two FAD residues, included to aid with orientation.The NADPH binding cavity of sub-unit A is clearly visible above the tricyclic isoalloxazine ring of FAD, whilst the trypanothione disulfide

binding cavity is situated on the opposite face of the isoalloxazine ring. As previously mentioned, the trypanothione disulfide binding cavity contains residues from both sub-units of the dimer, and the portion of sub-unit B that interacts with the trypanothione disulfide binding cavity of sub-unit A is clearly visible below the isoalloxazine ring.

The active site, with key residues depicted as ball and stick structures, is shown in Figure 55. Phe_{199} (A) forms a 'flap' over the NADPH pocket that folds out of the way to allow binding. The isoalloxazine ring of FAD (B) is located on top of the NADPH binding cavity whilst the rest of the FAD molecule points away from the active site with part of the adenine ring (C) visible to the right of the diagram. Just above the isoalloxazine ring, the active site disulfide bridge between Cys_{53} and Cys_{58} is visible (D). The trypanothione disulfide binding pocket is situated above the disulfide bridge and includes residues from both sub-units. Two such residues, $His_{461'}$ (E) and $Glu_{466'}$ (F), are involved in the catalytic cycle.

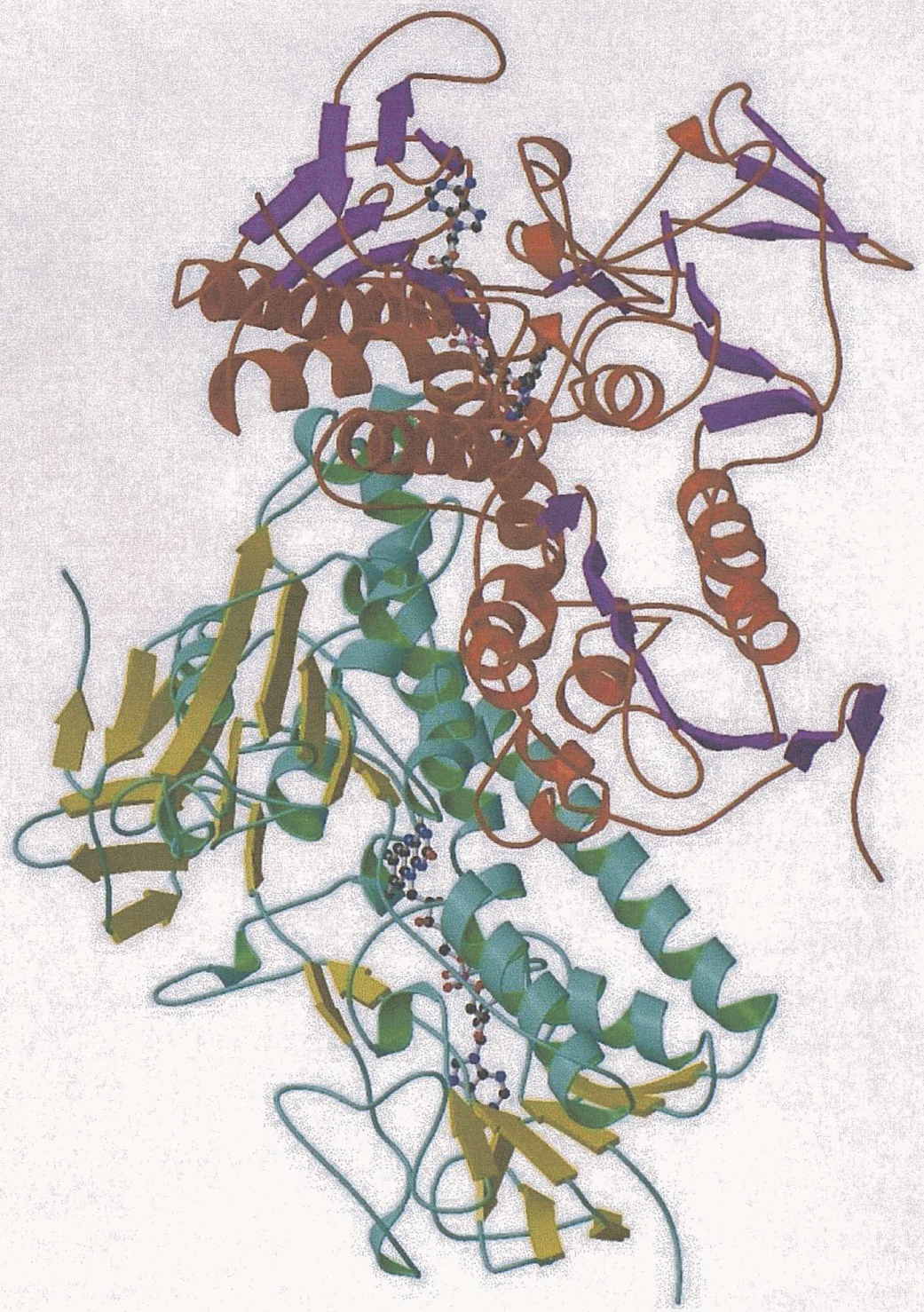

Figure 54: TR homodimer from crystal structure. β-sheets are depicted in yellow (sub-unit A) and purple (sub-unit B), α-helixes in turquoise (sub-unit A) and orange (sub-unit B). FAD is depicted in ball and stick to aid with orientation.

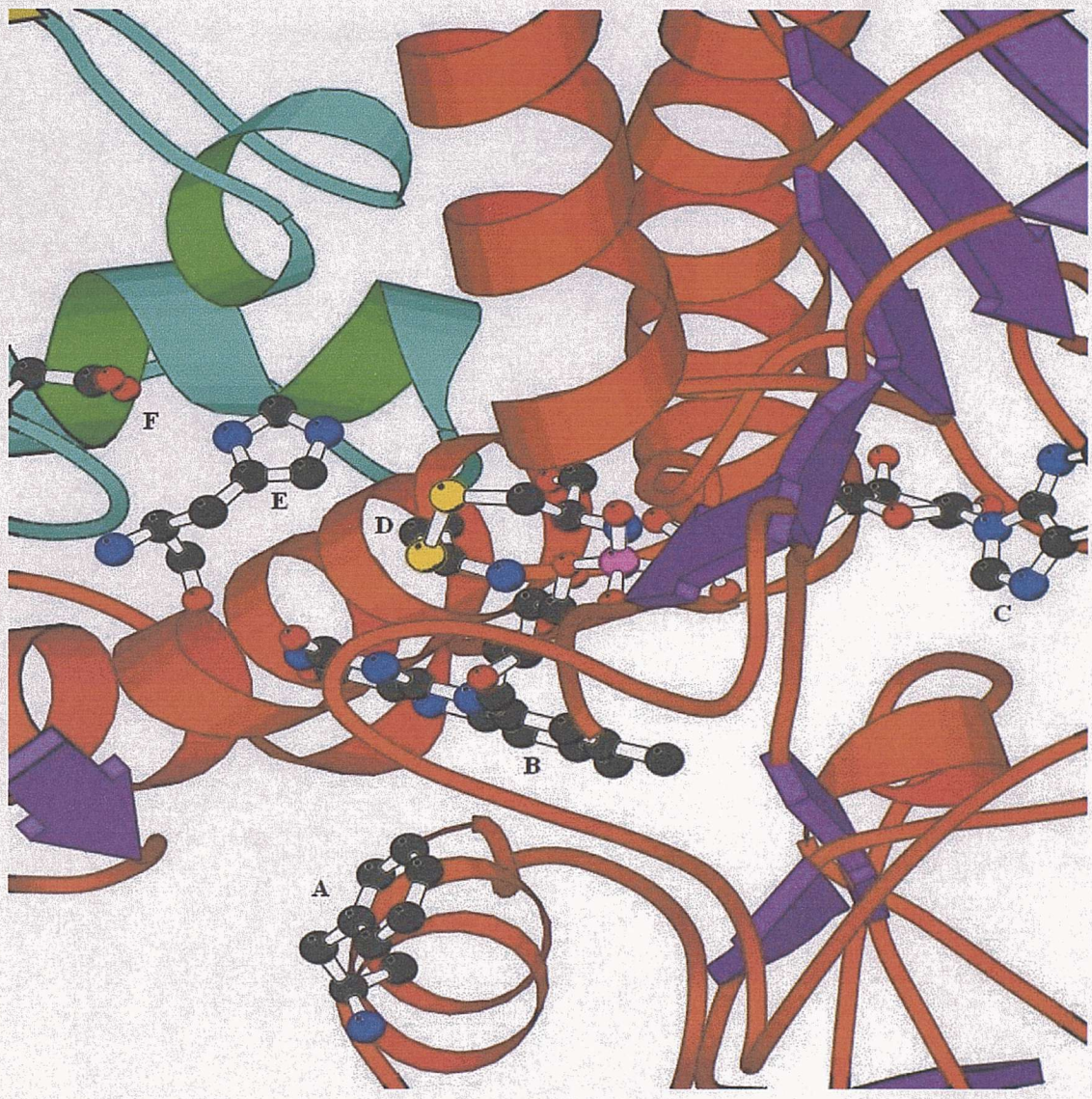

Figure 55: TR active site from crystal structure. The residues depicted in ball and stick are Phe_{199}, Cys_{53}, Cys_{58} and FAD of one sub-unit of the dimer, and $His_{461'}$ and $Glu_{466'}$ of the other sub-unit of the dimer (residues 325-360 removed for clarity).

2.12 Conclusions

The results reported in this chapter provide significant evidence for the mechanism of action of the lead compounds **110-112**. Kinetic analysis confirmed the non-competitive nature of inhibition with respect to both enzyme substrates. Further evidence for the non-competitive behaviour with respect to NADPH was obtained from the assay against glutamate dehydrogenase. The retention of activity upon a ten-fold concentration of enzyme, together with the observed specificity for TR, eliminated the

possibility of an aggregation mechanism. Inhibition *via* disruption of enzyme dimerisation was disproved by AUC and gel filtration analysis, which provided further evidence that no enzyme aggregation was taking place. Presumably, the inhibition occurs *via* an allosteric mechanism, whereby binding of the inhibitors at a site remote from either the disulfide or NADPH active sites or the dimer-interface region leads to a conformational change in the enzyme, modulating the active site.

CHAPTER 3

EXPLORING THE RELATIONSHIP BETWEEN STRUCTURE AND ACTIVITY

Having established the mechanism of action of the lead compounds **110-112**, the relationship between structure and activity was probed to aid the development of more potent inhibitors, aiming to identify key structural features necessary for activity and simplifying the relatively large lead compounds into smaller, more drug-like structures.

3.1 Library Design

Several structural elements were identified within the lead compounds capable of different binding interactions with the target enzyme (Figure 56).

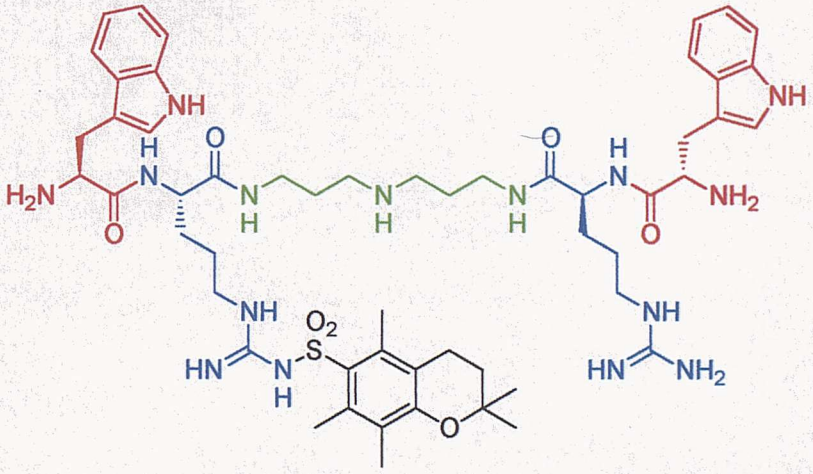

Figure 56: Structural elements identified within the lead compounds include the tryptophan residue (red), the arginine residue (blue), the Pmc group (black) and norspermidine (green).

These structural elements included aromatic hydrophobic regions (the indole ring of the tryptophan residue and the aromatic ring of the Pmc group) and polar/charged regions (the primary amino group of the tryptophan residue, the guanidine group of the arginine residue and the secondary amino group of the norspermidine portion). In

addition, the inhibitors were all based on a "two-armed" structure with derivatisation on both ends of norspermidine.

A library of compounds based on the lead compounds was synthesised and screened against TR, composed of compounds with one or more of the structural elements from the lead compounds removed. To investigate the importance of the two-armed structure a series of 15 compounds was prepared where one arm of norspermidine was derivatised with a structural element and the other arm was derivatised as a simple amide with varying alkyl chain length, or as a primary amino group. A number of compounds derivatised on both arms were also prepared (Figure 57). The library was completed with the synthesis of the dipeptides H-Trp-Arg-OH and H-Trp-Arg(Pmc)-OH, included to assess the importance of the norspermidine portion.

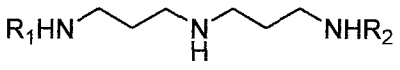

One-armed compounds	R_1 = Trp	R_2 = H
	Arg	$COCH_3$
	Arg(Pmc)	$CO(CH_2)_4CH_3$
	Trp-Arg	
	Trp-Arg(Pmc)	
Two-armed compounds	$R_1 = R_2$ = Trp	
	R_1 = Arg, R_2 = Arg(Pmc)	
	$R_1 = R_2$ = Arg(Pmc)	

Figure 57: Structure of one- and two-armed library members.

3.2 Library Synthesis

Solid-phase parallel synthesis utilised immobilised norspermidine with orthogonal protection on the primary amino groups to allow preparation of the library members functionalised on one arm alone. The resin was prepared using a Tfa/Dde strategy following a procedure developed within the group.[103] The first step in the synthesis was the orthogonal protection of norspermidine which was accomplished by sequential treatment with one equivalent of ethyl trifluoroacetate and 2-acetyldimedone. Both reagents are selective for primary amines and the reaction led to a mixture of the desired orthogonal protected compound **118** together with side products protected on both primary amino groups with either Tfa or Dde groups.[80,104] The poor yield of this reaction

was partly due to the significant quantities of these side products as well as difficulties in separating the products by chromatography. However, the reaction had the advantages of synthetic ease (avoiding multi-step procedures), used cheap starting materials and could be undertaken on a large scale. **118** was coupled to the activated linker **103** prior to allyl ester deprotection and coupling to aminomethyl polystyrene resin (1% DVB crosslinked) using standard HOBt/DIC activation (Scheme 8).

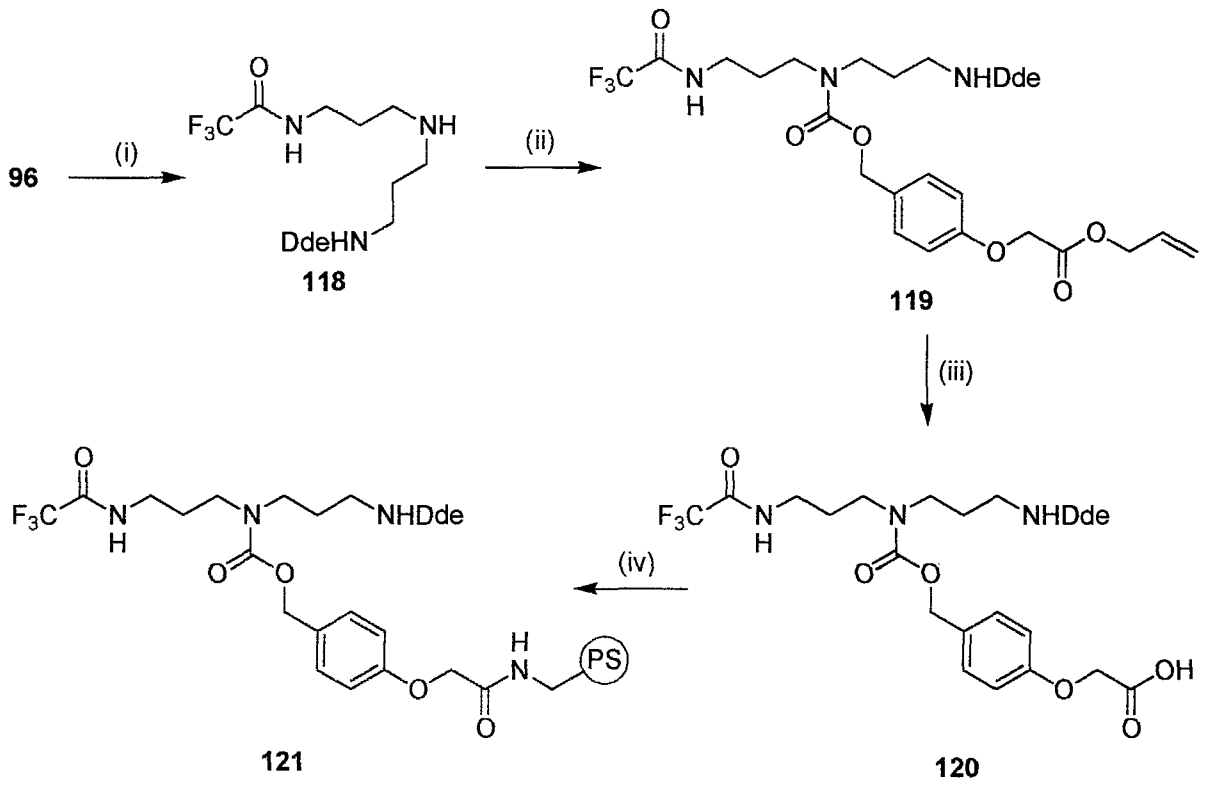

Scheme 8: Preparation of orthogonal protected norspermidine scaffold **121**.
Reagents and conditions: (i) Ethyl trifluoroacetate, MeOH, -78 °C to rt, 4 hrs, then 2-acetyldimedone, EtOH, 16 hrs, 16%. (ii) **103**, DMF, 16 hrs, 79%. (iii) $Pd(PPh_3)_4$, thiosalicylic acid, DCM/THF (1:1), 2 hrs, 65% (iv) aminomethyl polystyrene resin, HOBt, DIC, DCM/DMF (4:1), 16 hrs.

15 compounds were prepared from resin **121** using a multiple parallel approach (Scheme 9).

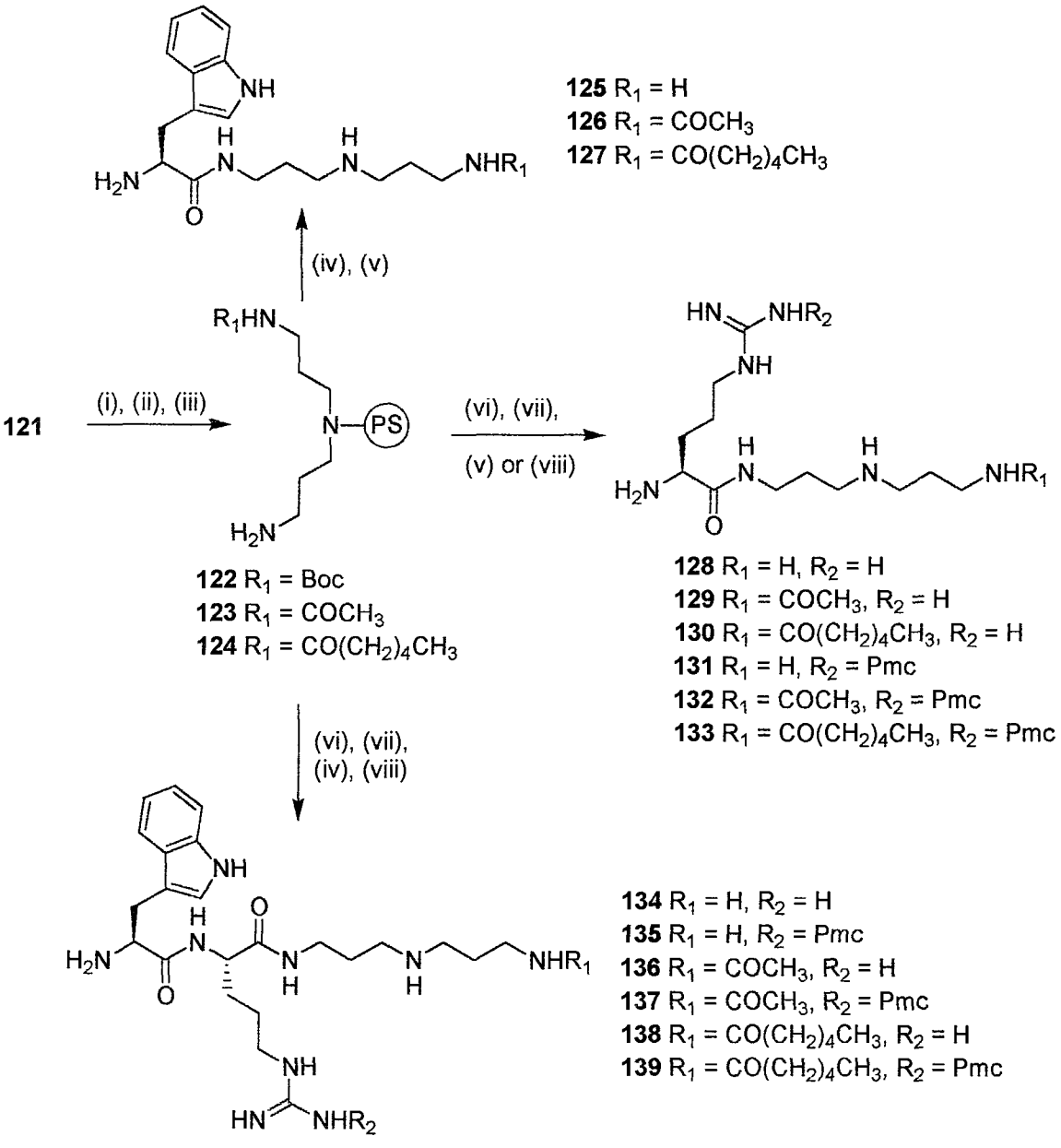

Scheme 9: Parallel synthesis of one-armed library members.

Reagents and conditions: (i) 5% H_2NNH_2/DMF, 30 min. (ii) Boc_2O, DIPEA, DCM, 2 hrs or acetic anhydride/pyridine (1:1), 30 mins or hexanoic anhydride/pyridine (1:1), 30 mins. (iii) 1M KOH/MeOH/THF (5:1:1), 2 x 2 hrs. (iv) Boc-Trp(Boc)-OH, HOBt, DIC, DCM/DMF (4:1), 2 hrs. (v) TFA/thioanisole/DCM/water (16:2:1:1), 2 hrs. (vi) Fmoc-Arg(Pmc)-OH, HOBt, DIC, DCM/DMF (4:1), 2 hrs. (vii) 20% piperidine/DMF, 2 x 10 min. (viii) TFA/thioanisole/DCM/water (10:2:7:1), 4 x 15 mins.

Following Dde deprotection, the resulting amine was capped with either Boc_2O, acetic anhydride or hexanoic anhydride to give **122**, **123** or **124**. Tfa deprotection was achieved by treatment with 1M KOH/MeOH/THF (5:1:1). Standard solid-phase peptide chemistry was then utilised to prepare the desired compounds **125-139**, which were purified by HPLC. Identical cleavage conditions were used for the synthesis of the Pmc-containing compounds **131-133**, **135**, **137** and **139** as were used for the preparation of **110-112**.

These cleavage conditions resulted in similar amounts of the desired Pmc-protected and deprotected compounds. Synthesis was very clean, as shown by the HPLC trace of the mixture of **136** and **137** obtained after cleavage from the resin (Figure 58).

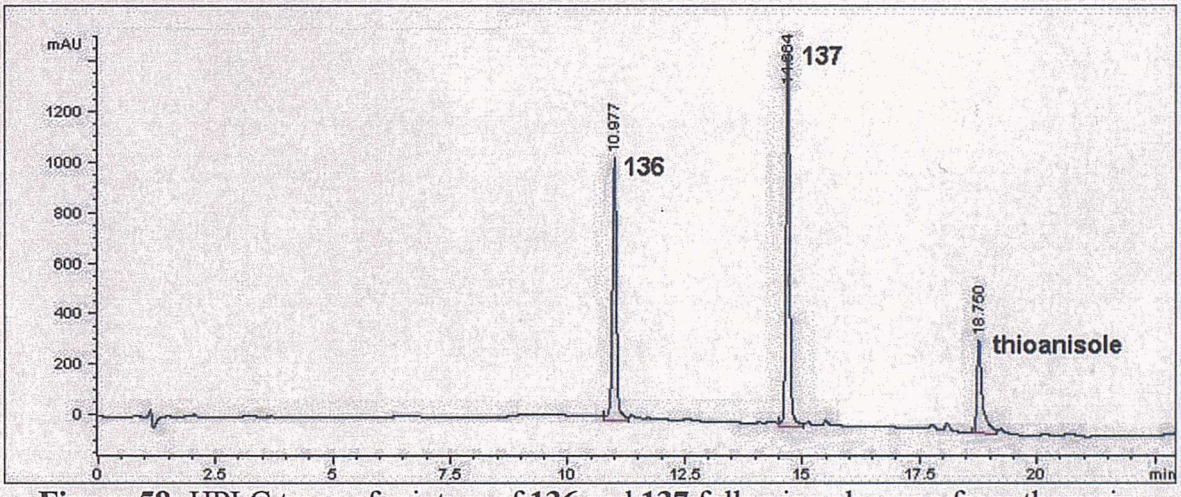

Figure 58: HPLC trace of mixture of **136** and **137** following cleavage from the resin.

The two-arm compounds **140-142** were prepared from resin **108** (Scheme 10). Following Dde-deprotection of **108**, standard solid phase peptide chemistry was used to couple either the tryptophan or arginine residues. Cleavage from the resin and HPLC purification again furnished the desired compounds.

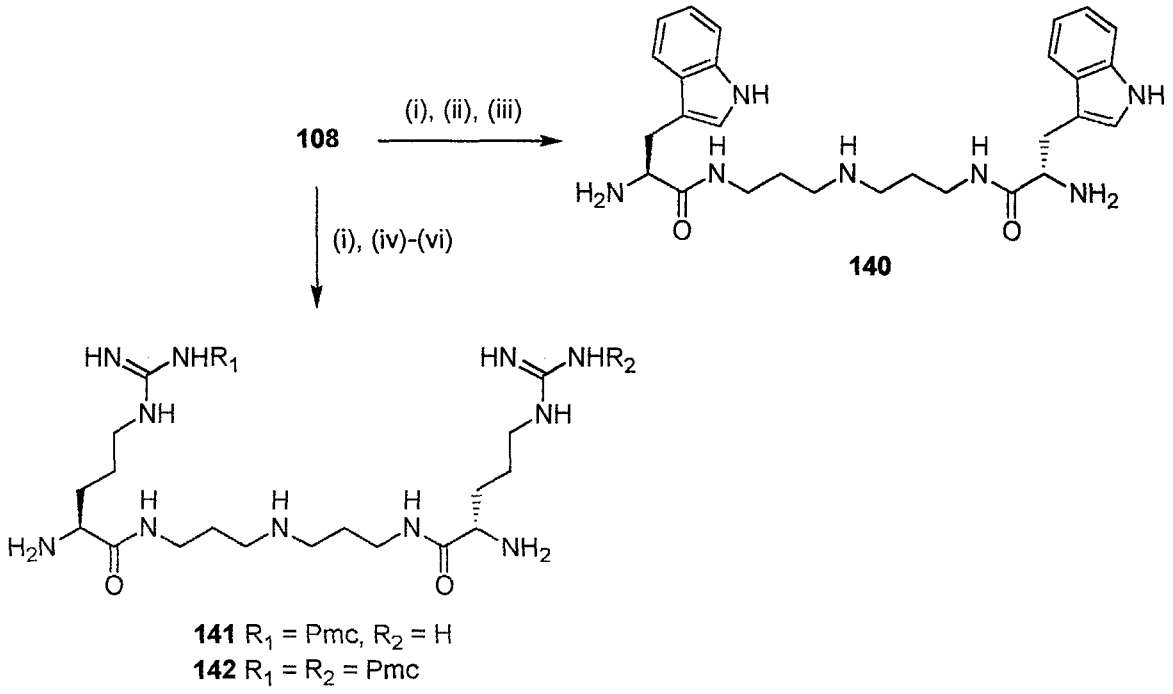

Scheme 10: Synthesis of **140-142**.

Reagents and conditions: (i) 5% H_2NNH_2/DMF, 30 min. (ii) Boc-Trp(Boc)-OH, HOBt, DIC, DCM, DMF, 2 hrs. (iii) TFA/thioanisole/DCM/water (16:2:1:1), 2 hrs. (iv) Fmoc-Arg(Pmc)-OH, HOBt, DIC, DCM, DMF, 2 hrs. (v) 20% piperidine/DMF, 2 x 10 min. (vi) TFA/thioanisole/DCM/water (10:2:7:1), 4 x 15 min.

Library synthesis was completed by the solution-phase synthesis of the dipeptides **145** and **146**. These were prepared by reaction of the NHS-ester of Boc-Trp(Boc)-OH **143** with H-Arg(Pmc)-OH in the presence of one equivalent of DIPEA to give **144** (Scheme 11). Subsequent treatment of **144** with TFA/thioanisole/DCM/water (10:2:7:1) for 30 minutes furnished a mixture of **145** and **146** which were purified by HPLC.

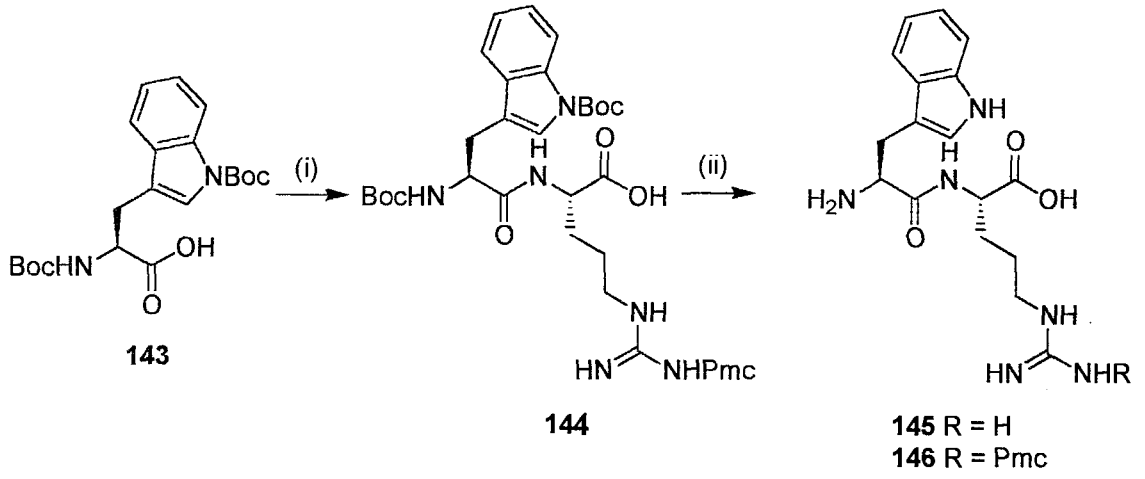

Scheme 11: Preparation of dipeptides **145** and **146**.

Reagents and conditions: (i) *N*-hydroxy succinimide, DCC, THF, 2 hrs then H-Arg(Pmc)-OH, DIPEA, DMF, 16 hrs, 77%. (ii) TFA/thioanisole/DCM/water (10:2:7:1), 30 min.

3.3 Library Screening

The inhibitor library was initially screened for activity against TR at a concentration of 100 μM (Figure 59). The screen was performed in triplicate as a single-point assay using nortrypanothione disulfide as substrate, and the lead compound **110** was included in the screen as a reference.

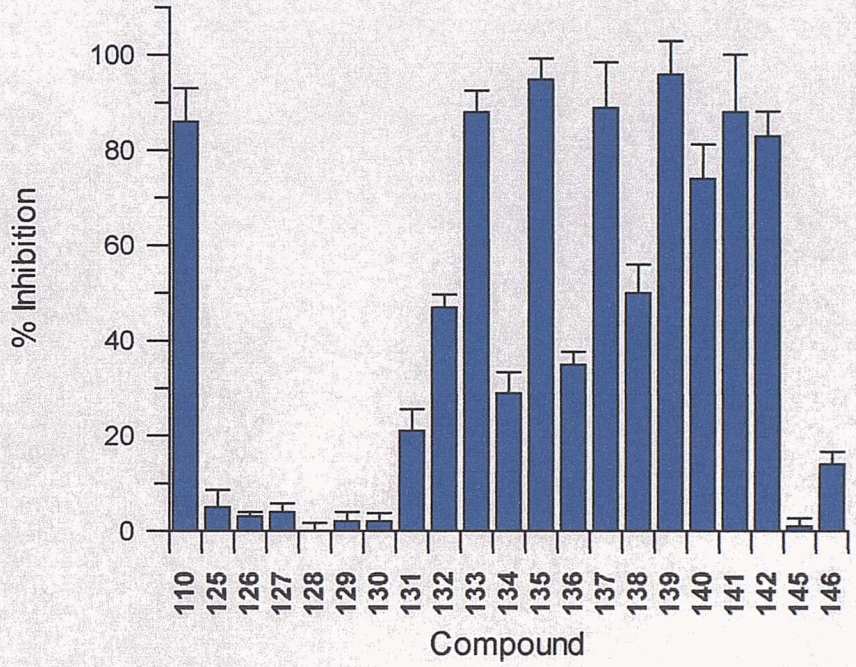

Figure 59: Inhibition of TR at an inhibitor concentration of 100 μM and a nortrypanothione disulfide concentration of 30 μM.

Significant activity was observed with compounds **131-142** of which the most active compounds were those containing the Trp-Arg(Pmc) moiety (**135**, **137** and **139**) and the two-armed compounds (**140-142**) which showed comparable inhibiton to **110**. Practically no activity was observed with the Trp-containing compounds **125-127** or the Arg-containing compounds **128-130**. The dipeptide **145** was also inactive, with the Pmc-containing analogue **146** showing only marginal activity.

Those compounds that showed significant inhibiton (i.e. >20%) were then screened at 10 μM (Figure 60).

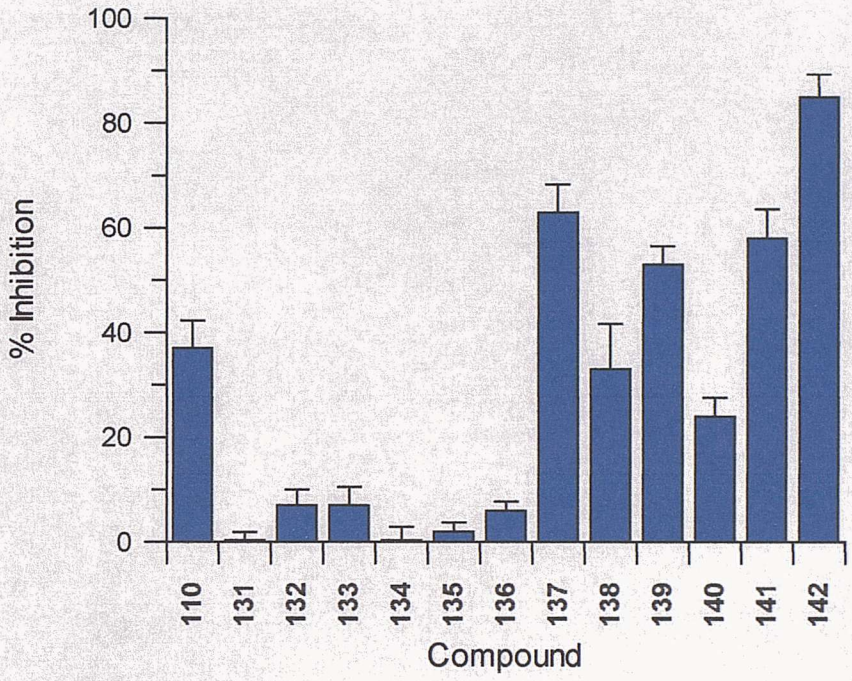

Figure 60: Inhibition of TR at an inhibitor concentration of 10 μM and a nortrypanothione disulfide concentration of 30 μM.

At 10 μM, activity comparable to **110** was observed with **133**, **135**, **137**, and **139-142**. With the exception of **133**, compounds bearing either the Arg(Pmc) or Trp-Arg moieties exhibited little or no inhibition.

Full kinetic analysis was then performed on compounds that exhibited significant activity at 100 μM to determine the K_i value for each as well as the type of inhibition exhibited.

3.4 Kinetic Analysis of Library Members Active at 100 μM

Kinetic analysis was performed on active library members as described for the lead compounds **110-112** (Section 2.7).

3.4.1 Arg(Pmc) Containing Compounds

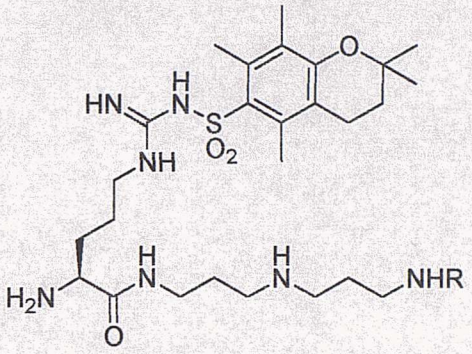

131 R = H (non-comp, K_i = 131 +/- 7.2 μM)
132 R = $COCH_3$ (non-comp, K_i = 68.8 +/- 3.2 μM)
133 R = $CO(CH_2)_4CH_3$ (non-comp, K_i = 6.5 +/- 0.2 μM)

Figure 61: Arg(Pmc) containing compounds **131-133**.

131-133 (Figure 61) displayed non-competitive inhibition as shown in the Eadie-Hofstee and Lineweaver-Burke plots (Figures 62-64). The compounds were considerably weaker inhibitors than the lead compounds **111** and **112**, with K_i values of 131 +/- 7.2, 68.8 +/- 3.2 and 6.5 +/- 0.2 μM, respectively.

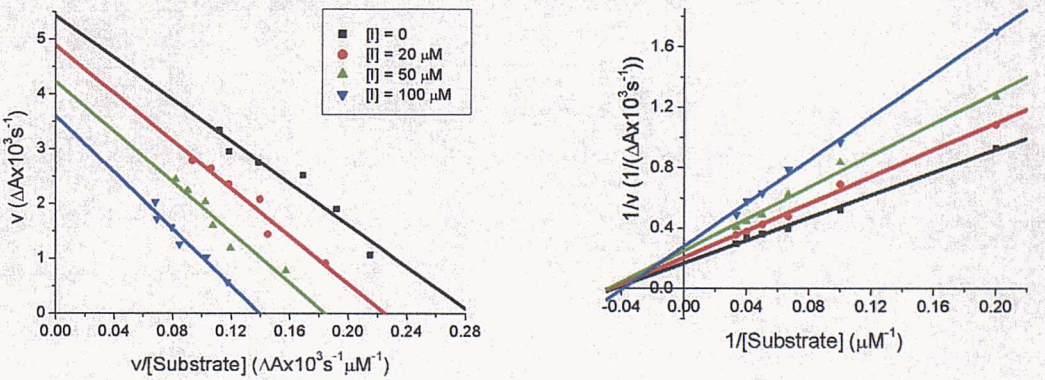

Figure 62: Inhibitor **131** - non-competitive behaviour (K_i = 131 +/- 7.2 μM).

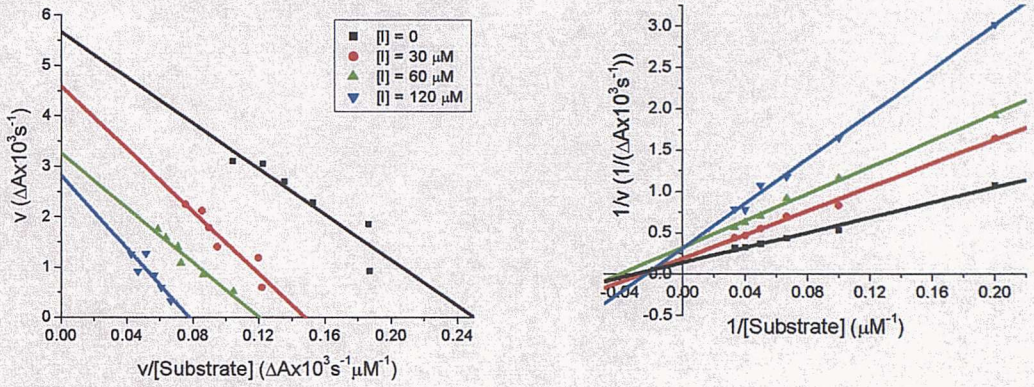

Figure 63: Inhibitor **132** - non-competitive behaviour (K_i = 68.8 +/- 3.2 μM).

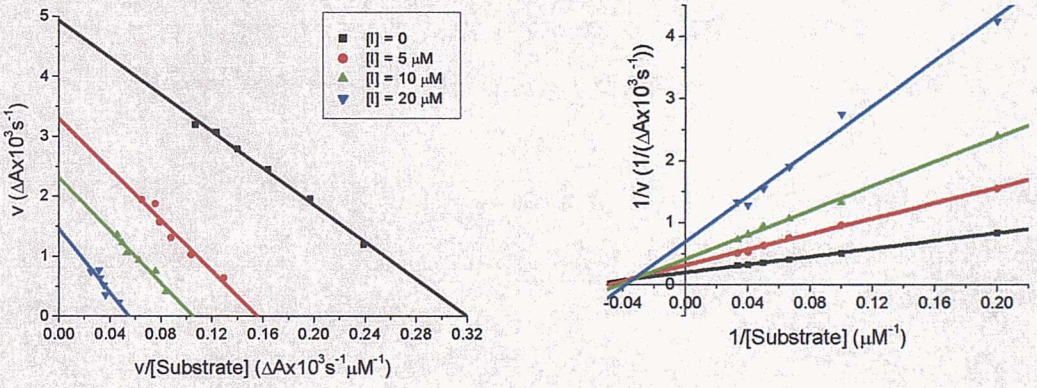

Figure 64: Inhibitor **133** - non-competitive behaviour (K_i = 6.5 +/- 0.2 μM).

The effect of the substituent on the second arm showed increased activity with increasing hydrophobic character. **133**, bearing the hexanoyl capping group, was more active than **132** bearing the acetyl capping group which in turn was more active than **131**, bearing the primary amino group.

3.4.2 Trp-Arg Containing Compounds

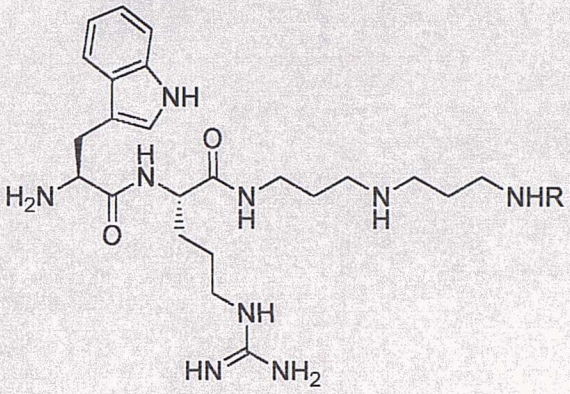

134 R = H (comp, K_i = 83.4 +/- 4.4 μM)
136 R = $COCH_3$ (comp, K_i = 68.5 +/- 5.8 μM)
138 R = $CO(CH_2)_4CH_3$ (comp, K_i = 23.5 +/- 2.0 μM)

Figure 65: Trp-Arg containing compounds **134**, **136** and **138**.

134, **136** and **138** (Figure 65) displayed competitive inhibition as shown in the Eadie-Hofstee and Lineweaver-Burke plots (Figures 66-68). Again a significant reduction in potency was observed compared to **111** and **112**, with measured K_i values of 83.4 +/- 4.4, 68.5 +/- 5.8 and 23.5 +/- 2.0 μM, respectively. An identical trend to **131-133** was observed with derivatisation on the second arm, with potency increasing with increasing hydrophobic nature.

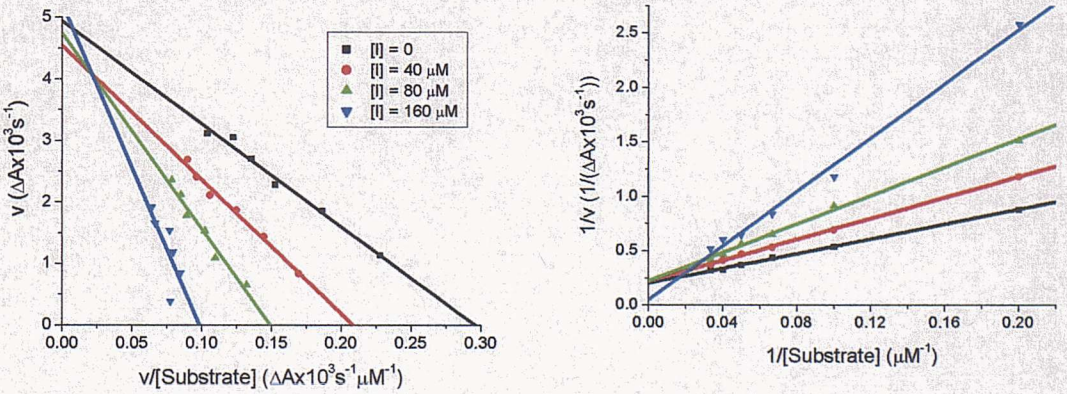

Figure 66: Inhibitor **134** - competitive behaviour (K_i = 83.4 +/- 4.4 μM).

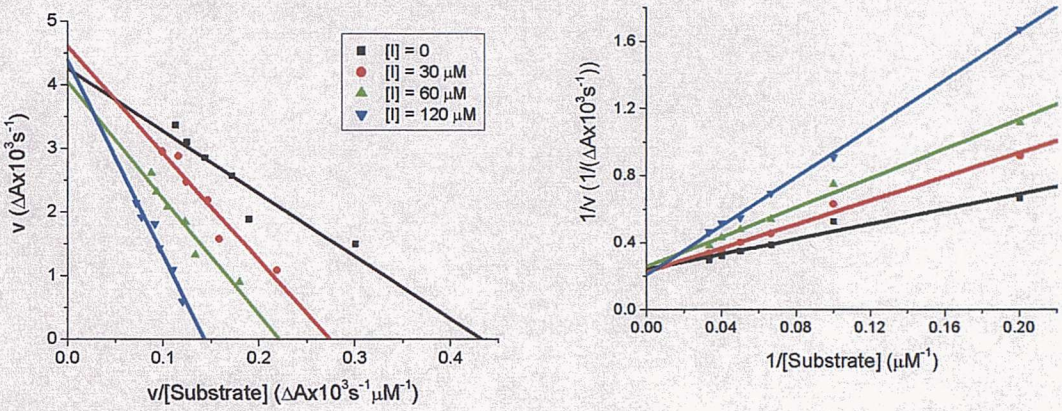

Figure 67: Inhibitor **136** - competitive behaviour (K_i = 68.5 +/- 5.8 μM).

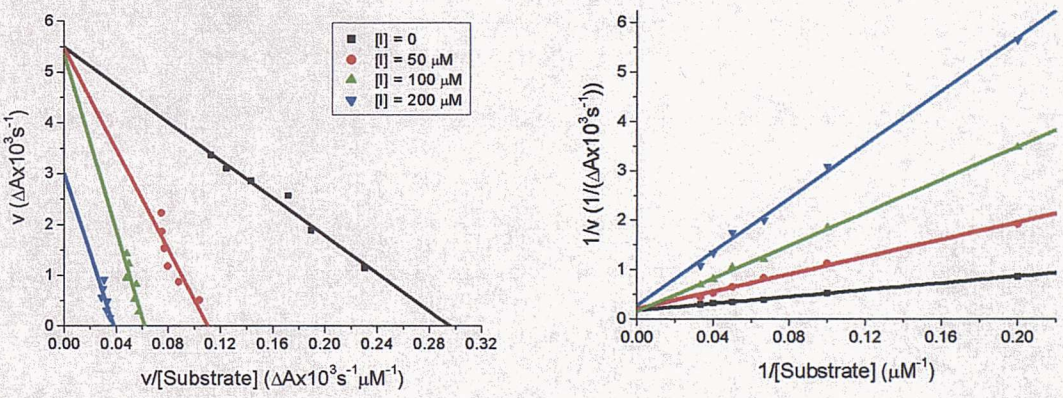

Figure 68: Inhibitor **138** - competitive behaviour (K_i = 23.5 +/- 2.0 μM).

3.4.3 Trp-Arg(Pmc) Containing Compounds

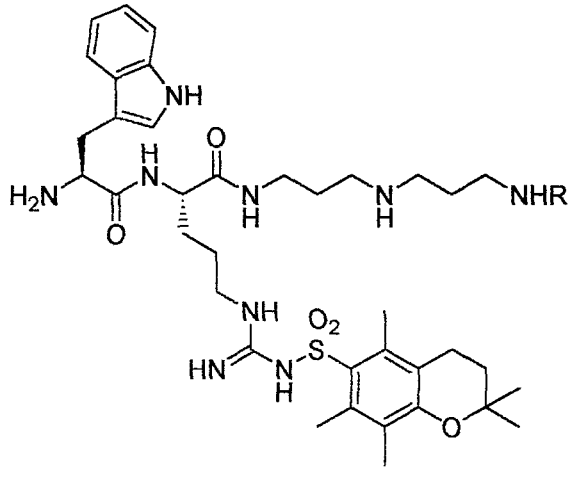

135 R = H (non-comp, K_i = 9.3 +/- 1.1 μM)
137 R = $COCH_3$ (non-comp, K_i = 11.5 +/- 0.4 μM)
139 R = $CO(CH_2)_4CH_3$ (non-comp, K_i = 5.9 +/- 0.2 μM)

Figure 69: Trp-Arg(Pmc) containing compounds **135**, **137** and **139**.

135, **137** and **139** (Figure 69) all displayed non-competitive inhibition as shown in the Eadie-Hofstee and Lineweaver-Burke plots (Figures 70-72). Although this was the most active subset of the one armed compounds, the activity of the compounds was significantly reduced compared to **111** and **112** with K_i values of 9.3 +/- 1.1, 11.5 +/- 0.4 and 5.9 +/- 0.2 μM, respectively. No clear correlation between activity and derivatisation on the second arm was observed.

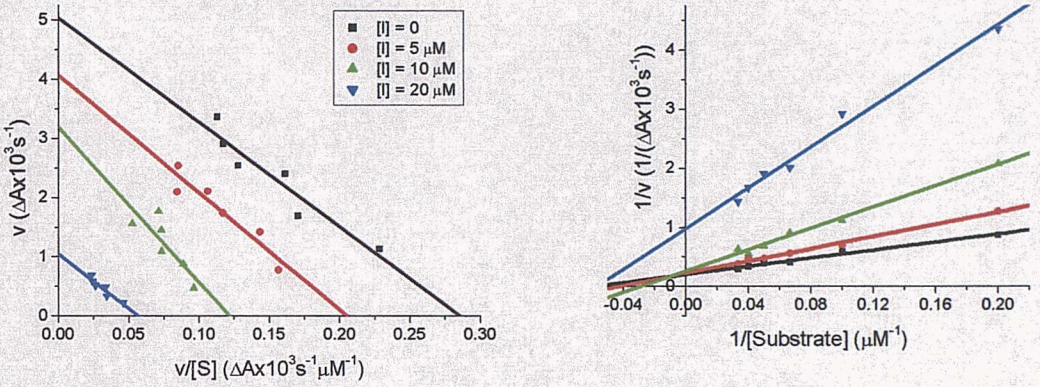

Figure 70: Inhibitor **135** - non-competitive behaviour (K_i = 9.3 +/- 1.1 μM).

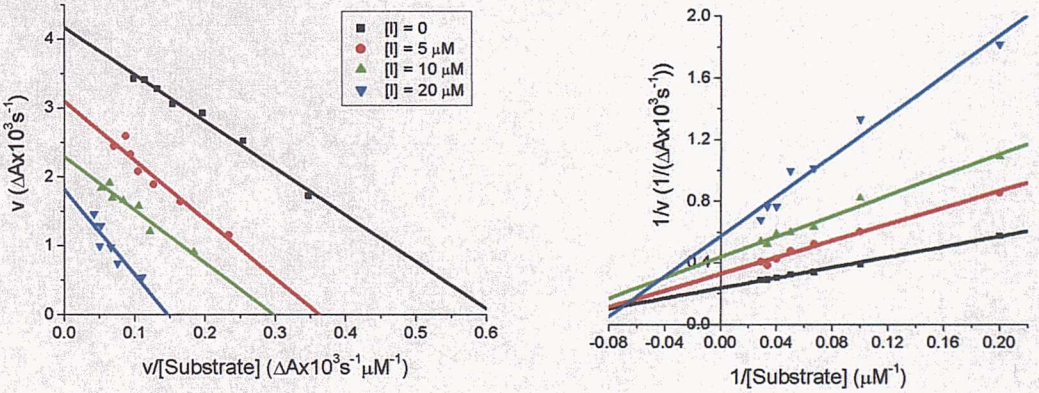

Figure 71: Inhibitor **137** - non-competitive behaviour (K_i = 11.5 +/- 0.4 μM).

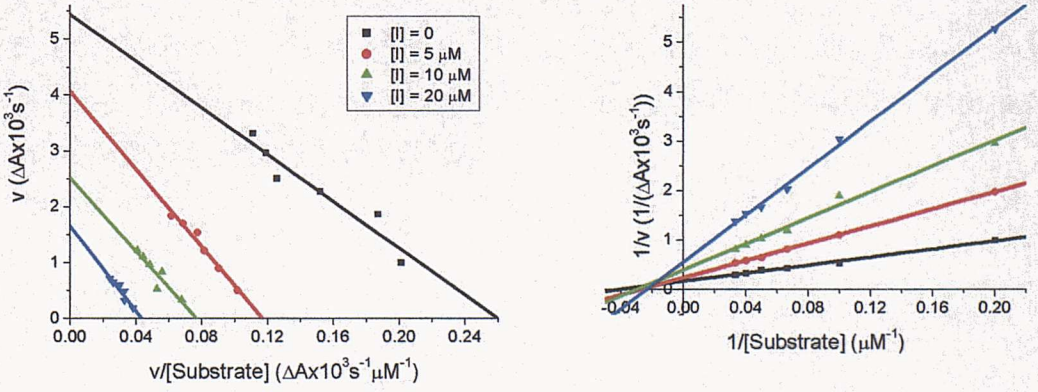

Figure 72: Inhibitor **139** - non-competitive behaviour (K_i = 5.9 +/- 0.2 nM).

3.4.4 Two-Armed Compounds

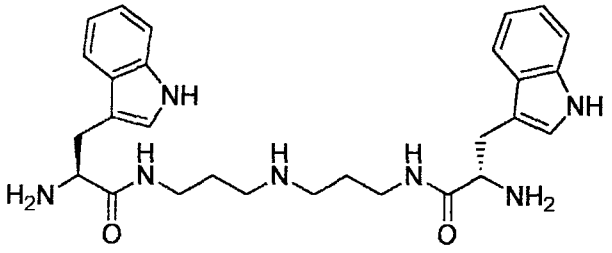

140 (comp, K_i = 19.1 +/- 1.1 μM)

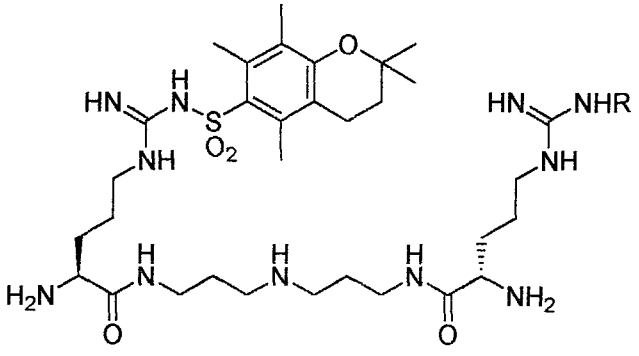

141 R = H (non-comp, K_i = 10.6 +/- 0.5 μM)
142 R = Pmc (non-comp, K_i = 2.9 +/- 0.3 μM)

Figure 73: Two-armed compounds **140-142**.

The two-armed compounds **140-142** (Figure 73) were the only sub-set that contained compounds that showed different modes of inhibition (Figures 74-76). **140** displayed competitive inhibition with a K_i value of 19.1 +/- 1.1 μM. **141** and **142** displayed non-competitive inhibition with K_i values of 10.6 +/- 0.5 and 2.9 +/- 0.3 μM, respectively. These were again significantly poorer than **111** and **112**, although **142** was the most potent of all the library members.

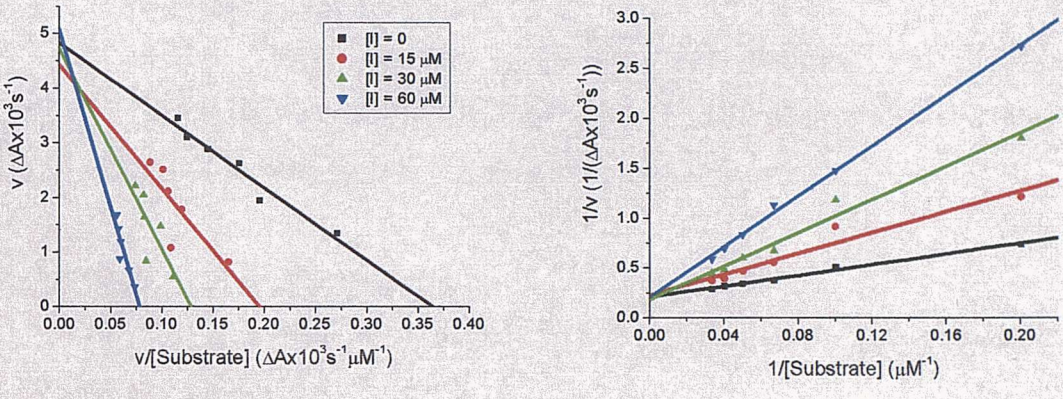

Figure 74: Inhibitor **140** - competitive behaviour (K_i = 19.1 +/- 1.1 μM).

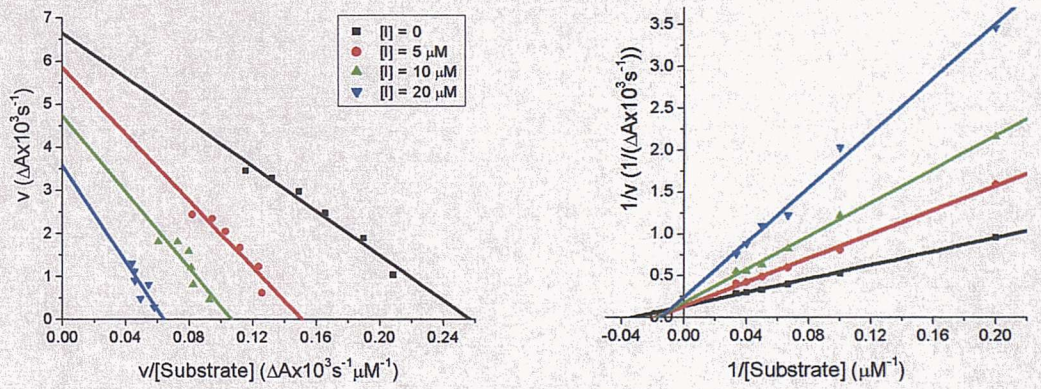

Figure 75: Inhibitor **141** - non-competitive behaviour (K_i = 10.6 +/- 0.5 μM).

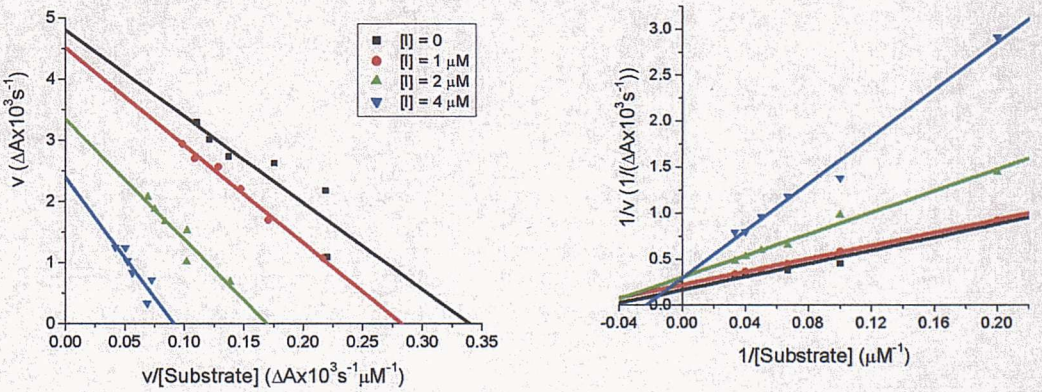

Figure 76: Inhibitor **142** - non-competitive behaviour (K_i = 2.9 +/- 0.3 μM).

3.5 Assay against Glutamate Dehydrogenase

The active library members (**131-142**) were screened against glutamate dehydrogenase at a concentration of 100 μM in an identical manner to **109-111** (Section 2.8). As found with inhibitors **110-112**, no activity was observed.

3.6 Structure-Activity Relationships

The results of the screening and kinetic assays of the norspermidine based compounds are summarised in Table 3.

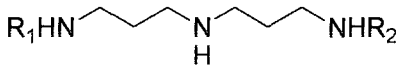

Compound	R_1	R_2	Mode	K_i
110	Trp-Arg	Trp-Arg	Non-competitive	14.3 +/- 0.5 μM
111	Trp-Arg(Pmc)	Trp-Arg	Non-competitive	220 +/- 15 nM
112	Trp-Arg(Pmc)	Trp-Arg(Pmc)	Non-competitive	160 +/- 8 nM
125	Trp	H	nd	>100
126	Trp	$COCH_3$	nd	>100
127	Trp	$CO(CH_2)_4CH_3$	nd	>100
128	Arg	H	nd	>100
129	Arg	$COCH_3$	nd	>100
130	Arg	$CO(CH_2)_4CH_3$	nd	>100
131	Arg(Pmc)	H	Non-competitive	131 +/- 7.2 μM
132	Arg(Pmc)	$COCH_3$	Non-competitive	68.8 +/- 3.2 μM
133	Arg(Pmc)	$CO(CH_2)_4CH_3$	Non-competitive	6.5 +/- 0.2 μM
134	Trp-Arg	H	Competitive	83.4 +/- 4.4 μM
135	Trp-Arg(Pmc)	H	Non-competitive	9.3 +/- 1.1 μM
136	Trp-Arg	$COCH_3$	Competitive	68.5 +/- 5.8 μM
137	Trp-Arg(Pmc)	$COCH_3$	Non-competitive	11.5 +/- 0.4 μM
138	Trp-Arg	$CO(CH_2)_4CH_3$	Competitive	23.5 +/- 2.0 μM
139	Trp-Arg(Pmc)	$CO(CH_2)_4CH_3$	Non-competitive	5.9 +/- 0.2 μM
140	Trp	Trp	Competitive	19.1 +/- 1.1 μM
141	Arg(Pmc)	Arg	Non-competitive	10.6 +/- 0.5 μM
142	Arg(Pmc)	Arg(Pmc)	Non-competitive	2.9 +/- 0.3 μM

Table 3: Summary of results of screening and enzyme kinetic analysis of lead compounds and library members.

Kinetic analysis surprisingly showed both competitive and non-competitive inhibitors within the library. The competitive inhibitors were similar in structure to many reported TR inhibitors, containing both a hydrophobic group and a polyamine, however

this was also true of other compounds in this series which displayed non-competitive behaviour! No improvement in potency compared to **111** and **112** was observed with any of the library members. Any change in structure was detrimental and resulted in an increase in K_i of at least an order of magnitude. In general, activity was related to structural similarity to **111** and **112**, with the most active derivative **142** being identical to **112** except for the absence of the tryptophan residues. Structural simplification led to a corresponding loss of activity.

The tryptophan residue: Removal of the tryptophan residue resulted in a loss of potency (compare **111** and **112** with **141** and **142**; **135**, **137** and **139** with **131-133**; and **134**, **136** and **138** with **128-130**. The lack of activity of **128-130** is not surprising as previously screened polyamines show little activity against TR.

The arginine residue: Removal of the arginine residue led to a change in mechanism (compare **110** with **140**) and a loss of potency (compare **134**, **136** and **138** with **125-127**). The lack of activity of **125-127** maybe due to the arginine residue in **134**, **136** and **138** acting as a spacer and placing the polyamine and hydrophobic groups at an optimum distance apart for binding. Alternatively, the arginine side-chain in **134**, **136** and **138** maybe involved in a binding interaction, increasing the potency of these compounds.

The Pmc group: The Pmc group was clearly important for potency, as the eight best inhibitors all contained this structural feature. Removal of the group led to an increase in K_i (compare **111** and **112** with **110**; **135**, **137** and **139** with **134**, **136** and **138**; and **131-133** with **128-130**). A change in mechanism also resulted (compare **135**, **137** and **139** with **134**, **136** and **138**).

One and two armed structure: The most potent compounds were derivatised on two arms of norspermidine, although significant activity was also observed with one armed compounds. No correlation between mode of action between either one or two armed structures was observed. In the one armed series, the more hydrophobic hexanoyl capping group generally gave the best inhibition, and the primary amino group proved inferior.

Norspermidine: The lack of activity of the dipeptides **145** and **146** demonstrated the importance of the polyamine portion of the inhibitors. The presence of the carboxylate moiety is almost certainly having a detrimental effect on the binding, as the

TR active site is known to disfavour the binding of negatively charged over positively charged compounds.

3.7 Conclusions

In summary, this chapter described the use of multiple parallel solid-phase chemistry in the synthesis of a library of compounds that were screened against TR. No improvement in potency from the lead compounds was observed, but SAR was developed and both competitive and non-competitive behaviour was observed. These results suggest that caution must be exercised when studying this protein as simple assumptions about binding sites and mode of action may not always be justified, given the observed change of mechanism from non-competitive to competitive upon small structural changes. The site of binding of the non-competitive inhibitors and specific interactions of the competitive inhibitors in the active site are currently under investigation by protein crystallography.

The findings presented in this thesis give a better understanding of the enzyme and this class of inhibitors and will aid the development of more effective enzyme inhibitors in the future.

CHAPTER 4

EXPERIMENTAL SECTION

4.1 General Information

^{1}H and ^{13}C NMR spectra were recorded on Bruker AC-300 (300 and 75 MHz, respectively) and Bruker DPX-400 spectrometers (400 and 100 MHz, respectively) in the solvents indicated at 298 K. Chemical shifts for proton and carbon spectra were reported on the δ scale in ppm and were referenced to residual protic solvent or natural abundance ^{13}C of the deuterated solvent. All coupling constants (*J* values) are given in Hz.

Low-resolution electrospray mass spectra were recorded on a VG Platform Quadrupole mass spectrometer. Low-resolution electron ionisation spectra were recorded on a Thermoquest Trace mass spectrometer. High-resolution electrospray mass spectra were recorded on a Bruker Apex III FT-ICR mass spectrometer.

IR spectra were recorded on a Bio-Rad ATR FT-IR fitted with a golden gate accessory. Samples were analysed as neat solids or oils.

Melting points were recorded on a Gallenkamp melting point apparatus and are uncorrected.

UV/VIS spectra and kinetic data were recorded on a Hewlett Packard HP8452A diode array spectrophotometer.

Fluorescence spectra and kinetic data were recorded on a Hitachi F2000 fluorescence spectrophotometer.

All reactiona were carried out at room temperature unless otherwise stated.

Thin layer chromatography was performed on Alugram® silica plates and visualized by ultra-violet light, stained with ninhydrin (0.3% ninhydrin and 3% acetic acid in *n*-butanol) or permanganate ($KMnO_4$ (3.00 g), K_2CO_3 (20.00 g), 5% aq. NaOH solution).

Column chromatography was performed using Sorbsil C60, 40-60 mesh silica or neutral, Brockmann I, 150 mesh alumina.

Analytical RP-HPLC was performed on a Hewlett Packard HP1100 chemstation equipped with a Phenomenex Prodigy C_{18} (150 x 4.6 mm) reverse phase column with a flow rate of 0.5 mL/min. Semi-preparative RP-HPLC was performed on a Hewlett

Packard HP1100 chemstation equipped with a Phenomenex Prodigy C_{18} (250 x 10 mm) reverse phase column with a flow rate of 2.5 mL/min. Mobile phase A was 0.1% TFA in water, mobile phase B was 0.042% TFA in MeCN.

Gradient 1 was T = 0 min, B = 10%, T = 10 min, B = 90%, T = 15 min, B = 90%.

Gradient 2 was T = 0 min, B = 0%, T = 5 min, B = 0%, T = 15 min, B = 60%, T = 16 min, B = 100%, T = 20 min, B = 100%.

Gradient 3 was T = 0 min, B = 0%, T = 40 min, B = 50%, T = 45 min, B = 90%, T = 50 min, B = 90%.

Gradient 4 was T = 0 min, B = 0%, T = 20 min, B = 25%, T = 22 min, B = 90%, T = 30 min, B = 90%.

4.1.1 General Procedures for Solid-Phase Chemistry

A: Peptide Coupling

Carboxylic acid (3 eq. relative to resin-bound amine) and HOBt (3 eq.) were dissolved in DCM/DMF (4:1, 1 mL per 100 mg of resin) and the resultant solution shaken for 10 min. DIC (3 eq.) was added and the resultant solution shaken for a further 10 min. The solution was added to the resin (pre-swollen in DCM (1 mL per 100 mg of resin) for 10 min) and the mixture shaken for 2 hours. The resin was filtered and washed sequentially with DMF, DCM, MeOH and Et_2O (3 mL per 100 mg of resin, 5 times with each). Reaction completion was monitored by the use of a qualitative ninhydrin test.

B: Dde Deprotection

The resin was swollen in DCM (1 mL per 100 mg of resin) for 10 min, filtered and treated with 5% v/v hydrazine in DMF (1 mL per 100 mg of resin) for 30 min. The resin was filtered and washed sequentially with DMF, DCM, MeOH and Et_2O (3 mL per 100 mg of resin, 5 times with each).

C: Fmoc Deprotection

The resin was swollen in DCM (1 mL per 100 mg of resin) for 10 min, filtered and treated with 20% v/v piperidine in DMF (1 mL per 100 mg of resin) for 2 x 10 min. The

resin was filtered and washed sequentially with DMF, DCM, MeOH and Et_2O (3 mL per 100 mg of resin, 5 times with each).

D: Trityl Deprotection with Concomitant Disulfide Formation

The resin was swollen in DCM (1 mL per 100 mg of resin) for 10 min, filtered and treated with a solution of I_2 (10 eq. relative to trityl group) in DMF (1 mL per 100 mg of resin) for 2 hours. The resin was filtered and washed sequentially with DMF, DCM, MeOH and Et_2O (3 mL per 100 mg of resin, 10 times with each).

E: Boc Protection

The resin was swollen in DCM (1 mL per 100 mg of resin) for 10 min, filtered and treated with a solution of Boc_2O (5 eq. relative to resin-bound amine) and DIPEA (2 eq.) in DCM (1 mL per 100 mg of resin) for 2 hours. The resin was filtered and washed sequentially with DMF, DCM, MeOH and Et_2O (3 mL per 100 mg of resin, 5 times with each). Reaction completion was monitored by the use of a qualitative ninhydrin test.

F: *N*-Capping with Acetic Anhydride

The resin was swollen in DCM (1 mL per 100 mg of resin) for 10 min, filtered and treated with a mixture of acetic anhydride and pyridine (1:1, 1 mL per 100 mg of resin) for 30 min. The resin was filtered and washed sequentially with DMF, DCM, MeOH and Et_2O (3 mL per 100 mg of resin, 5 times with each). Reaction completion was monitored by the use of a qualitative ninhydrin test.

G: *N*-Capping with Hexanoic Anhydride

The resin was swollen in DCM (1 mL per 100 mg of resin) for 10 min, filtered and treated with a mixture of hexanoic anhydride and pyridine (1:1, 1 mL per 100 mg of resin) for 30 min. The resin was filtered and washed sequentially with DMF, DCM, MeOH and Et_2O (3 mL per 100 mg of resin, 5 times with each). Reaction completion was monitored by the use of a qualitative ninhydrin test.

H: Tfa Deprotection

The resin was swollen in DCM (1 mL per 100 mg of resin) for 10 min, filtered and treated with a solution of 1M KOH/THF/MeOH (5:1:1, 1 mL per 100 mg of resin) for 2 x 2 hours. The resin was filtered and washed sequentially with DMF/water (1:1), MeOH/water (1:1), DMF, DCM, MeOH and Et_2O (3 mL per 100 mg of resin, 5 times with each).

I: Cleavage from the Resin with 80% TFA

The resin was swollen in DCM (1 mL per 100 mg of resin) for 10 min, filtered and treated with a mixture of TFA/thioanisole/DCM/water (16:2:1:1, 1 mL per 100 mg of resin) for 2 hours. The resin was filtered and washed with MeOH (3 mL per 100 mg of resin, 5 times), the filtrate and washings combined and concentrated *in vacuo*. The crude product was then dissolved in TFA, precipitated from ice-cold Et_2O, the precipitate collected by centrifugation and lyophilized.

J: Cleavage from the Resin with 50% TFA

The resin was swollen in DCM (1 mL per 100 mg of resin) for 10 min, filtered and treated with a mixture of TFA/thioanisole/DCM/water (10:2:7:1, 1 mL per 100 mg of resin) for 4 x 15 minutes at room temperature. The resin was filtered and washed with MeOH (3 mL per 100 mg of resin, 5 times), the filtrate and washings combined and concentrated *in vacuo*. The crude product was then dissolved in TFA, precipitated from ice-cold Et_2O, the precipitate collected by centrifugation and lyophilized.

Ninhydrin Analysis[105]

***Qualitative Test*:**

Reagent A (6 drops) and reagent B (2 drops) were added to a sample of resin (approx. 1-2 mg) in a small test tube and heated at 100 °C for 5 min. The intensity of colour (purple) in the solution gave a qualitative indication of the level of primary amine present on the resin.

***Quantitative Test*:**

Reagent A (6 drops) and reagent B (2 drops) were added to a known amount of dry resin (2-5 mg) and heated at 100 °C for 5 minutes. The tube was then cooled in cold water and 60% ethanol in water (2 mL) added. After thorough mixing, the solution was filtered and washed with 0.5 M Et_4NCl in DCM (2 x 0.5 mL) and made up to a total volume of 50 mL with 60% ethanol in water. The absorbance of the solution at 570 nm was then recorded against a control solution, prepared in the same way but without resin. The loading of primary amine groups on the resin was calculated *via*:

$$\text{Loading (mmol/g)} = [(A_{570} \times V \times 10^3 / (\varepsilon_{570} \times M)]$$

Where A_{570} is the measured absorbance at 570 nm minus the control reading, V is the total volume of the solution in mL, ε_{570} is the extinction coefficient at 570 nm (1.5×10^4) and M is the accurate mass of resin in mg.

Reagent A

Solution 1: To a solution of phenol (40.00 g, 0.43 mol) in absolute ethanol (10 mL) was added IWT TMD-8 ion exchange resin (4.00 g). The mixture was stirred at room temperature for 45 minutes and filtered.

Solution 2: A 10 mM aqueous solution of KCN (2 mL) was diluted with pyridine (98 mL) and stirred at room temperature for 45 minutes with IWT TMD-8 ion exchange resin (4.00 g). The solution was then filtered and mixed with solution 1.

Reagent B

Ninhydrin (2.50 g, 14 mmol) was dissolved in absolute ethanol (50 mL).

Quantitative Fmoc Test[106]

A known mass of dry resin (approx. 5 mg) was placed in a 25 mL volumetric flask, a solution of 20% piperidine in DMF (5 mL) was added and the mixture shaken for 15 minutes. The volume was then made up to 25 mL with 20% piperidine in DMF and the

absorbance recorded at 302 nm against a control solution of 20% piperidine in DMF. The loading of Fmoc groups on the resin was calculated *via*:

$$\text{Loading of Fmoc (mmol/g)} = (A_{302} \times V \times 10^3) / (\varepsilon_{302} \times M)$$

Where A_{302} is the absorbance at 302 nm minus the control reading, V is the total volume of the solution in mL, ε_{302} is the extinction coefficient at 302 nm (7800) and M is the accurate mass of resin in mg.

4.1.2 General Biological Procedures

Buffers and Solutions

Phosphate buffer:	50 mM K_2HPO_4, 1 mM EDTA, 0.1% BME, pH 7.5.
Ammonium acetate buffer:	50 mM NH_4OAc, 1 mM EDTA, pH 7.5.
Acrylamide mix:	acrylamide (29%, w/v) and bisacrylamide (1%, w/v) in water.
Separating buffer:	1.5 M Tris, pH 8.8.
SDS:	SDS (10%, w/v) aqueous solution.
Ammonium persulphate:	ammonium persulphate (10%, w/v) aqueous solution.
Stacking gel buffer:	0.5 M Tris, pH 6.8.
1 x SDS gel-loading buffer:	50 mM Tris, 100 mM dithiothreitol, 2% SDS, 0.1% bromophenol blue, 10% glycerol, pH 6.8.
Tank buffer:	25 mM Tris, 192 mM glycine, 0.1% SDS, PH 8.3.
Comassie blue stain:	0.125% comassie blue R-250, 50% MeOH, 10% acetic acid.
Destaining solution:	50% MeOH, 40% water, 10% acetic acid.
2 x TY culture:	bactopeptone (16 g/L), bacto-yeast extract (10 g/L) and NaCl (5 g/L) aqueous solution.

Protein concentration was determined by the Bradford assay[107]. All kinetic data were collected in triplicate and analysed by non linear regression with the aid of the commercial program Grafit.

SDS-PAGE: Gel Preparation and Running

A separating gel containing water, acrylamide mix, separating buffer, SDS, ammonium persulphate and TEMED (see Table 4 for quantities) was prepared and immediately poured between two plates. A layer of isobutanol was placed on top of the gel mix and the gel left to set for approximately 30 min. The isobutanol was removed, the top of the gel washed and 5% stacking gel (Table 4) poured onto the top of the running gel. A teflon comb was immediately inserted into the stacking gel and the gel left to set for approximately 30 min, following which the comb was carefully removed and the wells washed thoroughly with water. To each protein sample (20 μL) was added gel-loading buffer (20 μL) and the mixture heated at 100 °C for 3 min. After cooling, the samples (10-15 μL of each) were loaded onto the gel wells together with a lane of molecular weight markers (12.3, 17.2, 30.0, 42.7, 66.3 and 76-78 kDa) and the gel run at 200 V for approx. 45 min in tank buffer. The gel was then stained with comassie blue stain (2 x 30 s, microwave heating) before immersion in destaining solution overnight.

Component	Separating gel volume (mL)			Stacking gel volume (mL)
	6%	12%	15%	
water	5.3	3.3	2.3	1.4
acrylamide mix	2.0	4.0	5.0	0.33
separating buffer	2.5	2.5	2.5	0.25
SDS	0.1	0.1	0.1	0.02
ammonium persulphate	0.1	0.1	0.1	0.02
TEMED	0.008	0.004	0.004	0.002

Table 4: Composition of SDS-PAGE gels.

4.2 Experimental to Chapter 2

2-Acetyl dimedone[81]

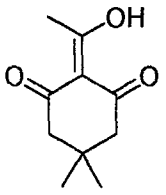

Dimedone (30.00 g, 214.0 mmol), DCC (44.16 g, 214.0 mmol), acetic acid (12.25 mL, 214.0 mmol) and DMAP (2.61 g, 21.4 mmol) were dissolved in DMF (350 mL) and stirred at room temperature for 16 hours. The reaction mixture was filtered, poured into water (350 mL) and extracted with EtOAc (4 x 200 mL). The organic extracts were combined and concentrated *in vacuo* to afford a dark yellow oil. The crude product was purified by column chromatography (silica gel, eluted with hexane/EtOAc, 17:3) to give the title compound as a pale yellow oil (31.09 g, 80%).

R_f	0.40 (hexane/EtOAc, 17:3).
^{1}H NMR	(400 MHz, $CDCl_3$): δ 2.63 (s, 3H, C=C(OH)C<u>H</u>$_3$), 2.55 (s, 2H, C<u>H</u>$_2$), 2.38 (s, 2H, C<u>H</u>$_2$), 1.10 (s, 6H, C(C<u>H</u>$_3$)$_2$).
^{13}C NMR	(100 MHz, $CDCl_3$): δ 203.4 (C), 198.8 (C), 196.1 (C), 113.3 (C), 53.4 (CH_2), 47.9 (CH_2), 31.6 (C), 29.5 (CH_3), 29.1 (CH_3).
FT-IR	ν (cm^{-1}): 2958, 2872, 1738, 1659, 1545.
LRMS	(ESI): 363.0 $[M-H]^-$ (100).
HPLC	8.4 min, 100% (λ = 220 nm, gradient 1).

N^1,N^9-*bis*-1-(4,4-Dimethyl-2,6-dioxocyclohexylidene)ethyl-norspermidine (98)[103]

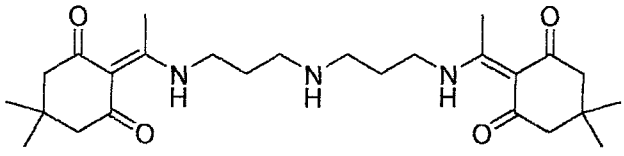

Norspermidine (0.96 mL, 6.9 mmol) and 2-acetyl dimedone (2.50 g, 13.7 mmol) were dissolved in ethanol (47 mL) and heated at reflux for 2 hrs. The solvent was removed *in vacuo* and the resulting yellow oil dissolved in EtOAc (50 mL), washed with water (3 x 50 mL), dried ($MgSO_4$) and concentrated *in vacuo* to give the title compound as a colourless oil (3.13 g, 99%).

R_f	0.39 (DCM/MeOH, 17:3).
^{1}H NMR	(400 MHz, $CDCl_3$): δ 13.40 (bs, 2H, 2 x C=C(CH_3)N<u>H</u>), 3.49 (m, 4H, 2 x C=C(CH_3)NHC<u>H</u>$_2$), 2.74 (t, 4H, J = 7, C<u>H</u>$_2$NHC<u>H</u>$_2$), 2.56 (s, 6H, 2 x C=C(C<u>H</u>$_3$)NH), 2.35 (s, 8H, 4 x COC<u>H</u>$_2$), 1.83 (tt, 4H, J = 7, 7, 2 x CH_2C<u>H</u>$_2$$CH_2$), 1.50 (bs, 1H, CH_2N<u>H</u>CH_2), 1.02 (s, 12H, 2 x C(C<u>H</u>$_3$)$_2$).
^{13}C NMR	(100 MHz, $CDCl_3$): δ 197.8 (C), 173.8 (C), 108.2 (C), 53.2 (CH_2), 47.1 (CH_2), 41.6 (CH_2), 30.4 (C), 29.7 (CH_2), 28.5 (CH_3), 18.2 (CH_3).
FT-IR	ν (cm^{-1}): 2954, 2867, 2958, 1633, 1567.
LRMS	(ESI): 460.4 $[M+H]^+$ (100), 919.8 $[2M+H]^+$ (18).
HRMS	(ESI): Found 460.3167, $C_{26}H_{42}N_3O_4$ requires 460.3170.
HPLC	6.3 min, 100% (λ = 220 nm, gradient 1).

N^1,N^{10}- *bis*-1-(4,4-Dimethyl-2,6-dioxocyclohexylidene)ethyl-spermidine (99)[82]

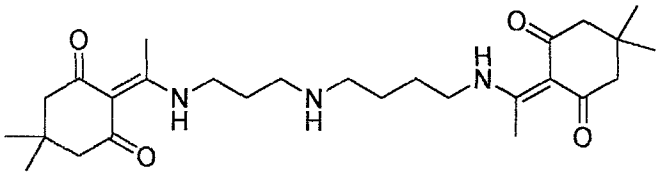

Spermidine (2.14 g, 14.7 mmol) and 2-acetyldimedone (5.36 g, 29.4 mmol) were dissolved in ethanol (100 mL) and heated at reflux for 2 hours. The solvent was removed *in vacuo* and the resulting yellow oil dissolved in EtOAc (100 mL), washed with water (3 x 100 mL), dried ($MgSO_4$) and concentrated *in vacuo* to give the title compound as a colourless oil (6.83 g, 98%).

R_f	0.42 (DCM/MeOH, 17:3).
^{1}H NMR	(400 MHz, $CDCl_3$): δ 13.44 (bs, 2H, 2 x C=C(CH_3)N<u>H</u>), 3.48 (m, 2H, C=C(CH_3)NHC<u>H</u>$_2$), 3.41 (m, 2H, C=C(CH_3)NHC<u>H</u>$_2$), 2.72 (t, 2H, J = 7, C<u>H</u>$_2$NHCH_2), 2.64 (t, 2H, J = 7, C<u>H</u>$_2$NHCH_2), 2.56 (m, 6H, 2 x C=C(C<u>H</u>$_3$)NH), 2.35 (s, 8H, 4 x COC<u>H</u>$_2$), 1.82 (m, 2H, NHCH_2C<u>H</u>$_2$CH_2NH), 1.73 (m, 2H, CH_2C<u>H</u>$_2$CH_2), 1.58 (m, 2H, CH_2C<u>H</u>$_2$CH_2), 1.02 (s, 12H, 2 x C(C<u>H</u>$_3$)$_2$).
^{13}C NMR	(100 MHz, $CDCl_3$): δ 198.1 (C), 173.9 (C), 108.3 (C), 53.3 (CH_2), 49.7 (CH_2), 47.1 (CH_2), 43.7 (CH_2), 41.7 (CH_2), 30.5 (CH_2), 30.0 (C), 28.7 (CH_3), 27.8 (CH_2), 27.3 (CH_2), 18.3 (CH_3).
FT-IR	ν (cm^{-1}): 2933, 1631, 1565, 1463, 1320.
LRMS	(ESI): 474.4 $[M+H]^+$ (100), 496.4 $[M+Na]^+$ (48).
HRMS	(ESI): Found 474.3319, $C_{27}H_{44}N_3O_4$ requires 474.3327.
HPLC	6.5 min, 100% (λ = 220 nm, gradient 1).

4-Formylphenoxyallylacetate (101)[86]

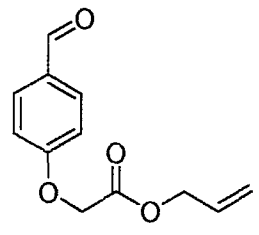

To a mixture of 4-hydroxybenzaldehyde (10.00 g, 81.9 mmol), KI (1.36 g, 8.2 mmol) and K_2CO_3 (27.18 g, 196.6 mmol) in MeCN (300 mL) was added allylchloroacetate (12.12 g, 90.1 mmol) dropwise. The reaction mixture was heated at reflux for 6 hours, cooled, filtered and the filtrate concentrated *in vacuo* to afford a yellow oil. The crude product was purified by column chromatography (silica gel, eluted with hexane/EtOAc, 17:3) to afford the title compound as a colourless oil (17.61 g, 97%).

R_f	0.42 (hexane/EtOAc, 1:1).
^{1}H NMR	(400 MHz, $CDCl_3$): δ 9.90 (s, 1H, C<u>H</u>O), 7.86 (d, 2H, J = 9, 2 x ArC<u>H</u>), 7.01 (d, 2H, J = 9, 2 x ArC<u>H</u>), 5.91 (ddt,1H, J = 18, 10.5, 6, C<u>H</u>=CH_2), 5.34 (dd, 1H, J = 18, 1, CH=CH<u>H</u>), 5.28 (dd, 1H, J = 10.5, 1, CH=C<u>H</u>H), 4.72 (s, 2H, OC<u>H</u>$_2$), 4.71 (d, 2H, J = 6, C<u>H</u>$_2$CH=CH_2).
^{13}C NMR	(100 MHz, $CDCl_3$): δ 192.1 (CH), 169.2 (C), 164.0 (C), 133.4 (CH), 132.6 (CH), 132.2 (C), 120.8 (CH), 116.3 (CH_2), 67.5 (CH_2), 66.6 (CH_2).
FT-IR	ν (cm^{-1}) 2833, 1755, 1687, 1598.
LRMS	(EI): 220.18 $[M]^+$ (56), 135.14 (100), 105.12 (71), 77.14 (70).

4-Hydroxymethylphenoxyallylacetate (102)[86]

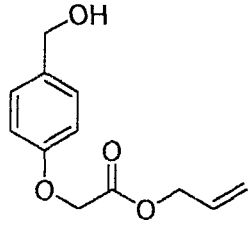

101 (17.50 g, 79.5 mmol), $NaBH_3CN$ (7.49 g, 119.0 mmol) and a trace of bromocreosol green were dissolved in THF/water (1:1, 180 mL) and stirred at 0 °C. The reaction mixture was maintained below pH 4.0 by the addition of conc. HCl over 2 hrs. The reaction mixture was concentrated *in vacuo*, the resulting residue taken into brine (200 mL) and extracted with EtOAc (3 x 100 mL). The combined extracts were concentrated *in vacuo* to afford a green oil, which was purified by column chromatography (silica gel, eluted with hexane/EtOAc, 7:3 to 1:1) to afford the title compound as a colourless oil (16.08 g, 91%).

R_f	0.32 (hexane/EtOAc, 1:1).
^{1}H NMR	(400 MHz, $CDCl_3$): δ 7.29 (d, 2H, J = 8.5, 2 x ArC<u>H</u>), 6.89 (d, 2H, J = 8.5, 2 x ArC<u>H</u>), 5.91 (ddt, 1H, J = 17, 10.5, 6, C<u>H</u>=CH_2), 5.34 (dd, 1H, J = 17, 1, CH=CH<u>H</u>), 5.27 (dd, 1H, J = 10.5, 1, CH=CH<u>H</u>), 4.70 (d, 2H, J = 6, $C\underline{H}_2CH=CH_2$), 4.65 (s, 2H, $OC\underline{H}_2$), 4.61 (s, 2H, $OC\underline{H}_2$).
^{13}C NMR	(100 MHz, $CDCl_3$): δ 168.9 (C), 157.7 (C), 134.6 (C), 131.7 (CH), 128.9 (CH), 119.4 (CH_2), 115.1 (CH), 66.2 (CH_2), 65.7 (CH_2), 65.1 (CH_2).
FT-IR	ν (cm^{-1}): 3388, 1758, 1612, 1586, 1510.
LRMS	(EI): 222.19 $[M]^+$ (38), 137.15 (45), 107.14 (85), 41.22 (100).

4'-Nitrophenyl-(4-hydroxymethylphenoxyallylacetate) carbonate (103)[86]

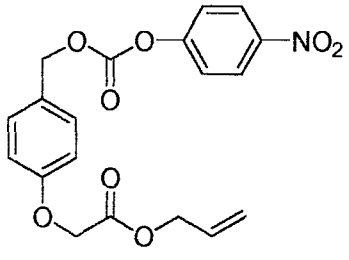

To a stirred solution of **102** (7.00 g, 31.5 mmol) and pyridine (3.05 mL, 37.8 mmol) in DCM (70 mL) at 0 °C was added 4-nitrophenylchloroformate (7.00 g, 34.7 mmol) in DCM (35 mL) dropwise over 20 min. The reaction was allowed to warm to room temperature, stirred for a further hour and concentrated *in vacuo*. The residue was taken into ice-cold HCl (1N, 100 mL) and extracted into EtOAc (2 x 100 mL). The organic extracts were combined, washed with brine (2 x 100 mL), dried ($MgSO_4$) and concentrated *in vacuo* to yield the title compound as a pale yellow solid (9.99 g, 82%).

R_f	0.58 (hexane/EtOAc, 1:1).
^{1}H NMR	(400 MHz, $CDCl_3$): δ 8.15 (d, 2H, J = 9, 2 x ArC<u>H</u>), 7.30-7.24 (m, 4H, 4 x ArC<u>H</u>), 6.83 (d, 2H, J = 8.5, 2 x ArC<u>H</u>), 5.82 (ddt, 1H, J = 17, 10.5, 6, C<u>H</u>=CH_2), 5.27-5.10 (m, 4H, CH=C<u>H_2</u>, OC<u>H_2</u>), 4.62-4.55 (m, 4H, OC<u>H_2</u>, C<u>H_2</u>CH=CH_2).
^{13}C NMR	(100 MHz, $CDCl_3$): δ 168.5 (C), 158.6 (C), 155.7 (C), 152.6 (C), 145.5 (C), 131.5 (CH), 130.8 (CH), 127.7 (C), 125.4 (CH), 121.8 (CH), 119.3 (CH_2), 115.0 (CH), 70.8 (CH_2), 66.1 (CH_2), 65.4 (CH_2).
FT-IR	ν (cm^{-1}): 1758, 1515, 1204, 1173, 1079.
HPLC	10.8 min, 100% (λ = 220 nm, gradient 1).

N^1,N^9-*bis*-1-(4,4-Dimethyl-2,6-dioxocyclohexylidene)ethyl-N^5-(4-(allyloxycarbonylmethoxy)phenyl-methoxycarbonyl)-norspermidine (104)

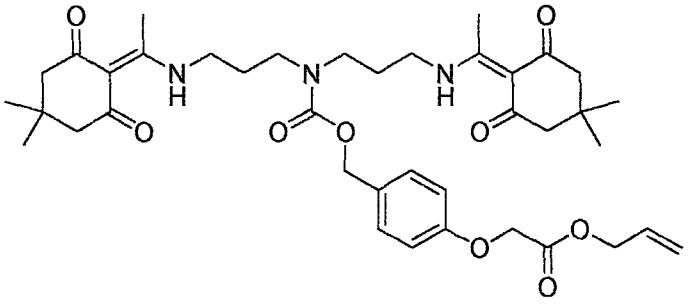

98 (3.00 g, 6.5 mmol) and **103** (3.03 g, 7.8 mmol) were dissolved in DMF (20 mL) and stirred at room temperature overnight. The reaction mixture was poured into 1M $KHSO_4$ (100 mL) and extracted with EtOAc (3 x 100 mL). The combined organic extracts were washed with water (5 x 100 mL), dried ($MgSO_4$) and concentrated *in vacuo*. The resulting oily residue was purified by column chromatography (silica gel, eluted with EtOAc then EtOAc/MeOH, 49:1) to give the title compound as a colourless oil (2.61 g, 74%).

R_f	0.20 (EtOAc/MeOH, 49:1).
^{1}H NMR	(400 MHz, $CDCl_3$): δ 13.50 (bs, 2H, 2 x NH), 7.28 (d, 2H, J = 9, 2 x ArCH), 6.86 (d, 2H, J = 9, 2 x ArCH), 5.91 (ddt, 1H, J = 17, 10.5, 5.5, CH=CH_2), 5.33 (dd, 1H, J = 17, 1, CH=CHH), 5.26 (dd, 1H, J = 10.5, 1, CH=CHH), 5.06 (s, 2H, OCH_2), 4.69 (d, 2H, J = 5.5, CH_2CH=CH_2), 4.65 (s, 2H, OCH_2), 3.43-3.30 (m, 8H, 2 x $CH_2CH_2CH_2$), 2.55-2.45 (m, 6H, 2 x C=C(CH_3)NH), 2.34 (s, 8H, 4 x $CH_2C(CH_3)_2$), 1.93-1.82 (m, 4H, 2 x $CH_2CH_2CH_2$), 1.01 (s, 12H, 2 x $C(CH_3)_2$).
^{13}C NMR	(100 MHz, $CDCl_3$): δ 197.3 (C), 173.6 (C), 168.5 (C), 157.8 (C), 156.2 (C), 131.5 (CH), 130.2 (CH), 129.7 (C), 119.3 (CH_2), 114.7 (CH), 108.0 (C), 67.2 (CH_2), 66.0 (CH_2), 65.3 (CH_2), 53.6 (CH_2), 45.1 (CH_2), 44.4 (CH_2), 40.7 (CH_2), 30.2 (C), 28.3 (CH_3), 17.9 (CH_3).
FT-IR	ν (cm^{-1}): 2955, 2859, 2958, 1758, 1636, 1570.

LRMS (ESI): 708.2 $[M+H]^+$ (100).

HRMS (ESI): Found 708.3865, $C_{39}H_{54}N_3O_9$ requires 708.3855.

HPLC 10.0 min, 100% (λ = 220 nm, gradient 1).

N^1,N^{10}-*bis*-1-(4,4-Dimethyl-2,6-dioxocyclohexylidene)ethyl-N^5-(4-(allyloxycarbonylmethoxy)phenyl-methoxycarbonyl)-spermidine (105)

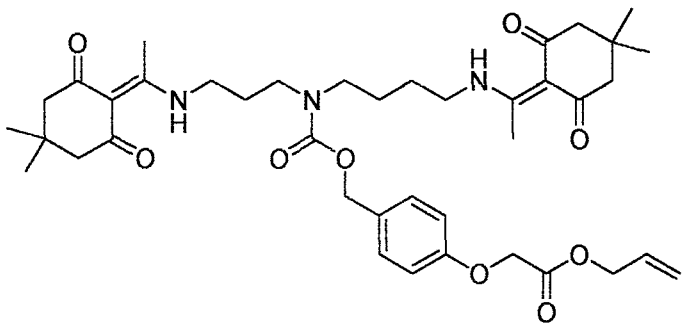

99 (3.08 g, 6.5 mmol) and **103** (3.03 g, 7.8 mmol) were reacted as above. The resulting oily residue was purified by column chromatography (silica gel, eluted with EtOAc then EtOAc/MeOH, 49:1) to yield the title compound as a colourless oil (3.03 g, 84%).

R_f 0.23 (EtOAc/MeOH, 49:1).

^{1}H NMR (400 MHz, $CDCl_3$): δ 13.52-13.41 (m, 2H, 2 x NH), 7.28 (d, 2H, J = 9, 2 x ArCH), 6.88 (d, 2H, J = 9, 2 x ArCH), 5.92 (ddt, 1H, J = 17.5, 10.5, 6, CH=CH_2), 5.34 (dd, 1H, J = 17.5, 1, CH=CHH), 5.27 (dd, 1H, J = 10.5, 1, CH=CHH), 5.06 (s, 2H, OCH_2), 4.71 (d, 2H, J = 6, CH_2CH=CH_2), 4.66 (s, 2H, OCH_2), 3.48-3.22 (m, 8H, 2 x $NHCH_2$, $CH_2N(CO_2)CH_2$), 2.58-2.41 (m, 6H, 2 x C=C(CH_3)NH), 2.35 (s, 8H, 4 x $CH_2C(CH_3)_2$), 1.98-1.84 (m, 2H, $NHCH_2CH_2CH_2NH$), 1.70-1.59 (m, 4H, $CH_2CH_2CH_2CH_2$), 1.02 (s, 12H, 2 x $C(CH_3)_2$).

^{13}C NMR (100 MHz, $CDCl_3$): δ 197.2 (C), 173.9 (C), 168.9 (C), 158.2 (C), 156.6 (C), 131.8 (CH), 130.4 (CH), 130.2 (C), 119.5 (CH_2), 115.1 (CH), 108.4 (C), 67.4 (CH_2), 66.3 (CH_2), 65.7 (CH_2), 53.9 (CH_2), 52.6 (CH_2), 47.2

(CH_2), 45.4 (CH_2), 43.3 (CH_2), 41.4 (CH_2), 30.5 (C), 28.7 (CH_3), 26.6 (CH_2), 18.3 (CH_3).

FT-IR ν (cm^{-1}): 2955, 1758, 1695, 1635, 1570.

LRMS (ESI): 722.5 $[M+H]^+$ (100), 744.5 $[M+Na]^+$ (100).

HRMS (ESI): Found 744.3830, $C_{40}H_{55}N_3O_9Na$ requires 744.3830.

HPLC 10.4 min, 100% (λ = 220 nm, gradient 1).

N^1,N^9-*bis*-1-(4,4-Dimethyl-2,6-dioxocyclohexylidene)ethyl-N^5-4-((carboxy-methyl)phenyl-methoxy-carbonyl)-norspermidine (106)

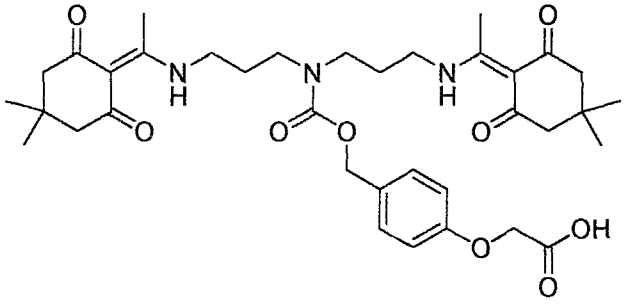

A solution of **104** (2.40 g, 3.4 mmol) in DCM/THF (1:1, 21 mL) was purged with N_2 for 1 hour. Thiosalicylic acid (1.05 g, 6.8 mmol) and $Pd(PPh_3)_4$ (0.39 g, 0.3 mmol) were added and the reaction mixture stirred at room temperature for 2 hours. Solvent was removed *in vacuo* and the resulting oily residue purified by column chromatography (silica gel, eluted with EtOAc then EtOAc/MeOH, 3:2) to yield the title compound as a colourless oil (1.59 g, 70%).

R_f 0.18 (EtOAc/MeOH, 2:1).

^{1}H NMR (400 MHz, $CDCl_3$): δ 13.40 (bs, 2H, 2 x NH), 7.30 (d, 2H, J = 8.5, 2 x ArCH), 6.88 (d, 2H, J = 8.5, 2 x ArCH), 5.08 (s, 2H, OCH_2), 4.67 (s, 2H, OCH_2), 3.43-25 (m, 8H, 2 x $CH_2CH_2CH_2$), 2.52-2.33 (m, 14H, 2 x C=C(CH_3)NH, 4 x $CH_2C(CH_3)_2$), 1.96-1.80 (m, 4H, 2 x $CH_2CH_2CH_2$), 1.03 (s, 12H, 2 x $C(CH_3)_2$).

^{13}C NMR (100 MHz, $CDCl_3$): δ 197.3 (C), 172.8 (C), 169.8 (C), 156.9 (C), 155.8 (C), 129.3 (CH), 128.7 (C), 113.6 (CH), 107.0 (C), 66.0 (CH_2), 65.2 (CH_2), 51.7 (CH_2), 42.0 (CH_2), 40.1 (CH_2), 29.1 (C), 27.2 (CH_3), 25.2 (CH_2), 16.9 (CH_3).

FT-IR ν (cm^{-1}): 2950, 1692, 1561.

LRMS (ESI): 668.5 $[M+H]^+$ (100), 690.5 $[M+Na]^+$ (40).

HRMS (ESI): Found 668.3563, $C_{36}H_{50}N_3O_9$ requires 668.3542.

HPLC 8.5 min, 100% (λ = 220 nm, gradient 1).

N^1,N^{10}-*bis*-1-(4,4-Dimethyl-2,6-dioxocyclohexylidene)ethyl-N^5-4-((carboxy-methyl)phenyl-methoxy-carbonyl))-spermidine (107)

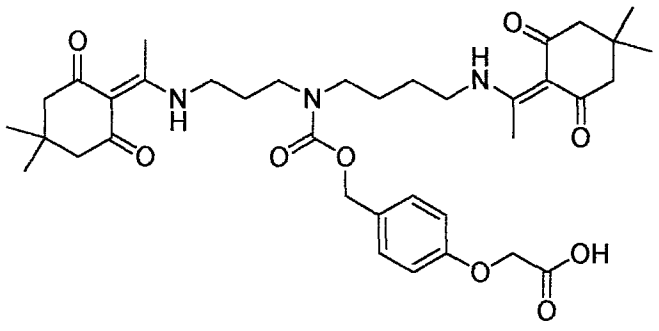

The allyl ester was removed from **105** (2.80g, 3.9 mmol) in an identical manner to the preparation of **106** described above to give the title compound as a colourless oil (2.09 g, 79%).

***R*$_f$** 0.22 (EtOAc/MeOH, 2:1).

^{1}H NMR (400 MHz, $CDCl_3$): δ 13.38 (bs, 2H, 2 x NH), 7.29 (d, 2H, J = 8.5, 2 x ArCH), 6.88 (d, 2H, J = 8.5, 2 x ArCH), 5.06 (s, 2H, OCH_2), 4.67 (s, 2H, OCH_2), 3.49-3.20 (m, 8H, 2 x $NHCH_2$, $CH_2N(CO_2)CH_2$), 2.57-2.28 (m, 14H, 2 x C=C(CH_3)NH, 4 x $CH_2C(CH_3)_2$), 1.95-1.79 (m, 2H, $NHCH_2CH_2CH_2NH$), 1.70-1.52 (m, 4H, $NHCH_2CH_2CH_2CH_2NH$), 1.03 (s, 12H, 2 x $C(CH_3)_2$).

^{13}C NMR (100 MHz, $CDCl_3$): δ 199.0 (C), 174.9 (C), 171.1 (C), 157.9 (C), 157.0 (C), 130.2 (CH), 129.6 (C), 114.8 (CH), 107.8 (C), 67.2 (CH_2), 65.2 (CH_2), 51.9 (CH_2), 46.4 (CH_2), 43.5 (CH_2), 41.6 (CH_2), 41.3 (CH_2), 30.3 (C), 28.2 (CH_2), 28.1 (CH_2), 28.0 (CH_3), 26.0 (CH_2), 16.6 (CH_3).

FT-IR ν (cm^{-1}): 2957, 1692, 1631, 1568.

LRMS (ESI): 682.5 $[M+H]^+$ (38), 704.5 $[M+Na]^+$ (100).

HRMS (ESI): Found 704.3497, $C_{37}H_{51}N_3O_9Na$ requires 704.3517.

HPLC 8.7 min, 100% (λ = 220 nm, gradient 1).

Polymer supported *N*^{1},*N*^{9}-*bis*-1-(4,4-dimethyl-2,6-dioxocyclohexylidene)ethyl-norspermidine (108)

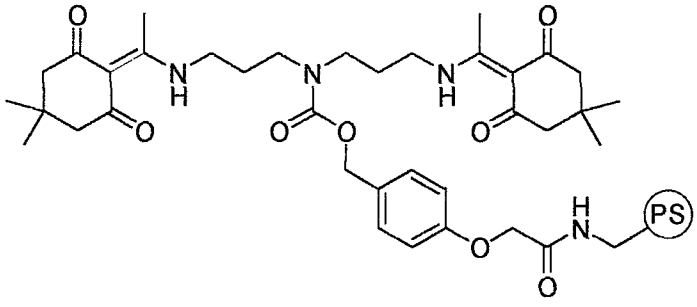

106 (1.50 g, 2.3 mmol) was coupled to aminomethyl-polystyrene resin (1% DVB cross-linked, 1.11 mmol/g, 1.35 g, 1.5 mmol, general procedure A with the exceptions that 1.5 eq. of reagents were used and the reaction was carried out overnight). A small portion of resin was treated according to general procedure B to remove the Dde groups and loading, measured by a quantitative ninhydrin test, determined to be 1.32 mmol/g of amine (equivalent to 0.66 mmol/g of norspermidine).

FT-IR ν (cm^{-1}): 2928, 1697, 1637, 1573, 1452.

Polymer supported N^1,N^{10}- *bis*-1-(4,4-dimethyl-2,6-dioxocyclohexylidene)ethyl-spermidine (109)

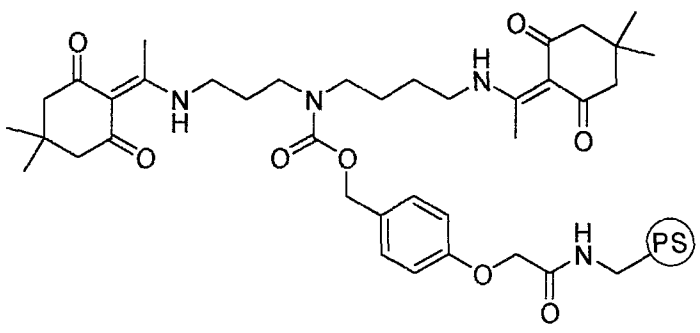

107 (1.95 g, 2.9 mmol) was coupled to aminomethyl-polystyrene resin (1% DVB cross-linked, 1.11 mmol/g, 1.72 g, 1.9 mmol) in an identical manner to the preparation of **108** described above. A small portion of resin was treated according to general procedure B to remove the Dde groups and loading, measured by quantitative ninhydrin test, determined to be 1.24 mmol/g of amine (equivalent to 0.62 mmol/g of spermidine).

FT-IR ν (cm^{-1}): 2929, 1697, 1637, 1573, 1453.

N^1,N^9-*bis*-(*L*-Tryptophanyl-*L*-arginyl)-norspermidine (110), N^1-*L*-tryptophanyl-*L*-arginyl-N^9-*L*-tryptophanyl-*L*-arginyl(2,2,5,7,8-pentamethylchroman-6-sulfonamide)-norspermidine (111), N^1,N^9-*bis*-(*L*-tryptophanyl-*L*-arginyl(2,2,5,7,8-pentamethylchroman-6-sulfonamide))-norspermidine (112)

The Dde groups of resin **108** (0.60 g, 0.4 mmol) were removed (general procedure B) and Fmoc-Arg(Pmc)-OH was coupled to the resulting amine-resin (general procedure A). The Fmoc group was then removed (general procedure C) and Boc-Trp(Boc)-OH was coupled to the resulting amine-resin (general procedure A). Cleavage from the resin was accomplished (general procedure J) and the desired compounds were purified as their TFA salts by semi-prep HPLC.

N^1,N^9-*bis*-(*L*-Tryptophanyl-*L*-arginyl)-norspermidine (110)

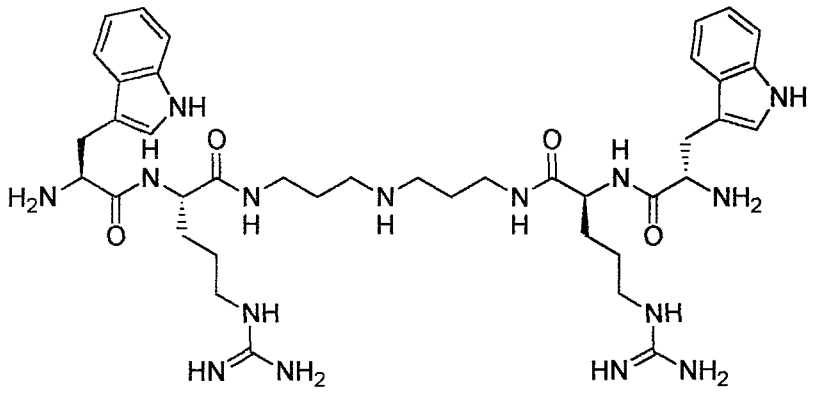

Semi-prep HPLC R_t = 22.4 min (gradient 3), yield = 25 mg, 7%.

^{1}H NMR (400 MHz, CD_3OD): δ 7.71 (d, 2H, J = 7.5, 2 x ArC<u>H</u>), 7.44 (d, 2H, J = 7.5, 2 x ArC<u>H</u>), 7.30 (s, 2H, 2 x ArC<u>H</u>), 7.19 (t, 2H, J = 7.5, 2 x ArC<u>H</u>), 7.11 (t, 2H, J = 7.5, 2 x ArC<u>H</u>), 4.36-4.27 (m, 4H, 2 x Arg αC<u>H</u>, 2 x Trp αC<u>H</u>), 3.50 (dd, 2H, J = 15, 6, 2 x Trp βCH<u>H</u>), 3.40-3.17 (m, 10H, 2 x Trp βCH<u>H</u>, 2 x Arg δC<u>H</u>$_2$, 2 x CONHC<u>H</u>$_2$), 2.99-2.93 (m, 4H, C<u>H</u>$_2$NHC<u>H</u>$_2$), 1.94-1.59 (m, 12H, 2 x Arg βC<u>H</u>$_2$, 2 x Arg γC<u>H</u>$_2$, 2 x NHCH$_2$C<u>H</u>$_2$CH$_2$NH).

^{13}C NMR (100 MHz, CD_3OD): δ 173.9 (C), 170.2 (C), 158.5 (C), 138.0 (C), 128.1 (C), 125.5 (CH), 122.8 (CH), 120.2 (CH), 119.0 (CH), 112.5 (CH), 107.7 (C), 54.6 (CH), 54.5 (CH), 46.2 (CH_2), 41.7 (CH_2), 36.9 (CH_2), 30.0 (CH_2), 28.5 (CH_2), 27.2 (CH_2), 26.1 (CH_2).

LRMS (ESI): 816.5 $[M+H]^+$ (100).

HRMS (ESI): Found 816.5103, $C_{40}H_{62}N_{15}O_4$ requires 816.5103.

HPLC 11.8 min, 100% (λ = 220 nm, gradient 2).

N^1-*L*-Tryptophanyl-*L*-arginyl(2,2,5,7,8-pentamethylchroman-6-sulfonamide)-N^9-*L*-tryptophanyl-*L*-arginyl-norspermidine (111)

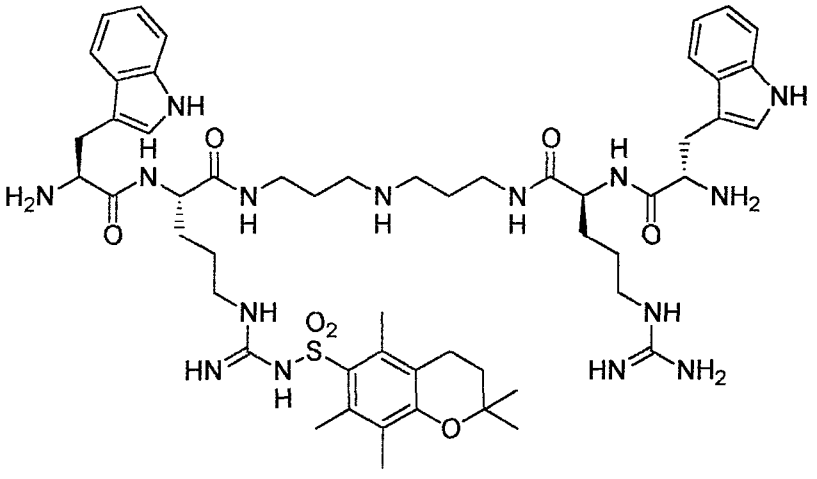

Semi-prep HPLC R_t = 33.8 min (gradient 3), yield = 23 mg, 5%.

^{1}H NMR (400 MHz, CD_3OD): δ 7.67 (d, 2H, J = 7.5, 2 x ArC<u>H</u>), 7.40 (d, 2H, J = 7.5, 2 x ArC<u>H</u>), 7.26 (s, 2H, 2 x ArC<u>H</u>), 7.15 (t, 2H, J = 7.5, 2 x ArC<u>H</u>), 7.06 (t, 2H, J = 7.5, 2 x ArC<u>H</u>), 4.40 (bs, 1H, Arg αC<u>H</u>), 4.33-4.22 (m, 3H, Arg αC<u>H</u>, 2 x Trp αC<u>H</u>), 3.50-3.42 (m, 2H, 2 x Trp βCH<u>H</u>), 3.31-3.11 (m, 10H, 2 x CONHC<u>H</u>$_2$, 2 x Trp βCH<u>H</u>, 2 x Arg δC<u>H</u>$_2$), 2.98-2.92 (m, 4H, C<u>H</u>$_2$NHC<u>H</u>$_2$), 2.65 (t, 2H, J = 6.5, ArC<u>H</u>$_2$), 2.59 (s, 3H, ArC<u>H</u>$_3$), 2.57 (s, 3H, ArC<u>H</u>$_3$), 2.11 (s, 3H, ArC<u>H</u>$_3$), 1.90-1.54 (m, 14H, 2 x Arg βC<u>H</u>$_2$, 2 x Arg γC<u>H</u>$_2$, 2 x NHCH$_2$C<u>H</u>$_2$CH$_2$NH, ArCH$_2$C<u>H</u>$_2$), 1.31 (s, 6H, C(C<u>H</u>$_3$)$_2$).

^{13}C NMR (100 MHz, CD_3OD): δ 174.5 (C), 174.2 (C), 170.4 (C), 170.1 (C), 158.7 (C), 154.9 (C), 138.2 (C), 136.6 (C), 136.2 (C), 134.3 (C), 128.3 (C), 125.7 (CH), 125.1 (C), 123.0 (CH), 120.4 (CH), 119.5 (C), 119.2 (CH), 112.6 (CH), 107.9 (C), 74.9 (C), 54.8 (CH), 54.5 (CH), 46.5 (CH_2), 46.5 (CH_2), 41.9 (CH_2), 37.1 (CH_2), 33.7 (CH_2), 30.3 (CH_2), 30.2 (CH_2), 28.7 (CH_2), 27.4 (CH_2), 27.4 (CH_2), 26.9 (CH_3), 26.3 (CH_2), 22.3 (CH_2), 19.0 (CH_3), 17.9 (CH_3), 12.3 (CH_3).

LRMS (ESI): 542.2 $[M+2H]^{2+}$ (100), 1082.9 $[M+H]^+$ (13).

HPLC 14.2 min, 100% (λ = 220 nm, gradient 2).

<u>*N*^{1},*N*^{9}-*bis*-(*L*-Tryptophanyl-*L*-arginyl(2,2,5,7,8-pentamethylchroman-6-sulfonamide))-norspermidine (112)</u>

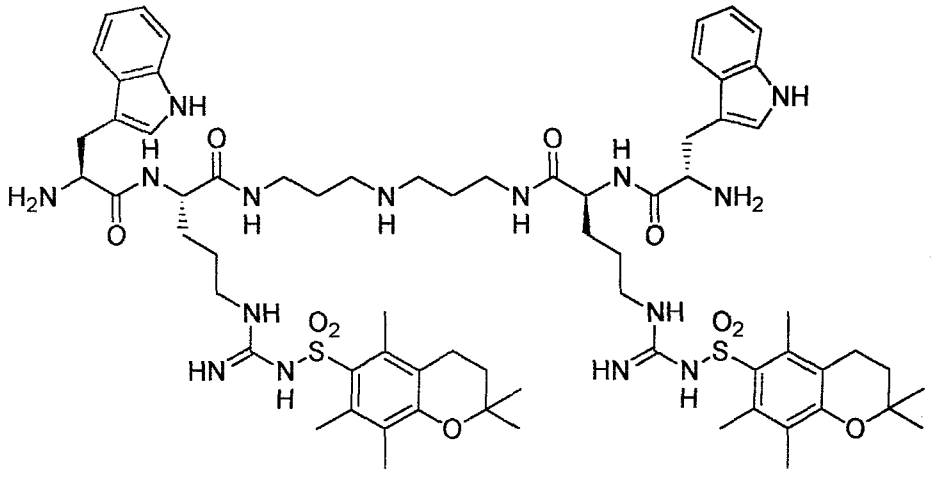

Semi-prep HPLC R_t = 43.5 min (gradient 3), yield = 28 mg, 5%.

^{1}H NMR (400 MHz, CD_3OD): δ 7.63 (d, 2H, *J* = 8, 2 x ArC<u>H</u>), 7.36 (d, 2H, *J* = 8, 2 x ArC<u>H</u>), 7.23 (s, 2H, 2 x ArC<u>H</u>), 7.11 (t, 2H, *J* = 8, 2 x ArC<u>H</u>), 7.03 (t, 2H, *J* = 8, 2 x ArC<u>H</u>), 4.39 (bs, 2H, 2 x Arg αC<u>H</u>), 4.22 (m, 2H, 2 x Trp αC<u>H</u>), 3.43 (dd, 2H, *J* = 15, 6, 2 x Trp βCH<u>H</u>), 3.33-3.16 (m, 8H, 2 x Trp βCH<u>H</u>, 2 x Arg δCH<u>H</u>, 2 x CONHC<u>H</u>$_2$), 3.13-3.07 (m, 2H, 2 x Arg δCH<u>H</u>), 2.98-2.94 (m, 4H, C<u>H</u>$_2$NHC<u>H</u>$_2$), 2.62 (t, 4H, *J* = 6.5, 2 x ArC<u>H</u>$_2$CH$_2$), 2.56 (s, 6H, 2 x ArC<u>H</u>$_3$), 2.54 (s, 6H, 2 x ArC<u>H</u>$_3$), 2.08 (s, 6H, 2 x ArC<u>H</u>$_3$), 1.90-1.75 (m, 10H, 2 x NHCH$_2$C<u>H</u>$_2$CH$_2$NH, 2 x ArCH$_2$C<u>H</u>$_2$, 2 x Arg βCH<u>H</u>), 1.74-1.63 (m, 2H, 2 x Arg βCH<u>H</u>), 1.60-1.51 (m, 4H, 2 x Arg γC<u>H</u>$_2$), 1.29 (s, 12H, 2 x C(C<u>H</u>$_3$)$_2$).

^{13}C NMR (100 MHz, CD_3OD): δ 174.4 (C), 170.2 (C),158.2 (C), 155.0 (C), 138.2 (C), 136.5 (C), 136.1 (C), 134.3 (C), 128.4 (C), 125.7 (CH), 125.2 (C), 122.9 (CH), 120.4 (CH), 119.5 (C), 119.2 (CH), 112.6 (CH), 107.9 (C), 75.0 (C), 54.8 (CH), 54.5 (CH), 46.6 (CH_2), 37.1 (CH_2), 33.7 (CH_2), 30.3

(CH_2), 28.8 (CH_2), 27.5 (CH_2), 26.9 (CH_3), 22.4 (CH_2), 19.1 (CH_3), 18.0 (CH_3), 12.3 (CH_3).

LRMS (ESI): 675.4 $[M+2H]^{2+}$ (100), 1349.0 $[M+H]^{+}$ (22).

HPLC 16.2 min, 100% (λ = 220 nm, gradient 2).

Nortrypanothione disulfide (115)[108]

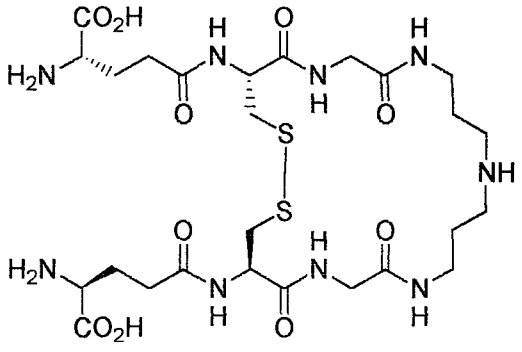

The Dde groups of resin **108** (0.60 g, 0.4 mmol) were removed (general procedure B) and Fmoc-Gly-OH was coupled to the resulting amine-resin (general procedure A with the exception that DMF was used as solvent). The Fmoc group was removed (general procedure C) and Fmoc-Cys(Trt)-OH coupled to the resulting amine-resin (general procedure A). The Fmoc group was removed (general procedure C) and Boc-Glu-O^{t}Bu coupled to the resulting amine-resin (general procedure A), trityl deprotection and disulfide-bond formation accomplished (general procedure D) and cleavage from the resin achieved (general procedure I). The desired compound was purified as the TFA salt by semi-prep HPLC.

Semi-prep HPLC R_t = 16.1 min (gradient 4), yield = 38 mg, 12%.

^{1}H NMR (400 MHz, D_2O): δ 4.92-4.86 (m, 2H, 2 x Cys αC$\underline{H}$), 4.18-3.95 (m, 6H, 2 x Gly αC$\underline{H}_2$, 2 x Glu αC$\underline{H}$), 3.56-3.43 (m, 4H, 2 x CONHC$\underline{H}_2$C$\underline{H}_2$), 3.40 (dd, 2H, J = 14, 6, 2 x Cys βCH$\underline{H}$), 3.25 (dd, 2H, J = 14, 6, 2 x Cys βCH$\underline{H}$), 3.20-3.13 (m, 4H, C$\underline{H}_2$NHC$\underline{H}_2$), 2.80-2.65 (m, 4H, 2 x Glu

γC$\underline{H}_2$), 2.42-2.30 (m, 4H, 2 x Glu βC$\underline{H}_2$), 2.11-2.00 (m, 4H, 2 x $CH_2C\underline{H}_2CH_2$).

^{13}C NMR (100 MHz, D_2O): δ 181.7 (C), 175.0 (C), 173.1 (C), 172.0 (C), 53.2 (CH), 52.9 (CH), 43.3 (CH_2), 38.3 (CH_2), 36.4 (CH_2), 31.3 (CH_2), 26.0 (CH_2), 26.0 (CH_2), 25.9 (CH_2).

LRMS (ESI): 730.4 $[M+Na]^+$ (100), 708.4 $[M+H]^+$ (5).

HPLC 8.1 min, 100% (λ = 220 nm, gradient 2).

Trypanothione disulfide (13)[108]

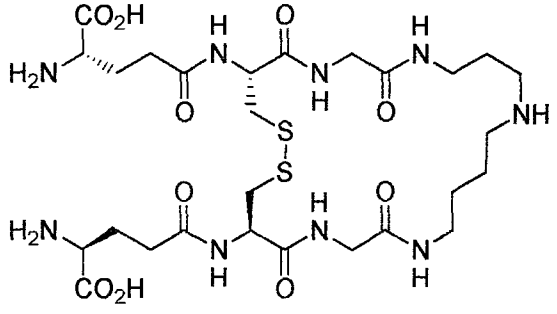

The title compound was prepared from resin **109** (0.50 g, 0.3 mmol) in an identical manner to the preparation of **115**. The desired compound was purified as the TFA salt by semi-prep HPLC.

Semi-prep HPLC R_t = 17.2 min (gradient 4), yield = 16 mg, 5%.

^{1}H NMR (400 MHz, D_2O): δ 4.92-4.85 (m, 2H, 2 x Cys αC$\underline{H}$), 4.15-4.05 (m, 4H, 2 x Gly αC$\underline{H}\underline{H}$, 2 x Glu αC$\underline{H}$), 4.00 (dd, 1H, J = 16.5, 7, 2 x Gly αC$\underline{H}\underline{H}$), 3.56-3.39 (m, 6H, 2 x Cys βC$\underline{H}\underline{H}$, 2 x $CONHC\underline{H}_2CH_2$), 3.27-3.15 (m, 6H, 2 x Cys βC$\underline{H}\underline{H}$, $C\underline{H}_2NHC\underline{H}_2$), 2.81-2.65 (m, 4H, 2 x Glu γC$\underline{H}_2$), 2.41-2.33 (m, 4H, 2 x Glu βC$\underline{H}_2$), 2.06 (m, 2H, $NHCH_2C\underline{H}_2CH_2NH$), 1.89-1.72 (m, 4H, $NHCH_2C\underline{H}_2C\underline{H}_2CH_2$).

^{13}C NMR (100 MHz, D_2O): δ 175.0 (C), 173.2 (C), 172.2 (C), 171.6 (C), 53.0 (CH), 52.8 (CH), 47.6 (CH_2), 45.0 (CH_2), 43.5 (CH_2), 43.4 (CH_2), 38.6 (CH_2), 38.1 (CH_2), 36.0 (CH_2), 31.2 (CH_2), 26.0 (CH_2), 25.8 (CH_2), 23.2 (CH_2).

LRMS (ESI): 722.5 $[M+H]^+$ (100).

HPLC 8.9 min, 100% (λ = 220 nm, gradient 2).

<u>*N*-Benzyloxycarbonylglycyl-3-dimethylaminopropylamide (117)</u>[39]

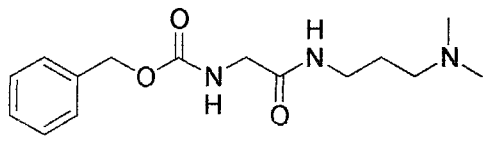

To a stirred solution of DCC (0.99 g, 4.8 mmol) in THF (15 mL) was added *N*-benzyloxycarbonylglycine (2.00 g, 9.6 mmol) and the resulting solution stirred at room temperature for 1 hour. The reaction mixture was filtered to remove the resulting white precipitate and to the filtrate was added 3-dimethylaminopropylamine (0.60 mL, 4.8 mmol) and the solution stirred at room temperature overnight. The solvent was removed *in vacuo* and the oily residue purified by column chromatography (alumina, eluted with EtOAc then EtOAc/MeOH, 4:1) to yield the title compound as a white solid (1.87 g, 67%).

Mpt 45-47 °C (lit = 46-48 °C).

***R*$_f$** 0.78 ($CHCl_3$/MeOH/conc. ammonium hydroxide, 6:3:1).

^{1}H NMR (CD_3OD, 400 MHz): δ 7.39 (m, 5H, 5 x ArC<u>H</u>), 5.15 (s, 2H, $CO_2C\underline{H}_2$), 3.79 (s, 2H, $NHC\underline{H}_2CO$), 3.31 (m, 2H, $NHC\underline{H}_2CH_2$), 2.71 (t, 2H, J = 7.5, $N(CH_3)_2C\underline{H}_2$), 2.52 (s, 6H, $N(C\underline{H}_3)_2$), 1.82 (tt, 2H, J = 7.5, 7.5 $CH_2C\underline{H}_2CH_2$).

^{13}C NMR (CD_3OD, 100 MHz): δ 172.7 (C), 159.1 (C), 138.1 (C), 129.5 (CH), 129.1 (CH), 128.9 (CH), 67.8 (CH_2), 57.4 (CH_2), 45.0 (CH_2), 44.6 (CH_3), 37.9 (CH_2), 27.1 (CH_2).

FT-IR (v, cm^{-1}): 3280, 1713, 1662, 1455, 1241.

LR-MS (ESI): 294.1 $[M+H]^+$ (100), 316.1 $[M+Na]^+$ (48).

Glycine-3-dimethylaminopropylamide[39]

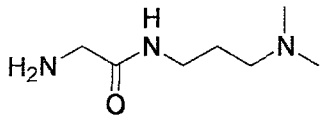

N_2 was bubbled through a solution of **117** (0.50 g, 1.7 mmol) in EtOH (5 mL) for 30 min. 10% Pd/charcoal (24 mg, 0.2 mmol) was added and the reaction mixture stirred under H_2 overnight. The reaction mixture was filtered through celite and the filtrate concentrated *in vacuo* to give the title compound as a colourless oil (0.26 g, 95%).

R_f	0.51 ($CHCl_3$/MeOH/conc. ammonium hydroxide, 6:3:1).
^{1}H NMR	(CD_3OD, 400 MHz): δ 3.30 (m, 4H, $NH_2C\underline{H}_2$, $NHC\underline{H}_2$), 2.56 (t, 2H, J = 7.5, $(CH_3)_2NC\underline{H}_2$), 2.42 (s, 6H, $N(C\underline{H}_3)_2$), 1.79 (tt, 2H, J = 7.5, 7.5, $CH_2C\underline{H}_2CH_2$).
^{13}C NMR	(CD_3OD, 100 MHz): δ 172.8 (C), 57.7 (CH_2), 45.0 (CH_3), 44.5 (CH_2), 38.1 (CH_2), 27.7 (CH_2).
FT-IR	(v, cm^{-1}): 3288, 1650, 1548, 1463.
LR-MS	(ESI): 182.1 $[M+Na]^+$ (100), 160.1 $[M+H]^+$ (57).

***N*-Benzyloxycarbonyl-*L*-cysteinylglycine-3-dimethylaminopropylamide disulfide (14)**[39]

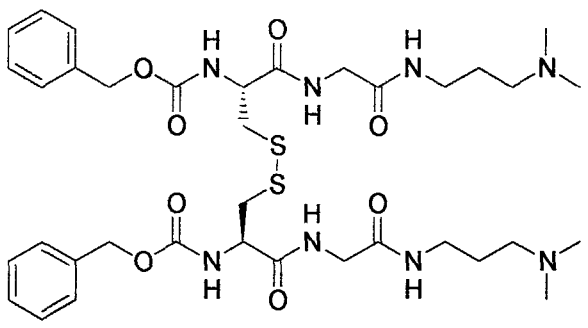

To a stirred solution of glycine-3-dimethylaminopropylamide (0.20 g, 1.3 mmol), *N*,*N*'-benzyloxycarbonyl-*L*-cysteine disulfide (0.32 g, 0.6 mmol) and HOBt (0.17 g, 1.2 mmol) in DMF (2 mL) at 0 °C was added DIC (188 μL, 1.2 mmol). The reaction mixture was stirred at room temperature overnight and concentrated *in vacuo* to yield a colourless oil, which was purified by column chromatography (alumina, eluted with DCM/MeOH, 6:1) to give the title compound as a white solid (0.24 g, 38%).

Mpt 124-126 °C (lit = 126-128 °C).

R_f 0.55 (nBuOH/ H_2O/Ac-OH, 5:3:2).

^{1}H NMR (CD_3OD, 400 MHz): δ 7.46-7.27 (m, 10H, 10 x ArC<u>H</u>), 5.18 (s, 4H, 2 x ArC<u>H_2</u>), 4.58-4.46 (m, 2H, 2 x Cys αC<u>H</u>), 3.97-3.78 (m, 4H, 2 x Gly αC<u>H_2</u>), 3.35-3.24 (m, 6H, 2 x Cys βCH<u>H</u>, 2 x NHC<u>H_2</u>CH_2), 3.09-2.99 (m, 2H, 2 x Cys βCH<u>H</u>), 2.80-2.72 (m, 4H, 2 x C<u>H_2</u>$N(CH_3)_2$), 2.59 (s, 12H, 2 x $N(C\underline{H}_3)_2$), 1.90-1.73 (m, 4H, 2 x $CH_2C\underline{H}_2CH_2$).

^{13}C NMR (CD_3OD, 100 MHz): δ 173.5 (C), 171.8 (C), 158.7 (C), 138.0 (C), 129.5 (CH), 129.1 (CH), 128.7 (CH), 68.0 (CH_2), 57.2 (CH_2), 56.0 (CH), 44.5 (CH_3), 43.9 (CH_2), 41.2 (CH_2), 37.7 (CH_2), 26.9 (CH_2).

LR-MS (ESI): 396.5 $[M+2H]^{2+}$ (100).

<u>Preparation and Purification of *T. Cruzi* Trypanothione Reductase</u>

E. Coli (DE3) cells (transformed with pIBITczTR, containing the *T. Cruzi* TR gene and an ampicillin resistance marker) were plated out on 2 x TY media containing ampicillin (100 mM) and grown overnight at 37 °C. 2 x TY media (100 mL) containing ampicillin (100 mM) was inoculated with a single colony of cells and grown overnight at 37 °C. 2 x TY media (4 x 1.25 L) containing ampicillin (100 mM) was inoculated with the cell culture (4 x 12.5 mL) and grown at 37 °C. The optical density of the cultures was monitored at 600 nm against a media blank to determine when cell growth reached the end of log-phase. IPTG (4 x 0.63 mmol) was added to the cultures after 2.25 hrs and the cultures grown at 37 °C for a further 2.25 hrs, by which time cell growth, as determined by optical density, had begun to slow. The culture was cooled to 4 °C and the cells harvested by centrifugation (12 K RPM, 8 min) to give 20.42 g of cells that were frozen

at –80 °C. The frozen cells were resuspended in phosphate buffer (60 mL) with the addition of lysozyme solution (600 μL, 10 mg/mL). The cells were lysed by sonication on ice (20 x 30 s) and the protein concentration determined to be 20 mg/mL by Bradford assay. PEI (2 mL, 5% aqueous solution) was added to precipitate the DNA and the mixture centrifuged twice (12 K RPM, 30 min, then 17 K RPM, 30 min). The resulting clear supernatant (65 mL) was initially purified by ammonium sulfate precipitation, with the careful addition of ammonium sulfate in three portions (7.4 g, 20% saturation, 8.0 g, 40% saturation, 8.5 g, 60% saturation) over 3 x 45 min at 4 °C. The precipitate from each cut was collected by centrifugation (10 K RPM, 10 min) and resuspended in phosphate buffer (10 mL each). Following SDS-PAGE analysis (Figure 78), the 0-20% cut was discarded and the 20-40 and 40-60% cuts dialysed against phosphate buffer (1 L, 2 x 30 min, 1 x 2 hr, 1 x 12 hr).

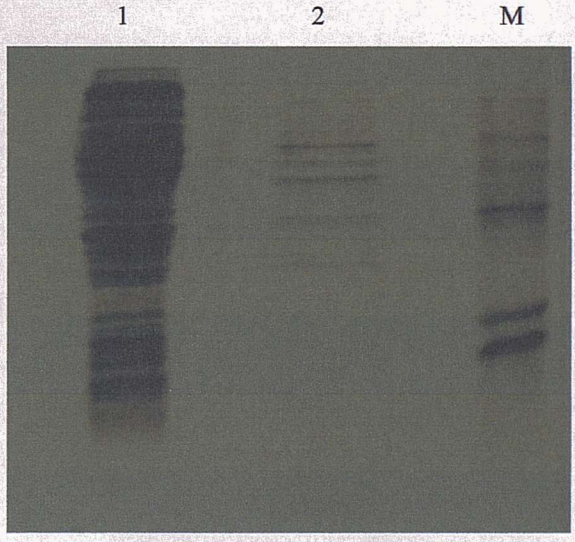

Figure 78: 15% SDS-PAGE gel of the (1) 20-60% and (2) 0-20% ammonium sulfate cuts with molecular weight markers (M).

The two samples were combined, diluted to a total volume of 90 mL and purified by affinity column chromatography (2',5'-ADP sepharose 4B, Amersham Pharmacia Biotech). The crude protein was loaded onto the column at a flow rate of 3.5 mL/min, the column washed with phosphate buffer (100 mL) before a salt gradient elution (0-0.5 M

KCl over 150 mL) with 5.25 mL fractions collected. Fractions with a protein concentration greater than 0.1 mg/mL were analysed by SDS-PAGE.

TR was observed to be the major species, with a number of small impurities also apparent, in fractions 11-29 which were combined and concentrated to a total volume of 10 mL using an Amicon concentrator (30 KDa MWCO), dialysed against phosphate buffer (1 L, 2 x 30 min, 1 x 2 hr, 1 x 12 hr) and diluted to a total volume of 90 mL. The crude protein was loaded onto an ion-exchange column (DEAE sephacel, Amersham Pharmacia Biotech) at 2 mL/min and the column washed with phosphate buffer (150 mL) before salt gradient elution (0-1 M KCl over 150 mL) with 6 mL fractions collected. TR did not bind to the column but eluted in the flow through and wash.

The flow through and wash fractions were combined and concentrated as before to give a total volume of 10 mL and protein concentration (determined by Bradford assay and UV absorbance at 458 nm, ε_{458} for FAD = 11.2 $mM^{-1}cm^{-1}$)[34] was 1 mg/mL, giving a total recovery of 10 mg of protein.

Determination of Kinetic Parameters of Substrates and TR

Initial rates of reaction were recorded at 340 nm in assays of a total volume of 1 mL which contained ammonium acetate buffer (50 mM NH_4OAc, pH 7.5), EDTA (1 mM), TR (2 nM), NADPH (100 μM) and various known concentrations of trypanothione disulfide **13** (10-200 μM). The K_m was determined to be 55 +/- 5 μM (lit = 50 μM).[39]

[Substrate] (μM)	v ($\Delta Asec^{-1}$ x 10^3)
10	1.048
20	2.144
40	3.291
80	4.950
120	5.562
160	5.999
200	6.136

Table 5: Initial rate data for trypanothione disulfide **13** K_m determination.

K_m for alternative substrate **14** was determined in an identical manner as for trypanothione except a concentration of TR of 1 nM was used. A value of 27 +/- 3 μM was obtained (lit = 24 μM).[39]

[Substrate] (μM)	v ($\Delta Asec^{-1} \times 10^3$)
10	0.756
25	1.113
50	1.400
75	1.811
100	1.968
150	2.092
200	2.047

Table 6: Initial rate data for alternative substrate **14** K_m determination.

K_m for nortrypanothione **115** was determined to be 17 +/- 1 μM in an identical manner as for alternative substrate **14** (lit = 28 μM).[87]

[Substrate] (μM)	v ($\Delta Asec^{-1} \times 10^3$)
10	0.982
20	1.377
40	1.764
80	2.053
120	2.221
160	2.350

Table 7: Initial rate data for nortrypanothione disulfide **115** K_m determination.

Enzymatic Assays with Nortrypanothione as Variable Substrate

Kinetic analysis were performed in assays of a total volume of 1 mL which contained ammonium acetate buffer (50 mM NH_4OAc, pH 7.5), EDTA (1 mM), NADPH (100 μM), TR (2 nM) and various known concentrations of nortrypanothione disulfide.

Initial rates were recorded at 340 nm at inhibitor concentrations estimated to be 0.5, 1 and 2 K_i.

[Substrate] (μM)	v (ΔAsec^{-1} x 10^3) at specified [Inhibitor]			
	0	8 μM	16 μM	32 μM
5	0.842	0.541	0.377	0.233
12	1.898	1.058	0.767	0.527
19	2.572	1.556	1.097	0.681
26	3.104	2.117	1.413	0.872
33	3.520	2.343	1.814	1.110
40	3.942	2.595	1.853	1.285
V_{max} [a]	7.532	6.344	5.102	4.400

[a]value obtained from Grafit non-linear regression analysis

Table 8: Initial rate data for N^1,N^9-*bis*-(*L*-tryptophanyl-*L*-arginyl)-norspermidine (**110**).

[Substrate] (μM)	v (ΔAsec^{-1} x 10^3) at specified [Inhibitor]			
	0	50 nM	100 nM	200 nM
5	1.173	0.969	0.753	0.528
12	2.021	1.875	1.599	1.162
19	2.768	2.307	1.776	1.277
26	3.001	2.799	2.223	1.564
33	3.404	2.958	2.245	1.660
40	3.511	3.046	2.564	1.831
V_{max}	5.241	4.424	3.528	2.676

Table 9: Initial rate data for N^1-*L*-tryptophanyl-*L*-arginyl(2,2,5,7,8-pentamethylchroman-6-sulfonamide)-N^9-*L*-tryptophanyl-*L*-arginyl-norspermidine (**111**).

[Substrate] (μM)	v ($\Delta Asec^{-1}$ x 10^3) at specified [Inhibitor]			
	0	125 nM	250 nM	500 nM
5	1.055	0.589	0.381	0.266
12	2.226	1.155	0.626	0.544
19	2.679	1.394	0.913	0.700
26	3.100	1.683	1.132	0.768
33	3.221	1.970	1.280	0.954
40	3.481	1.861	1.384	1.101
V_{max}	5.068	2.866	2.593	1.966

Table 10: Initial rate data for N^1,N^9-*bis*-(*L*-tryptophanyl-*L*-arginyl(2,2,5,7,8-pentamethylchroman-6-sulfonamide))-norspermidine (**112**).

Enzymatic Analysis with NADPH as Variable Substrate

Kinetic analysis was performed in assays of a total volume of 1 mL which contained ammonium acetate buffer (50 mM NH_4OAc, pH 7.5), EDTA (1 mM), alternative substrate **14** (300 μM), TR (2 nM) and various known concentrations of NADPH. Initial rates were recorded by monitoring of the fluorescence of NADPH (λ_{ex} = 340 nm, λ_{em} = 460 nm) at inhibitor concentrations estimated to be 0.5, 1 and 2 K_i.

[Substrate] (μM)	v (ΔFs^{-1}) at specified [Inhibitor]			
	0	50 nM	100 nM	200 nM
0.10	0.141	0.105	0.063	0.039
0.28	0.317	0.188	0.128	0.073
0.46	0.429	0.260	0.183	0.114
0.64	0.517	0.353	0.236	0.146
0.82	0.587	0.391	0.302	0.185
1.00	0.657	0.422	0.309	0.214
V_{max}	1.220	0.782	0.732	0.795

Table 11: Initial rate data for N^1-*L*-tryptophanyl-*L*-arginyl(2,2,5,7,8-pentamethylchroman-6-sulfonamide)-N^9-*L*-tryptophanyl-*L*-arginyl-norspermidine (**111**) with NADPH as variable substrate.

Assay against Glutamate Dehydrogenase

Kinetic analyses were performed in assays of a total volume of 1 mL which contained sodium phosphate buffer (100 mM NaH_2PO_4, pH 7.5), EDTA (1 mM), NADPH (100 μM), α-ketogluarate (250 μM), NH_4Cl (50 mM) and glutamate dehydrogenase (10 μM). Initial rates were recorded at 340 nm at a inhibitor concentrations of 100 μM. Data were collected in triplicate and compared to a control containing no inhibitor to determine the % inhibition. No inhibition was observed with **110-112** or with **131-142**.

Effect of Enzyme Concentration

Kinetic analyses were performed in assays of a total volume of 1 mL which contained ammonium acetate buffer (50 mM NH_4OAc, pH 7.5), EDTA (1 mM), NADPH (100 μM), TR (1.1 or 11 nM) and nortrypanothione disulfide (30 μM). Initial rates were recorded at 340 nm at inhibitor concentrations of 125, 250 and 500 nM. Data were collected in triplicate and compared to a control containing no inhibitor to determine the % inhibition (Table 14)

[TR] (nM)	[**111**] (nM)	v ($\Delta Asec^{-1} \times 10^3$)	v control ($\Delta Asec^{-1} \times 10^3$)	% Inhibition
1.1	125	0.344	0.484	29
1.1	250	0.319	0.484	44
1.1	500	0.232	0.484	52
11	125	2.499	4.235	41
11	250	1.948	4.235	54
11	500	1.440	4.235	66

Table 12: Initial rate data from aggregation inhibition investigation.

Gel Filtration Chromatography Studies

Gel filtration studies were performed on a Gilson HPLC system (234 autoinjector, 321 pump, 155 UV/Vis detector) equipped with a Sephadex G-200 column (Amersham Pharmacia Biotech), eluted with. 50 mM Na_3PO_4/150 mM NaCl pH 7.0 buffer at a flow rate of 0.5 mL/min with UV detection at 220 and 280 nm. A calibration curve was generated by plotting $Log_{10}M_r$ against retention time with 6 standard proteins (4 mg/mL, 20 µl, Table 13 and Figure 79). The calibration curve in the absence of **111** gave an R^2 value of 0.98. TR (1 mg/mL, 20 µL) was analysed and had a retention time of 25.0 min, equating to a M_r of 103.0 kDa. The column was then equilibrated with buffer containing **111** (10 µM) and the calibration curve regenerated. The calibration curve in the presence of **111** gave an R^2 value of 0.97. TR (1 mg/mL, 20 µL) and **111** (10 µM), incubated at room temperature for 30 min, had a retention time of 24.7 min, equating to a M_r of 105.3 kDa.

Sample	M_r (kDa)	$Log_{10}MWt$	R_t (min)	R_t (min) + **111** (10 μM)
horse myoglobin	17	4.230	32.3	32.3
carbonic anhydrase	29	4.462	30.8	30.6
chicken egg albumin	43	4.633	28.2	26.9
bovine serum albumin	66	4.820	25.2	25.2
β-amylase	200	5.301	21.9	22.0
blue dextran	2000	6.301	14.6	14.6

Table 13: Retention time of gel filtration standards in presence and absence of **111**.

(a) (b)

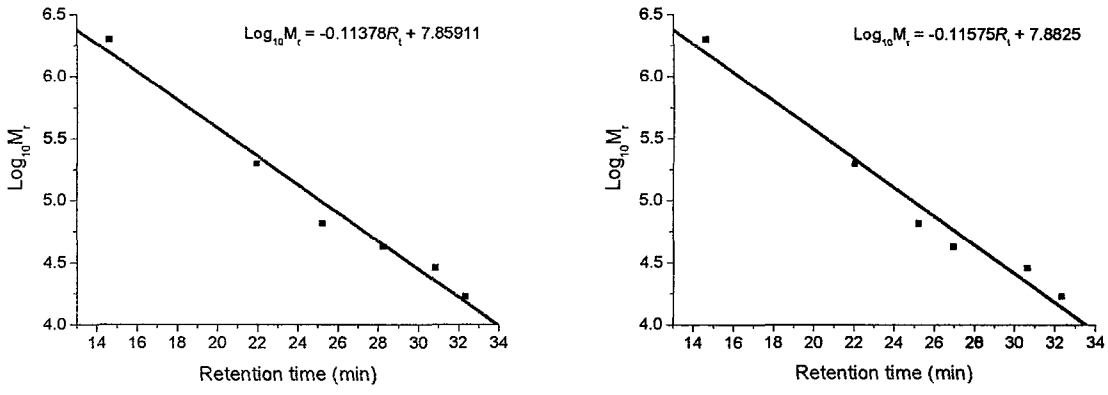

Figure 79: Calibration curve of gel filtration standards in (a) absence and (b) presence of **111** (10 μM), showing equation of line of best-fit.

Protein X-Ray Crystallography

Structure determination and refinement:

Data were processed using programmes of the CCP4 suite.[109] The structure was solved by molecular replacement using the programme MOLREP[110] with the previously solved structure from *T. cruzi* as the model.[111] The model was then refined using the CNS suite of programmes[112] and model building carried out using the graphics interface QUANTA (Molecular Simulations Inc, USA). Following initial inspection of the *2Fo-Fc* and *Fo-Fc*

electron density maps positive difference density was seen for the prosthetic group FAD in both monomers. Thus, two molecules of FAD were included in further rounds of refinement and model building. Owing to the low resolution of the structure, electron density for the ligand remained uninterpretable. A summary of data collection and refinement statistics are shown in Table 14.

Data processing	
Number of reflections	222310
Number of unique reflections	20948
R_{sym} (outer shell)	13.9 (51.9)
$\langle I \rangle / \langle \sigma I \rangle$ (outer shell)	3.3 (1.3)
Completeness (%)	100
Multiplicity	10.6
Refinement	
Resolution range (Å)	40 – 3.1
R_{factor} (%)	28
R_{free} (%)	33
Number of reflections in working set	19899
Number of reflections in test set	1012
Number of protein atoms	7466
Number of non-protein atoms	106
RMS bond length deviation (Å)	0.01
RMS bond angle deviation (°)	1.50

Table 14: Summary of data collection and refinement statistics

4.3 Experimental to Chapter 3

N^1-Trifluoroacetyl-N^9-1-(4,4-dimethyl-2,6-dioxocyclohexylidene)ethyl-norspermidine (118)[103]

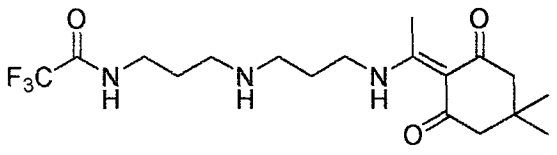

To a stirred solution of norspermidine (10.20 g, 78.0 mmol) in MeOH (51 mL) was added a solution of ethyltrifluoroacetate (11.04 g, 78.0 mmol) in MeOH (36 mL) dropwise at -78 °C. The resulting solution was stirred at -78 °C for 1 hour then allowed to warm to room temperature for a further 4 hours before being concentrated *in vacuo* to yield a colourless oil. To a stirred solution of the oil in DCM (102 mL) was added a solution of 2-acetyl dimedone (14.16 g, 78.0 mmol) in DCM (87 mL) dropwise and the resulting solution stirred at room temperature for 12 hours. The resulting solution was concentrated *in vacuo* to yield a yellow oil, which was purified by column chromatography (silica gel, eluted with DCM/MeOH, 17:3) to give the title compound as a colourless oil (4.79 g, 16%).

R_f	0.35 (DCM/MeOH, 17:3).
^{1}H NMR	(400 MHz, $CDCl_3$): δ 13.41 (bs, 1H, C=C(CH_3)N<u>H</u>), 8.91 (bs, 1H, CON<u>H</u>), 3.47 (m, 4H, C=C(CH_3)NHC<u>H</u>$_2$, CONHC<u>H</u>$_2$), 2.80 (m, 2H, CH_2NHC<u>H</u>$_2$), 2.74 (m, 2H, CH_2NHC<u>H</u>$_2$), 2.54 (s, 3H, C=C(C<u>H</u>$_3$)NH), 2.34 (s, 4H, 2 x COC<u>H</u>$_2$), 2.20 (s, 1H, CH_2N<u>H</u>CH_2), 1.85 (m, 2H, CH_2C<u>H</u>$_2$CH_2), 1.75 (m, 2H, CH_2C<u>H</u>$_2$CH_2), 1.01 (s, 6H, C(C<u>H</u>$_3$)$_2$).
^{13}C NMR	(100 MHz, $CDCl_3$): δ 198.2 (C), 173.9 (C), 155.6 (q, J = 37, C), 116.4 (q, J = 288, C), 108.3 (C), 53.1 (CH_2), 48.4 (CH_2), 46.9 (CH_2), 41.4 (CH_2), 39.7 (CH_2), 30.4 (C), 29.1 (CH_2), 28.5 (CH_3), 27.5 (CH_2), 18.1 (CH_3).
FT-IR	ν (cm^{-1}): 3263, 2955, 2864, 1712, 1627, 1570.
LRMS	(ESI): 392.3 $[M+H]^+$ (100).

HRMS (ESI): Found 392.2151, $C_{18}H_{29}F_3N_3O_3$ requires 392.2156.

HPLC 7.0 min, 100% (λ = 220 nm, gradient 1).

N^1-Trifluoroacetyl-N^5-(4-(allyloxycarbonylmethoxy)phenyl-methoxycarbonyl)-N^9-1-(4,4-dimethyl-2,6-dioxocyclohexylidene)ethyl-norspermidine (119)[103]

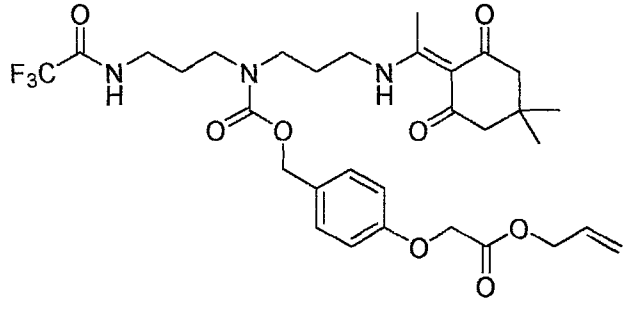

118 (4.69 g, 12.0 mmol) and **103** (5.56 g, 14.4 mmol) were dissolved in DMF (37 mL) and stirred at room temperature overnight. The reaction mixture was poured into 1M $KHSO_4$ (150 mL) and extracted with EtOAc (3 x 150 mL). The combined organic extracts were washed with water (5 x 150 mL), dried ($MgSO_4$) and concentrated *in vacuo* and the resulting oily residue was purified by column chromatography (silica gel, eluted with EtOAc then EtOAc/MeOH, 49:1) to give the title compound as a colourless oil (6.05 g, 79%).

R_f 0.30 (EtOAc/hexane, 4:1).

^{1}H NMR (400 MHz, $CDCl_3$): δ 13.5 (bs, 1H, C=C(CH_3)N$\underline{H}$), 8.00 (bs, 1H, CON$\underline{H}$), 7.29 (d, 2H, J = 8.5, 2 x Ar$\underline{CH}$), 6.88 (d, 2H, J = 8.5, 2 x Ar$\underline{CH}$), 5.93 (ddt, 1H, J = 17, 10.5, 6, $CH_2\underline{CH}$=CH_2), 5.35 (dd, 1H, J = 17, 1, CH_2CH=C$\underline{H}$H), 5.28 (dd, 1H, J = 10.5, 1, CH_2CH=CH$\underline{H}$), 5.09 (s, 2H, O$\underline{CH_2}$), 4.71 (d, 2H, J = 6, $\underline{CH_2}CH$=CH_2), 4.66 (s, 2H, O$\underline{CH_2}$), 3.35-3.25 (m, 8H, 2 x $\underline{CH_2}CH_2\underline{CH_2}$), 2.50 (s, 3H, C=C(C$\underline{H_3}$)), 2.36 (s, 4H, 2 x $\underline{CH_2}C(CH_3)_2$), 1.90 (m, 2H, $CH_2\underline{CH_2}CH_2$), 1.75 (m, 2H, $CH_2\underline{CH_2}CH_2$), 1.03 (s, 6H, C(C$\underline{H_3}$)$_2$).

^{13}C NMR (100 MHz, $CDCl_3$): δ 199.4 (C), 197.0 (C), 173.9 (C), 168.8 (C), 158.3 (C), 157.7 (q, J = 38, C), 157.5 (C), 131.7 (CH), 130.5 (CH), 129.7 (C), 119.5 (CH_2), 116.0 (q, J = 286, C), 115.1 (CH), 108.3 (C), 67.8 (CH_2), 66.2 (CH_2), 65.6 (CH_2), 53.8 (CH_2), 52.6 (CH_2), 44.5 (CH_2), 44.2 (CH_2), 41.0 (CH_2), 36.3 (CH_2), 30.4 (C), 28.6 (CH_3), 28.2 (CH_2), 27.3 (CH_2), 18.2 (CH_3).

FT-IR ν (cm^{-1}): 3269, 2955, 2864, 1758, 1718, 1571.

LRMS (ESI): 662.5 $[M+Na]^+$ (100), 640.5 $[M+H]^+$ (13).

HRMS (ESI): Found 640.2835, $C_{31}H_{41}F_3N_3O_8$ requires 640.2840.

<u>N^1-Trifluoroacetyl-N^5-((carboxy-methyl)phenyl-methoxy-carbonyl)-N^9-1-(4,4-dimethyl-2,6-dioxocyclohexylidene)ethyl-norspermidine (120)</u>[103]

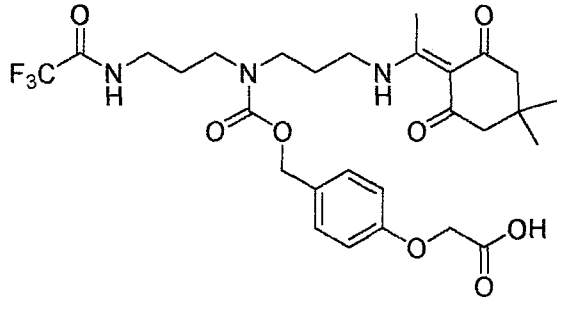

A solution of **119** (5.91 g, 9.2 mmol) in DCM/THF (1:1, 57 mL) was purged with N_2 for 1 hour. Thiosalicylic acid (2.86 g, 18.5 mmol) and $Pd(PPh_3)_4$ (1.06 g, 0.9 mmol) were added and the reaction mixture stirred at room temperature for 2 hours. The solvent was removed *in vacuo* and the resulting oily residue purified by column chromatography (silica gel, eluted with EtOAc then EtOAc/MeOH, 3:2) to give the title compound as a colourless oil (3.60 g, 65%).

***R*$_f$** 0.15 (EtOAc/MeOH, 2:1).

^{1}H NMR (400 MHz, $CDCl_3$): δ 13.36 (bs, 1H, C=C(CH_3)N<u>H</u>), 8.00 (bs, 1H, CON<u>H</u>), 7.27 (d, 2H, J = 8.5, ArC<u>H</u>), 6.88 (d, 2H, J = 8.5, ArC<u>H</u>), 5.07 (s, 2H, OC<u>H$_2$</u>), 4.64 (s, 2H, OC<u>H$_2$</u>), 3.34-3.32 (m, 8H, 2 x C<u>H$_2$</u>C<u>H$_2$</u>C<u>H$_2$</u>), 2.37

(m, 7H, C=C(C$\underline{H}_3$), 2 x COC$\underline{H}_2$C(CH$_3$)$_2$), 1.85 (m, 2H, CH$_2$C$\underline{H}_2$CH$_2$), 1.75 (m, 2H, CH$_2$C$\underline{H}_2$CH$_2$), 1.02 (s, 6H, C(C$\underline{H}_3$)$_2$).

^{13}C NMR (100 MHz, $CDCl_3$): δ 198.9 (C), 174.4 (C), 171.3 (C), 158.3 (C), 157.7(q, J = 37, C), 157.5 (C), 130.6 (CH), 129.5 (C), 116.0 (q, J = 287, C), 115.0 (CH), 108.3 (C), 67.8 (CH_2), 65.5 (CH_2), 52.8 (CH_2), 44.3 (CH_2), 41.2 (CH_2), 36.4 (CH_2), 30.5 (C), 28.5 (CH_3), 28.3 (CH_2), 28.1 (CH_2), 18.3 (CH_3).

FT-IR ν (cm^{-1}): 3293, 3018, 2958, 1720, 1560.

LRMS (ESI): 600.4 $[M+H]^+$ (100), 622.5 $[M+Na]^+$ (93).

HRMS (ESI): Found 600.2530, $C_{28}H_{37}F_3N_3O_8$ requires 600.2527.

Polymer supported N^1-trifluoroacetyl-N^9-1-(4,4-dimethyl-2,6-dioxocyclohexylidene)ethyl-norspermidine (121)

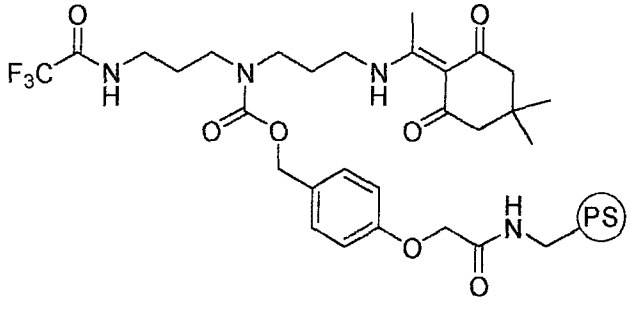

120 (3.40 g, 5.7 mmol) was coupled to aminomethyl-polystyrene resin (1% DVB cross-linked, 1.11 mmol/g, 3.41 g, 3.8 mmol, general procedure A with the exceptions that 1.5 eq. of reagents were used and the reaction was carried out overnight). A small portion of resin was treated according to general procedure B to remove the Dde group and loading, measured by a quantitative ninhydrin test, determined to be 0.54 mmol/g of norspermidine.

FT-IR ν (cm^{-1}): 2925, 1670, 1574, 1452, 1212.

Library characterisation

All compounds were characterised by ^{1}H NMR, LRMS, HRMS and HPLC. A representative sample (approximately 40%) were also characterised by ^{13}C NMR.

N^1-*L*-Tryptophanyl-norspermidine (125)

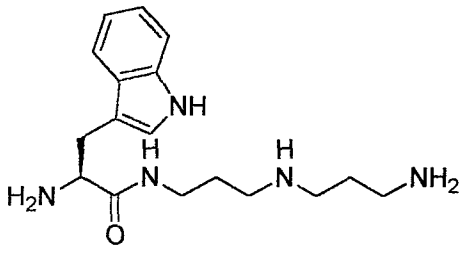

The Dde group of resin **121** (0.20 g, 0.1 mmol) was removed (general procedure B) and the resulting amine-resin Boc-protected (general procedure E). The Tfa group was removed (general procedure H) and Boc-Trp(Boc)-OH coupled to the resulting amine-resin (general procedure A). Cleavage from the resin was accomplished (general procedure I) and the desired compound was purified as the TFA salt by semi-prep HPLC.

Semi-prep HPLC R_t = 20.8 min (gradient 4), yield = 7 mg, 16%.

^{1}H NMR (400 MHz, CD_3OD): δ 7.63 (d, 1H, J = 8, ArC<u>H</u>), 7.41 (d, 1H, J = 8, ArC<u>H</u>), 7.23 (s, 1H, ArC<u>H</u>), 7.17 (t, 1H, J = 8, ArC<u>H</u>), 7.09 (t, 1H, J = 8, ArC<u>H</u>), 4.11 (t, 1H, J = 7.5, Trp αC<u>H</u>), 3.44-3.17 (m, 4H, Trp βC<u>H_2</u>, CONHC<u>H_2</u>), 3.10-2.98 (m, 4H, C<u>H_2</u>CH_2C<u>H_2</u>NH_2), 2.81 (t, 2H, J = 7.5, CONHCH_2CH_2C<u>H_2</u>), 2.13-2.02 (m, 2H, C<u>H_2</u>C$H_2$$NH_2$), 1.84-1.73 (m, 2H, CONHCH_2C<u>H_2</u>).

LRMS (ESI): 318.2 $[M+H]^+$ (100).

HRMS (ESI): Found 318.2287, $C_{17}H_{28}N_5O$ requires 318.2288.

HPLC 10.8 min, 100% (λ = 220 nm, gradient 2).

N^1- *L*-Tryptophanyl-N^9-acetyl-norspermidine (126)

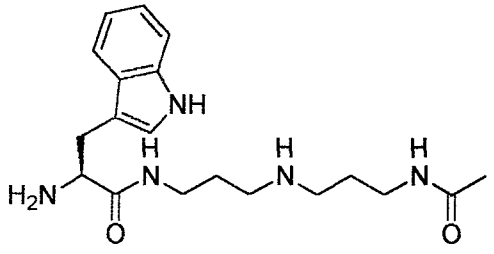

The Dde group of resin **121** (0.20 g, 0.1 mmol) was removed (general procedure B) and the resulting amine-resin capped with acetic anhydride (general procedure F). The Tfa group was removed (general procedure H) and Boc-Trp(Boc)-OH coupled to the resulting amine-resin (general procedure A). Cleavage from the resin was accomplished (general procedure I) and the desired compound was purified as the TFA salt by semi-prep HPLC.

Semi-prep HPLC R_t = 22.4 min (gradient 4), yield = 16 mg, 34%.

^{1}H NMR (400 MHz, CD_3OD): δ 7.63 (d, 1H, J = 8, ArC<u>H</u>), 7.42 (d, 1H, J = 8, ArC<u>H</u>), 7.24 (s, 1H, ArC<u>H</u>), 7.15 (t, 1H, J = 8, ArC<u>H</u>), 7.09 (t, 1H, J = 8, ArC<u>H</u>), 4.13 (t, 1H, J = 7.5, Trp αC<u>H</u>), 3.39 (dd, 1H, J = 14.5, 7.5, Trp βCH<u>H</u>), 3.35-3.21 (m, 5H, Trp βC<u>H</u>H, 2 x CONHC<u>H</u>$_2$), 2.88 (t, 2H, J = 7, C<u>H</u>$_2$NHCH$_2$), 2.69 (t, 2H, J = 7, C<u>H</u>$_2$NHCH$_2$), 1.99 (s, 3H, C<u>H</u>$_3$), 1.85 (tt, 2H, J = 7, 7, CH$_2$C<u>H</u>$_2$CH$_2$), 1.75 (tt, 2H, J = 7, 7, CH$_2$C<u>H</u>$_2$CH$_2$).

^{13}C NMR (100 MHz, CD_3OD): δ 174.4 (C), 170.8 (C), 138.2 (C), 128.4 (C), 125.5 (CH), 122.9 (CH), 119.2 (CH), 112.7 (CH), 108.2 (C), 55.3 (CH), 46.4 (CH_2), 46.1 (CH_2), 37.3 (CH_2), 36.9 (CH_2), 28.7 (CH_2), 27.6 (CH_2), 27.1 (CH_2), 22.5 (CH_3).

LRMS (ESI): 360.2 $[M+H]^+$ (100), 382.2 $[M+Na]^+$ (25).

HRMS (ESI): Found 360.2392, $C_{19}H_{30}N_5O_2$ requires 360.2394.

HPLC 11.2 min, 100% (λ = 220 nm, gradient 2).

N^1-*L*-Tryptophanyl-N^9-hexanoyl-norspermidine (127)

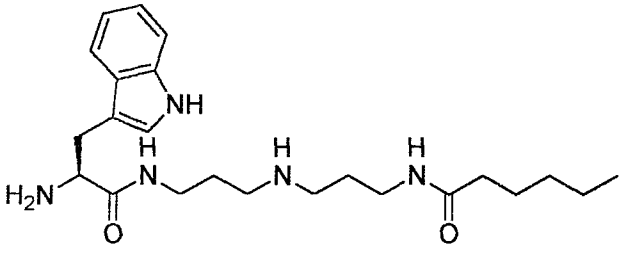

The Dde group of resin **121** (0.20 g, 0.1 mmol) was removed (general procedure B) and the resulting amine-resin capped with hexanoic anhydride (general procedure G). The Tfa group was removed (general procedure H) and Boc-Trp(Boc)-OH coupled to the resulting amine-resin (general procedure A). Cleavage from the resin was accomplished (general procedure I) and the desired compound was purified as the TFA salt by semi-prep HPLC.

Semi-prep HPLC R_t = 28.9 min (gradient 4), yield = 11 mg, 21%.

^{1}H NMR (400 MHz, CD_3OD): δ 7.51 (d, 1H, J = 8, ArC<u>H</u>), 7.29 (d, 1H, J = 8, ArC<u>H</u>), 7.12 (s, 1H, ArC<u>H</u>), 7.03 (t, 1H, J = 8, ArC<u>H</u>), 6.97 (t, 1H, J = 8, ArC<u>H</u>), 3.99 (t, 1H, J = 7.5, Trp αC<u>H</u>), 3.32-3.08 (m, 6H, Trp βC<u>H</u>$_2$, 2 x CONHC<u>H</u>$_2$), 2.76 (t, 2H, J = 7, CH_2NHC<u>H</u>$_2$), 2.59 (t, 2H, J = 7.5, CH_2NHC<u>H</u>$_2$), 2.11 (t, 2H, J = 7.5, COC<u>H</u>$_2$), 1.78-1.47 (m, 6H, $COCH_2$C<u>H</u>$_2$, 2 x $NHCH_2$C<u>H</u>$_2$), 1.29-1.14 (m, 4H, C<u>H</u>$_2$C<u>H</u>$_2$$CH_3$), 0.81 (t, 3H, J = 7, C<u>H</u>$_3$).

LRMS (ESI): 416.3 $[M+H]^+$ (100).

HRMS (ESI): Found 416.3025, $C_{23}H_{38}N_5O_2$ requires 416.3020.

HPLC 13.0 min, 100% (λ = 220 nm, gradient 2).

N^1-*L*-Arginyl-norspermidine (128)

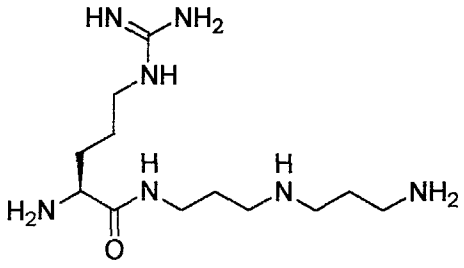

The Dde group of resin **121** (0.20 g, 0.1 mmol) was removed (general procedure B) and the resulting amine-resin Boc-protected (general procedure E). The Tfa group was removed (general procedure H) and Fmoc-Arg(Pmc)-OH coupled to the resulting amine-resin (general procedure A). The Fmoc group was removed (general procedure C) and cleavage from the resin accomplished (general procedure I) to give the title compound as the TFA salt.

Yield = 17 mg, 59 %.

^{1}H NMR (400 MHz, CD_3OD): δ 4.11 (q, 1H, J = 6.5, Arg αC<u>H</u>), 3.57-3.14 (m, 10H, Arg δC<u>H</u>$_2$, C<u>H</u>$_2$CH$_2$C<u>H</u>$_2$NHC<u>H</u>$_2$CH$_2$C<u>H</u>$_2$), 2.29-1.99 (m, 6H, Arg βC<u>H</u>$_2$, CH$_2$C<u>H</u>$_2$CH$_2$NHCH$_2$C<u>H</u>$_2$CH$_2$), 1.84-1.74 (m, 2H, Arg γC<u>H</u>$_2$).

^{13}C NMR (100 MHz, CD_3OD): δ 170.7 (C), 158.1 (C), 53.9 (CH), 46.3 (CH_2), 45.7 (CH_2), 41.4 (CH_2), 37.6 (CH_2), 37.4 (CH_2), 29.1 (CH_2), 26.6 (CH_2), 26.3 (CH_2), 24.9 (CH_2).

LRMS (ESI): 288.4 (100%) $[M+H]^+$.

HRMS (ESI): Found 288.2506, $C_{12}H_{30}N_7O$ requires 288.2506.

N^1-*L*-Arginyl-N^9-acetyl-norspermidine (129)

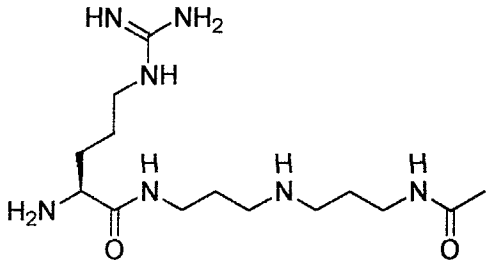

The Dde group of resin **121** (0.20 g, 0.1 mmol) was removed (general procedure B) and the resulting amine-resin capped with acetic anhydride (general procedure F). The Tfa group was removed (general procedure H) and Fmoc-Arg(Pmc)-OH coupled to the resulting amine-resin (general procedure A). The Fmoc group was removed (general procedure C) and cleavage from the resin accomplished (general procedure I) to give the title compound as the TFA salt.

Yield = 23 mg, 70%.

^{1}H NMR (400 MHz, CD_3OD): δ 3.97 (bs, 1H, Arg αC<u>H</u>), 3.46-3.23 (m, 6H, Arg δC<u>H</u>$_2$, 2 x CONHC<u>H</u>$_2$), 3.11-3.01 (m, 4H, C<u>H</u>$_2$NHC<u>H</u>$_2$), 2.05-1.87 (m, 9H, Arg βC<u>H</u>$_2$, 2 x NHCH$_2$C<u>H</u>$_2$CH$_2$NH, C<u>H</u>$_3$), 1.77-1.67 (m, 2H, Arg γC<u>H</u>$_2$).

^{13}C NMR (100 MHz, CD_3OD): δ 174.2 (C), 170.7 (C), 158.7 (C), 54.0 (CH), 46.6 (CH_2), 41.5 (CH_2), 37.4 (CH_2), 37.1 (CH_2), 29.6 (CH_2), 27.5 (CH_2), 27.2 (CH_2), 25.3 (CH_2), 22.5 (CH_3).

LRMS (ESI): 330.4 $[M+H]^+$ (100), 352.4 $[M+Na]^+$ (8).

HRMS (ESI): Found 330.2605, $C_{14}H_{32}N_7O_2$ requires 330.2612.

N^1-*L*-Arginyl-N^9-hexanoyl-norspermidine (130)

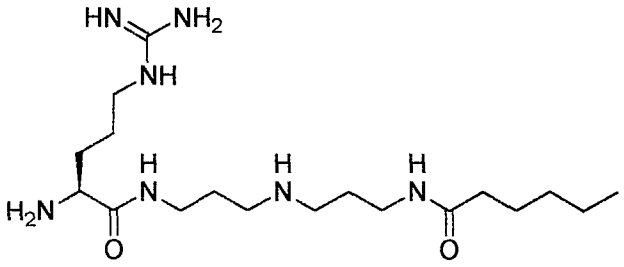

The Dde group of resin **121** (0.20 g, 0.1 mmol) was removed (general procedure B) and the resulting amine-resin capped with hexanoic anhydride (general procedure F). The Tfa group was removed (general procedure H) and Fmoc-Arg(Pmc)-OH coupled to the resulting amine-resin (general procedure A). The Fmoc group was removed (general procedure C) and cleavage from the resin accomplished (general procedure I) to give the title compound as the TFA salt.

Yield = 28 mg, 73%.

^{1}H NMR (400 MHz, CD_3OD): δ 3.98 (bs, 1H, Arg αC<u>H</u>), 3.48-3.24 (m, 6H, Arg δC<u>H</u>$_2$, 2 x CONHC<u>H</u>$_2$), 3.12-3.05 (m, 4H, C<u>H</u>$_2$NHC<u>H</u>$_2$), 2.25 (t, 2H, J = 7.5, COC<u>H</u>$_2$), 2.08-1.89 (m, 6H, Arg βC<u>H</u>$_2$, 2 x NHCH$_2$C<u>H</u>$_2$CH$_2$NH), 1.79-1.58 (m, 4H, Arg γC<u>H</u>$_2$, COCH$_2$C<u>H</u>$_2$), 1.42-1.29 (m, 4H, CH$_3$C<u>H</u>$_2$C<u>H</u>$_2$), 0.95 (t, 3H, J = 7, C<u>H</u>$_3$).

^{13}C NMR (100 MHz, CD_3OD): δ 177.3 (C), 170.7 (C), 158.8 (C), 54.0 (CH), 46.6 (CH_2), 46.5 (CH_2), 41.4 (CH_2), 37.4 (CH_2), 37.0 (CH_2), 32.6 (CH_2), 29.6 (CH_2), 27.6 (CH_2), 27.2 (CH_2), 26.7 (CH_2), 25.3 (CH_2), 23.4 (CH_2), 14.3 (CH_3).

LRMS (ESI): 386.5 $[M+H]^+$ (100).

N^1-*L*-Arginyl(2,2,5,7,8-pentamethylchroman-6-sulfonamide)-norspermidine (131)

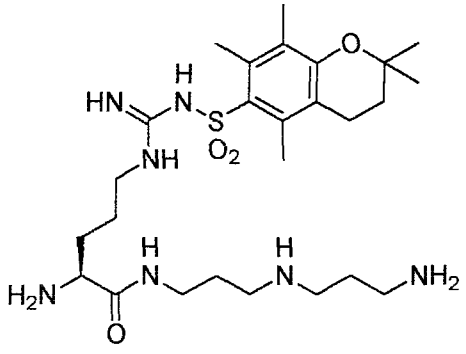

The Dde group of resin **121** (0.20 g, 0.1 mmol) was removed (general procedure B) and the resulting amine-resin Boc-protected (general procedure E). The Tfa group was removed (general procedure H) and Fmoc-Arg(Pmc)-OH coupled to the resulting amine-resin (general procedure A). The Fmoc group was removed (general procedure C) and cleavage from the resin accomplished (general procedure J). The desired compound was purified as the TFA salt by semi-prep HPLC.

Semi-prep HPLC R_t = 32.4 min (gradient 4), yield = 13 mg, 19%.

^{1}H NMR (400 MHz, CD_3OD): δ 3.98 (t, 1H, J = 6.5, Arg αC<u>H</u>), 3.52-3.32 (m, 4H, Arg δC<u>H</u>$_2$, CONHC<u>H</u>$_2$), 3.23-3.08 (m, 6H, $H_2NC\underline{H}_2CH_2C\underline{H}_2NHC\underline{H}_2$), 2.72 (t, 2H, J = 6.5, ArC<u>H</u>$_2$), 2.63 (s, 3H, ArC<u>H</u>$_3$), 2.61 (s, 3H, ArC<u>H</u>$_3$), 2.18-2.09 (m, 5H, ArC<u>H</u>$_3$, $NHCH_2C\underline{H}_2CH_2NH$), 2.08-1.86 (m, 6H, Arg βC<u>H</u>$_2$, $NHCH_2C\underline{H}_2CH_2NH$, $ArCH_2C\underline{H}_2$), 1.67 (tt, 2H, J = 7, 7, Arg γC<u>H</u>$_2$), 1.36 (s, 6H, $C(C\underline{H}_3)_2$).

LRMS (ESI): 554.4 $[M+H]^+$ (100), 576.4 $[M+H]^+$ (70).

HRMS (ESI): Found 554.3498, $C_{26}H_{48}N_7O_4S$ requires 554.3483.

HPLC 13.7 min, 100% (λ = 220 nm, gradient 2).

N^1-*L*-Arginyl(2,2,5,7,8-pentamethylchroman-6-sulfonamide)-N^9-acetyl-norspermidine (132)

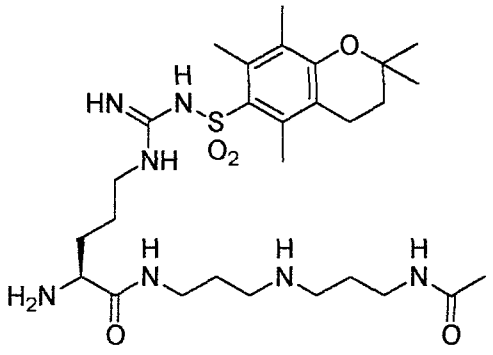

The Dde group of resin **121** (0.20 g, 0.1 mmol) was removed (general procedure B) and the resulting amine-resin capped with acetic anhydride (general procedure F). The Tfa group was then removed (general procedure H) and Fmoc-Arg(Pmc)-OH coupled to the resulting amine-resin (general procedure A). The Fmoc group was removed (general procedure C) and cleavage from the resin accomplished (general procedure J). The desired compound was purified as the TFA salt by semi-prep HPLC.

Semi-prep HPLC R_t = 34.3 min (gradient 4), yield = 15 mg, 21%.

^{1}H NMR (400 MHz, CD_3OD): δ 3.99 (t, 1H, J = 6.5, Arg αC<u>H</u>), 3.50-3.19 (m, 6H, 2 x CONHC<u>H</u>$_2$, Arg δC<u>H</u>$_2$), 3.12-2.95 (m, 4H, C<u>H</u>$_2$NHC<u>H</u>$_2$), 2.73 (t, 2H, J = 7, ArC<u>H</u>$_2$), 2.62 (s, 3H, ArC<u>H</u>$_3$), 2.60 (s, 3H, ArC<u>H</u>$_3$), 2.15 (s, 3H, ArC<u>H</u>$_3$), 2.04-1.86 (m, 11H, COC<u>H</u>$_3$, ArCH$_2$C<u>H</u>$_2$, Arg βC<u>H</u>$_2$, 2 x NHCH$_2$C<u>H</u>$_2$CH$_2$NH), 1.68 (t, 2H, J = 7, Arg γC<u>H</u>$_2$), 1.36 (s, 6H, C(C<u>H</u>$_3$)$_2$).

LRMS (ESI): 596.5 $[M+H]^+$ (100), 618.5 $[M+Na]^+$ (35).

HRMS (ESI): Found 596.3581, $C_{28}H_{50}N_7O_5S$ requires 596.3589.

HPLC 14.1 min, 100% (λ = 220 nm, gradient 2).

N^1-*L*-Arginyl(2,2,5,7,8-pentamethylchroman-6-sulfonamide)-N^9-hexanoyl-norspermidine (133)

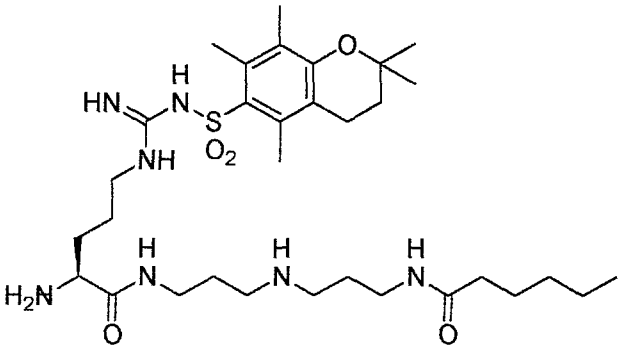

The Dde group of resin **121** (0.20 g, 0.1 mmol) was removed (general procedure B), the resulting amine-resin capped with hexanoic anhydride (general procedure G) and the Tfa group removed (general procedure H). Fmoc-Arg(Pmc)-OH was coupled to the resulting amine-resin (general procedure A), the Fmoc group removed (general procedure C) and cleavage from the resin accomplished (general procedure J). The desired compound was purified as the TFA salt by semi-prep HPLC.

Semi-prep HPLC R_t = 39.3 min (gradient 4), yield = 8 mg, 10%.

^{1}H NMR (400 MHz, CD_3OD): δ 4.01 (t, 1H, J = 6.5, Arg αC<u>H</u>), 3.54-3.18 (m, 6H, Arg δC<u>H</u>$_2$, 2 x CONHC<u>H</u>$_2$), 3.13-3.05 (m, 4H, C<u>H</u>$_2$NHC<u>H</u>$_2$), 2.72 (t, 2H, J = 6.5, ArC<u>H</u>$_2$), 2.62 (s, 3H, ArC<u>H</u>$_3$), 2.61 (s, 3H, ArC<u>H</u>$_3$), 2.24 (t, 2H, J = 7.5, COC<u>H</u>$_2$), 2.15 (s, 3H, ArC<u>H</u>$_3$), 2.07-1.86 (m, 8H, Arg βC<u>H</u>$_2$, ArCH$_2$C<u>H</u>$_2$, 2 x NHCH$_2$C<u>H</u>$_2$CH$_2$NH), 1.73-1.59 (m, 4H, COCH$_2$C<u>H</u>$_2$, Arg γC<u>H</u>$_2$), 1.40-1.30 (m, 10H, CH$_3$C<u>H</u>$_2$C<u>H</u>$_2$, C(C<u>H</u>$_3$)$_2$), 0.95 (t, 3H, J = 7, C<u>H</u>$_3$CH$_2$).

LRMS (ESI): 652.5 $[M+H]^+$ (100), 674.5 $[M+Na]^+$ (100), 326.9 $[M+2H]^{2+}$ (70).

HRMS (ESI): Found 652.4213, $C_{32}H_{58}N_7O_5S$ requires 652.4215.

HPLC 15.0 min, 100% (λ = 220 nm, gradient 2).

N^1-*L*-Tryptophanyl-*L*-arginyl-norspermidine (134), N^1-*L*-tryptophanyl-*L*-arginyl(2,2,5,7,8-pentamethylchroman-6-sulfonamide)-norspermidine (135)

The Dde group of resin **121** (0.40 g, 0.2 mmol) was removed (general procedure B), the resulting amine-resin Boc-protected (general procedure E) and the Tfa group removed (general procedure H). Fmoc-Arg(Pmc)-OH was coupled to the resulting amine-resin (general procedure A), the Fmoc group removed (general procedure C) and Boc-Trp(Boc)-OH coupled to the resulting amine-resin (general procedure A). Cleavage from the resin was accomplished (general procedure J) and the desired compounds were purified as the TFA salts by semi-prep HPLC.

N^1-*L*-Tryptophanyl-*L*-arginyl-norspermidine (134)

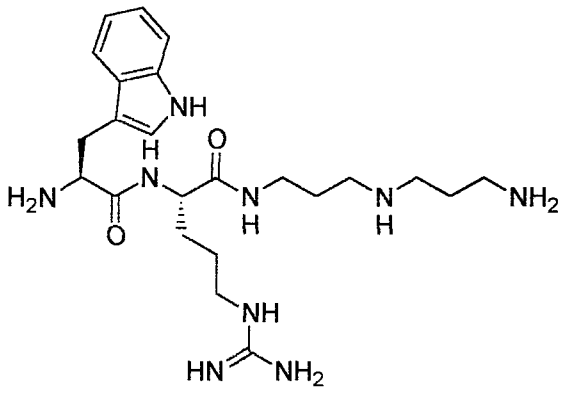

Semi-prep HPLC R_t = 18.2 min (gradient 4), yield = 7 mg, 6%.

^{1}H NMR (400 MHz, CD_3OD): 7.69 (d, 1H, J = 7.5, ArC<u>H</u>), 7.41 (d, 1H, J = 7.5, ArC<u>H</u>), 7.27 (s, 1H, ArC<u>H</u>), 7.17 (t, 1H, J = 7.5, ArC<u>H</u>), 7.09 (t, 1H, J = 7.5, ArC<u>H</u>), 4.36-4.23 (m, 2H, Arg αC<u>H</u>, Trp αC<u>H</u>), 3.49 (dd, 1H, J = 15, 6, Trp βCH<u>H</u>), 3.38-2.97 (m, 11H, Trp βC<u>H</u>H, Arg δC<u>H</u>$_2$, NHC<u>H</u>$_2$CH$_2$C<u>H</u>$_2$NHC<u>H</u>$_2$CH$_2$C<u>H</u>$_2$NH$_2$), 2.13-2.05 (m, 2H, C<u>H</u>$_2$CH$_2$NH$_2$), 1.93-1.56 (m, 6H, Arg βC<u>H</u>$_2$, Arg γC<u>H</u>$_2$, NHCH$_2$C<u>H</u>$_2$CH$_2$NH).

LRMS (ESI): 474.4 $[M+H]^+$ (100).

HRMS (ESI): Found 474.3291, $C_{23}H_{40}N_9O_2$ requires 474.3299.

HPLC 10.8 min, 100% (λ = 220 nm, gradient 2).

N^1-*L*-Tryptophanyl-*L*-arginyl(2,2,5,7,8-pentamethylchroman-6-sulfonamide)-norspermidine (135)

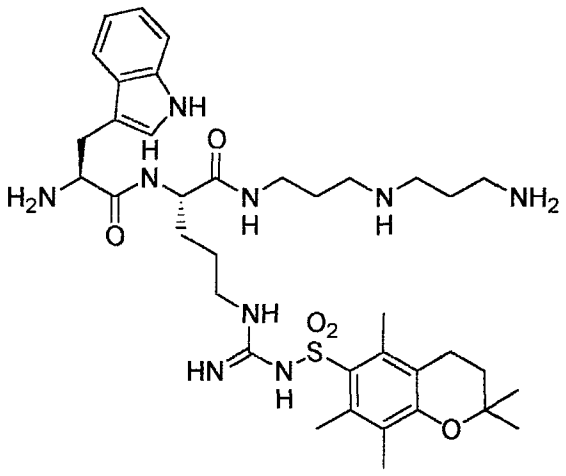

Semi-prep HPLC R_t = 35.6 min (gradient 4), yield = 11 mg, 6%.

^{1}H NMR (400 MHz, CD_3OD): δ 7.67 (d, 1H, J = 8, ArC<u>H</u>), 7.39 (d, 1H, J = 8, ArC<u>H</u>), 7.25 (s, 1H, ArC<u>H</u>), 7.15 (t, 1H, J = 8, ArC<u>H</u>), 7.07 (t, 1H, J = 8, ArC<u>H</u>), 4.44 (bs, 1H, Arg αC<u>H</u>), 4.23 (dd, 1H, J = 8, 6, Trp αC<u>H</u>), 3.46 (dd, 1H, J = 15, 6, Trp βCH<u>H</u>), 3.38-3.19 (m, 3H, Trp βC<u>H</u>H, CONHC<u>H</u>$_2$), 3.17-3.00 (m, 8H, Arg δC<u>H</u>$_2$, C<u>H</u>$_2$NHC<u>H</u>$_2$CH$_2$C<u>H</u>$_2$), 2.68 (t, 2H, J = 6.5, ArC<u>H</u>$_2$), 2.59 (s, 3H, ArC<u>H</u>$_3$), 2.57 (s, 3H, ArC<u>H</u>$_3$), 2.13-2.04 (m, 5H, ArC<u>H</u>$_3$, C<u>H</u>$_2$CH$_2$NH$_2$), 1.95-1.79 (m, 5H, Arg βCH<u>H</u>, ArCH$_2$C<u>H</u>$_2$, NHCH$_2$C<u>H</u>$_2$CH$_2$NH), 1.77-1.55 (m, 3H, Arg βCH<u>H</u>, Arg γC<u>H</u>$_2$), 1.31 (s, 6H, C(C<u>H</u>$_3$)$_2$).

LRMS (ESI): 740.5 $[M+H]^+$ (90), 370.9 $[M+2H]^{2+}$ (90).

HRMS (ESI): Found 740.4285, $C_{37}H_{58}N_9O_5S$ requires 740.4276.

HPLC 14.2 min, 100% (λ = 220 nm, gradient 2).

N^1-*L*-Tryptophanyl-*L*-arginyl-N^9-acetyl-norspermidine (136), N^1-*L*-tryptophanyl-*L*-arginyl(2,2,5,7,8-pentamethylchroman-6-sulfonamide)-N^9-acetyl-norspermidine (137)

The Dde group of resin **121** (0.40 g, 0.2 mmol) was removed (general procedure B), the resulting amine-resin capped with acetic anhydride (general procedure F) and the Tfa group removed (general procedure H). Fmoc-Arg(Pmc)-OH was coupled to the resulting amine-resin (general procedure A), the Fmoc group removed (general procedure C) and Boc-Trp(Boc)-OH coupled to the resulting amine-resin (general procedure A). Cleavage from the resin was accomplished (general procedure J) and the desired compounds were purified as the TFA salts by semi-prep HPLC.

N^1-*L*-Tryptophanyl-*L*-arginyl-N^9-acetyl-norspermidine (136)

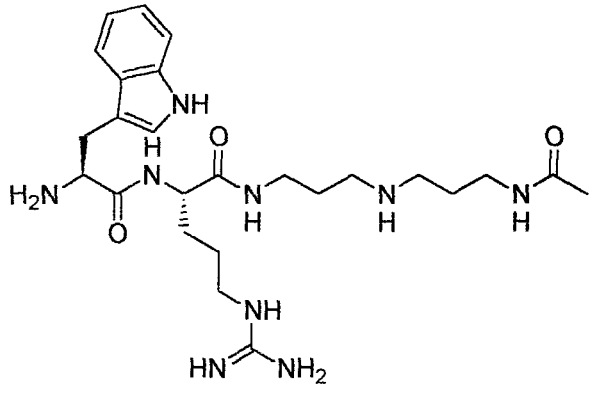

Semi-prep HPLC R_t = 19.4 min (gradient 4), yield = 16 mg, 13%.

^{1}H NMR (400 MHz, CD_3OD): δ 7.66 (d, 1H, J = 8, ArC<u>H</u>), 7.39 (d, 1H, J = 8, ArC<u>H</u>), 7.26 (s, 1H, ArC<u>H</u>), 7.15 (t, 1H, J = 8, ArC<u>H</u>), 7.06 (t, 1H, J = 8, ArC<u>H</u>), 4.30-4.24 (m, 2H, Arg αC<u>H</u>, Trp αC<u>H</u>), 3.45 (dd, 1H, J = 15, 6.5, Trp βC<u>H</u>H), 3.38-3.16 (m, 7H, Trp βCH<u>H</u>, 2 x CONHC<u>H</u>$_2$, Arg δC<u>H</u>$_2$), 2.96-2.88 (m, 4H, C<u>H</u>$_2$NHC<u>H</u>$_2$), 1.95 (s, 3H, C<u>H</u>$_3$CO), 1.90-1.80 (m, 4H, 2 x NHCH$_2$C<u>H</u>$_2$CH$_2$NH), 1.78-1.57 (m, 4H, Arg βC<u>H</u>$_2$, Arg γC<u>H</u>$_2$).

^{13}C NMR (100 MHz, CD_3OD): δ 174.3 (C), 174.2 (C), 170.4 (C), 158.7 (C), 138.1 (C), 128.4 (C), 125.8 (CH), 122.9 (CH), 120.4 (CH), 119.2 (CH), 112.6 (CH), 107.9 (C), 54.9 (CH), 54.8 (CH), 46.5 (CH_2), 46.3 (CH_2), 41.9 (CH_2), 37.0 (CH_2), 36.9 (CH_2), 30.1 (CH_2), 28.7 (CH_2), 27.6 (CH_2), 27.4 (CH_2), 26.3 (CH_2), 22.5 (CH_3).

LRMS (ESI): 258.9 $[M+2H]^{2+}$ (100), 516.5 $[M+H]^+$ (46).

HRMS (ESI): Found 516.3410, $C_{25}H_{42}N_9O_3$ requires 516.3405.

HPLC 11.1 min, 100% (λ = 220 nm, gradient 2).

N^1-*L*-Tryptophanyl-*L*-arginyl(2,2,5,7,8-pentamethylchroman-6-sulfonamide)-N^9-acetyl-norspermidine (137)

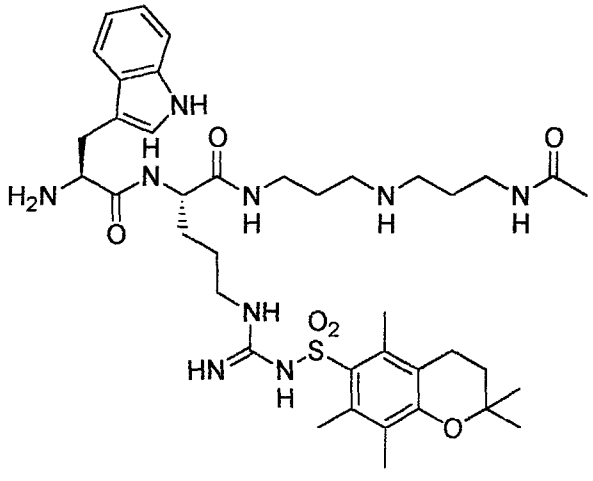

Semi-prep HPLC R_t = 37.0 min (gradient 4), yield = 21 mg, 12%.

^{1}H NMR (400 MHz, CD_3OD): δ 7.70 (d, 1H, *J* = 8, ArC<u>H</u>), 7.42 (d, 1H, *J* = 8, ArC<u>H</u>), 7.29 (s, 1H, ArC<u>H</u>), 7.18 (t, 1H, *J* = 8, ArC<u>H</u>), 7.10 (t, 1H, *J* = 8, ArC<u>H</u>), 4.46 (bs, 1H, Arg αC<u>H</u>), 4.26 (t, 1H, *J* = 7, Trp αC<u>H</u>), 3.49 (dd, 1H, *J* = 15, 6, Trp βCH<u>H</u>), 3.37-3.23 (m, 5H, Trp βC<u>H</u>H, 2 x CONHC<u>H</u>$_2$), 3.20-3.12 (m, 2H, Arg δC<u>H</u>$_2$), 3.05-2.97 (m, 4H, C<u>H</u>$_2$NHC<u>H</u>$_2$), 2.71 (t, 2H, *J* = 6.5, ArC<u>H</u>$_2$CH$_2$), 2.62 (s, 3H, ArC<u>H</u>$_3$), 2.61 (s, 3H, ArC<u>H</u>$_3$), 2.14 (s, 3H, ArC<u>H</u>$_3$), 1.98 (s, 3H, COC<u>H</u>$_3$), 1.92-1.82 (m, 6H, 2 x

NHCH$_2$C$\underline{H}_2$CH$_2$NH, ArCH$_2$C$\underline{H}_2$), 1.80-1.69 (m, 2H, Arg βC$\underline{H}_2$), 1.67-1.58 (m, 2H, Arg γC$\underline{H}_2$), 1.35 (s, 6H, C(C$\underline{H}_3$)$_2$) .

^{13}C NMR (100 MHz, CD_3OD): δ 174.5 (C), 174.3 (C), 170.2 (C), 158.6 (C), 154.9 (C), 138.3 (C), 136.5 (C), 136.1 (C), 134.4 (C), 128.4 (C), 125.7 (CH), 125.1 (C), 123.0 (CH), 119.5 (CH), 119.2 (C), 119.0 (CH), 112.6 (CH), 107.9 (C), 75.0 (C), 54.8 (CH), 54.4 (CH), 46.6 (CH_2), 46.5 (CH_2), 37.0 (CH_2), 33.8 (CH_2), 30.3 (CH_2), 28.8 (CH_2), 27.7 (CH_2), 27.5 (CH_2), 26.9 (CH_3), 22.5 (CH_2), 22.4 (CH_3), 19.0 (CH_3), 17.9 (CH_3), 12.3 (CH_3).

LRMS (ESI): 782.7 $[M+H]^+$ (100), 804.7 $[M+Na]^+$ (55).

HRMS (ESI): Found 782.4357, $C_{39}H_{60}N_9O_6S$ requires 782.4382.

HPLC 14.7 min, 100% (λ = 220 nm, gradient 2).

$\underline{N^1\text{-}L\text{-Tryptophanyl-}L\text{-arginyl-}N^9\text{-hexanoyl-norspermidine (138), }N^1\text{-}L\text{-tryptophanyl-}L\text{-arginyl(2,2,5,7,8-pentamethylchroman-6-sulfonamide)-}N^9\text{-hexanoyl-norspermidine (139)}}$

The Dde group of resin **121** (0.40 g, 0.2 mmol) was removed (general procedure B), the resulting amine-resin capped with hexanoic anhydride (general procedure G) and the Tfa group removed (general procedure H). Fmoc-Arg(Pmc)-OH was coupled to the resulting amine-resin (general procedure A), the Fmoc group removed (general procedure C) and Boc-Trp(Boc)-OH coupled to the resulting amine-resin (general procedure A). Cleavage from the resin was accomplished (general procedure J) and the desired compounds were purified as the TFA salts by semi-prep HPLC.

N^1-*L*-Tryptophanyl-*L*-arginyl-N^9-hexanoyl-norspermidine (138)

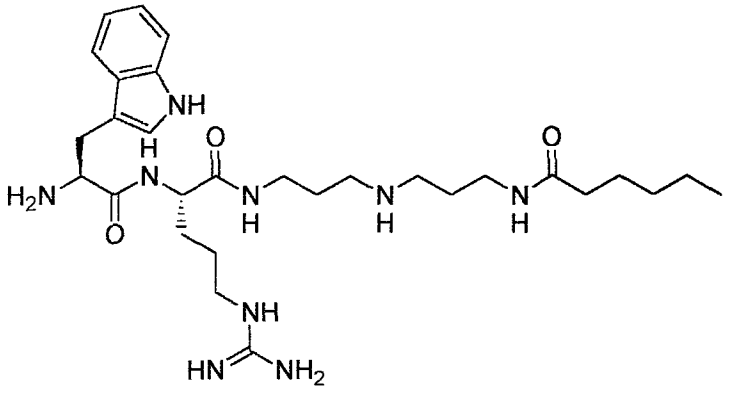

Semi-prep HPLC R_t = 26.6 min (gradient 4), yield = 14 mg, 10%.

^{1}H NMR (400 MHz, CD_3OD): δ 7.70 (d, 1H, J = 8, ArC<u>H</u>), 7.42 (d, 1H, J = 8, ArC<u>H</u>), 7.28 (s, 1H, ArC<u>H</u>), 7.18 (t, 1H, J = 8, ArC<u>H</u>), 7.10 (t, 1H, J = 8, ArC<u>H</u>), 4.33 (dd, 1H, J = 8, 6, Arg αC<u>H</u>), 4.27 (dd, 1H, J = 8, 6, Trp αC<u>H</u>), 3.49 (dd, 1H, J = 15, 6, Trp βC<u>H</u>H), 3.38-3.20 (m, 7H, Trp βCH<u>H</u>, Arg δC<u>H</u>$_2$, 2 x CONHC<u>H</u>$_2$), 3.03-2.90 (m, 4H, C<u>H</u>$_2$NHC<u>H</u>$_2$), 2.22 (t, 2H, J = 7.5, COC<u>H</u>$_2$), 1.90-1.59 (m, 10H, Arg βC<u>H</u>$_2$, Arg γC<u>H</u>$_2$, 2 x NHCH$_2$C<u>H</u>$_2$CH$_2$NH, C<u>H</u>$_2$CH$_2$CO), 1.39-1.27 (m, 4H, CH$_3$C<u>H</u>$_2$C<u>H</u>$_2$), 0.92 (t, 3H, J = 7, C<u>H</u>$_3$CH$_2$).

LRMS (ESI): 286.9 $[M+2H]^{2+}$ (100), 572.4 $[M+H]^+$ (70), 594.4 $[M+Na]^+$ (15).

HRMS (ESI): Found 572.4041, $C_{29}H_{50}N_9O_3$ requires 572.4031.

HPLC 12.8 min, 100% (λ = 220 nm, gradient 2).

N^1-*L*-Tryptophanyl-*L*-arginyl(2,2,5,7,8-pentamethylchroman-6-sulfonamide)-N^9-hexanoyl-norspermidine (139)

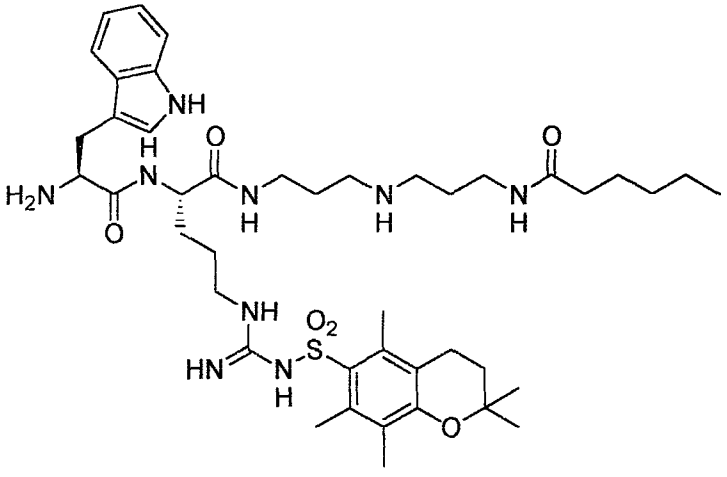

Semi-prep HPLC R_t = 41.7 min (gradient 4), yield = 14 mg, 7%.

^{1}H NMR (400 MHz, CD_3OD): δ 7.71 (d, 1H, J = 8, ArC<u>H</u>), 7.44 (d, 1H, J = 8, ArC<u>H</u>), 7.29 (s, 1H, ArC<u>H</u>), 7.19 (t, 1H, J = 8, ArC<u>H</u>), 7.11 (t, 1H, J = 8, ArC<u>H</u>), 4.50 (bs, 1H, Arg αC<u>H</u>), 4.26 (t, 1H, J = 7, Trp αC<u>H</u>), 3.49 (dd, 1H, J = 15, 6, Trp βC<u>H</u>H), 3.39-3.14 (m, 7H, Trp βCH<u>H</u>, Arg δC<u>H</u>$_2$, 2 x CONHC<u>H</u>$_2$), 3.09-2.97 (m, 4H, C<u>H</u>$_2$NHC<u>H</u>$_2$), 2.72 (t, 2H, J = 7, ArC<u>H</u>$_2$CH$_2$), 2.63 (s, 3H, ArC<u>H</u>$_3$), 2.61 (s, 3H, ArC<u>H</u>$_3$), 2.22 (t, 2H, J = 7.5, COC<u>H</u>$_2$), 2.15 (s, 3H, ArC<u>H</u>$_3$), 1.97-1.83 (m, 6H, ArCH$_2$C<u>H</u>$_2$, 2 x NHCH$_2$C<u>H</u>$_2$CH$_2$NH), 1.82-1.71 (m, 2H, Arg βC<u>H</u>$_2$), 1.70-1.57 (m, 4H, C<u>H</u>$_2$CH$_2$CO, Arg γC<u>H</u>$_2$), 1.39-1.28 (m, 10H, C(C<u>H</u>$_3$)$_2$, CH$_3$C<u>H</u>$_2$C<u>H</u>$_2$), 0.94 (t, 3H, J = 7, C<u>H</u>$_3$CH$_2$).

LRMS (ESI): 420.0 $[M+2H]^{2+}$ (100), 860.7 $[M+Na]^+$ (50), 838.7 $[M+H]^+$ (45).

HRMS (ESI): Found 838.5002, $C_{43}H_{68}N_9O_6S$ requires 838.5008.

HPLC 15.5 min, 100% (λ = 220 nm, gradient 2).

N^1,N^9-*bis*-(*L*-Tryptophanyl)-norspermidine (140)

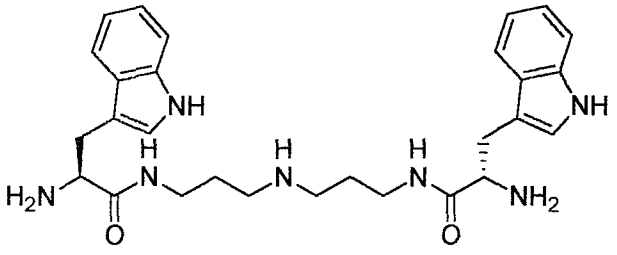

The Dde groups of resin **108** (0.20 g, 0.13 mmol) were removed (general procedure B), Boc-Trp(Boc)-OH coupled to the resulting amine-resin (general procedure A) and cleavage from the resin accomplished (general procedure I). The desired compound was purified as the TFA salt by semi-prep HPLC.

Semi-prep HPLC R_t = 21.4 min (gradient 4), yield = 17 mg, 21%.

^{1}H NMR (400 MHz, CD_3OD): δ 7.62 (d, 2H, J = 7.5, 2 x ArC<u>H</u>), 7.40 (d, 2H, J = 7.5, 2 x ArC<u>H</u>), 7.22 (s, 2H, 2 x ArC<u>H</u>), 7.16 (t, 2H, J = 7.5, 2 x ArC<u>H</u>), 7.08 (t, 2H, J = 7.5, 2 x ArC<u>H</u>), 4.11 (t, 2H, J = 7.5, 2 x Trp αC<u>H</u>), 3.42-3.16 (m, 8H, 2 x Trp βC<u>H</u>$_2$, 2 x CONHC<u>H</u>$_2$), 2.65 (t, 4H, J = 7, C<u>H</u>$_2$NHC<u>H</u>$_2$), 1.71 (tt, 4H, J = 7, 7, 2 x $CH_2C\underline{H}_2CH_2$).

^{13}C NMR (100 MHz, CD_3OD): δ 170.9 (C), 138.2 (C), 128.4 (CH), 125.5 (CH), 123.0 (CH), 120.3 (CH), 119.1 (CH), 112.7 (C), 108.1 (C), 55.3 (CH), 46.2 (CH_2), 37.4 (CH_2), 28.8 (CH_2), 27.1 (CH_2).

LRMS (ESI): 504.4 $[M+H]^+$ (100), 526.4 $[M+Na]^+$ (11).

HRMS (ESI): Found 504.3087, $C_{28}H_{38}N_7O_2$ requires 504.3082.

HPLC 12.3 min, 100% (λ = 220 nm, gradient 2).

N^1-*L*-Arginyl(2,2,5,7,8-pentamethylchroman-6-sulfonamide)-N^9-*L*-arginyl-norspermidine (141), N^1,N^9-*bis*-(*L*-Arginyl(2,2,5,7,8-pentamethylchroman-6-sulfonamide))-norspermidine (142)

The Dde groups of resin **108** (0.40 g, 0.26 mmol) were removed (general procedure B), Fmoc-Arg(Pmc)-OH coupled to the resulting amine-resin (general procedure A) and the Fmoc group removed (general procedure C). Cleavage from the resin was accomplished (general procedure J) and the desired compounds were purified as the TFA salts by semi-prep HPLC.

N^1-*L*-Arginyl(2,2,5,7,8-pentamethylchroman-6-sulfonamide)-N^9-*L*-arginyl-norspermidine (141)

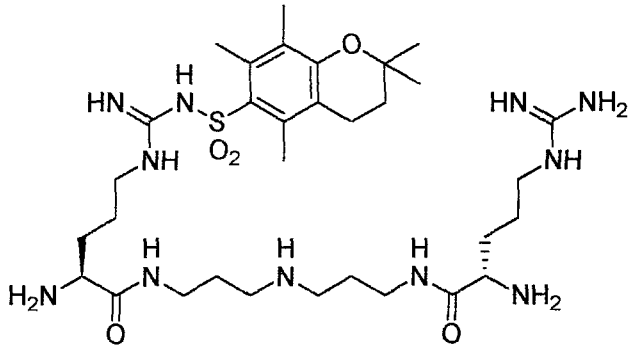

Semi-prep HPLC R_t = 31.0 min (gradient 4), yield = 14 mg, 7%.

^{1}H NMR (400 MHz, CD_3OD): δ 3.97-3.87 (m, 2H, 2 x Arg αC<u>H</u>), 3.50-3.16 (m, 8H, 2 x Arg δC<u>H</u>$_2$, 2 x CONHC<u>H</u>$_2$), 3.10 (t, 4H, J = 7.5, C<u>H</u>$_2$NHC<u>H</u>$_2$), 2.69 (t, 2H, J = 7, ArC<u>H</u>$_2$CH$_2$), 2.59 (s, 3H, ArC<u>H</u>$_3$), 2.58 (s, 3H, ArC<u>H</u>$_3$), 2.12 (s, 3H, ArC<u>H</u>$_3$), 2.03-1.83 (m, 10H, 2 x Arg βC<u>H</u>$_2$, 2 x NHCH$_2$C<u>H</u>$_2$CH$_2$NH, ArCH$_2$C<u>H</u>$_2$), 1.74-1.61 (m, 4H, 2 x Arg γC<u>H</u>$_2$), 1.33 (s, 6H, C(C<u>H</u>$_3$)$_2$).

LRMS (ESI): 356.1 $[M+2H]^{2+}$ (100), 710.7 $[M+H]^+$ (23).

HRMS (ESI): Found 710.4500, $C_{32}H_{60}N_{11}O_5S$ requires 710.4494.

HPLC 13.3 min, 100% (λ = 220 nm, gradient 2).

N^1,N^9-*bis*-(*L*-Arginyl(2,2,5,7,8-pentamethylchroman-6-sulfonamide))-norspermidine (142)

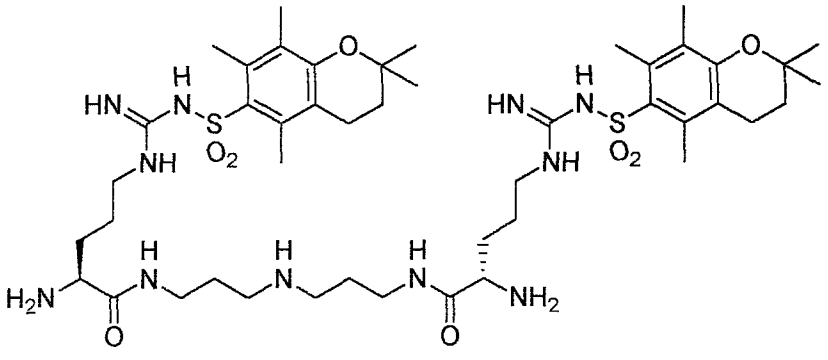

Semi-prep HPLC R_t = 40.7 min (gradient 4), yield = 18 mg, 6%.

^{1}H NMR (400 MHz, CD_3OD): δ 3.96 (t, 2H, J = 6.5, 2 x Arg αC<u>H</u>), 3.50-3.08 (m, 12H, 2 x NHC<u>H</u>$_2$CH$_2$C<u>H</u>$_2$NH, 2 x Arg δC<u>H</u>$_2$), 2.67 (t, 4H, J = 7, 2 x ArC<u>H</u>$_2$CH$_2$), 2.58 (s, 6H, 2 x ArC<u>H</u>$_3$), 2.56 (s, 6H, 2 x ArC<u>H</u>$_3$), 2.11 (s, 6H, 2 x ArC<u>H</u>$_3$), 2.03-1.81 (m, 12H, 2 x Arg βC<u>H</u>$_2$, 2 x ArCH$_2$C<u>H</u>$_2$, 2 x NHCH$_2$C<u>H</u>$_2$CH$_2$NH), 1.64 (tt, 4H, J = 7, 7, 2 x Arg γC<u>H</u>$_2$), 1.32 (s, 12H, 2 x C(C<u>H</u>$_3$)$_2$).

LRMS (ESI): 489.1 $[M+2H]^{2+}$ (100), 998.6 $[M+Na]^+$ (12).

HRMS (ESI): Found 976.5475, $C_{46}H_{78}N_{11}O_8S_2$ requires 976.5471.

HPLC 15.5 min, 100% (λ = 220 nm, gradient 2).

Boc-*L*-tryptophanyl-(Boc)-N^G-2,2,5,7,8-pentamethylchroman-6-sulfonamide-*L*-arginine (144)

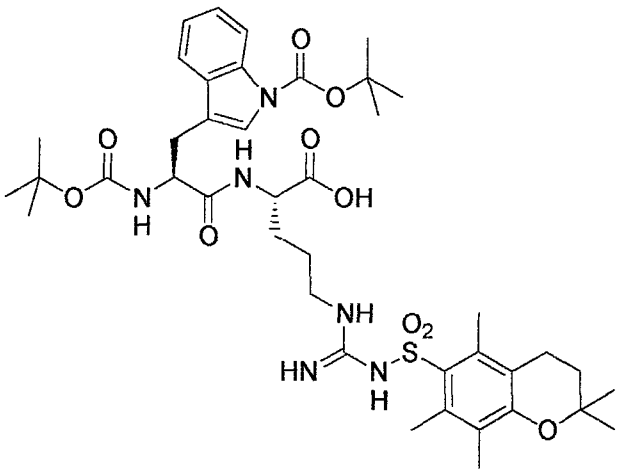

To a stirred solution of Boc-Trp(Boc)-OH (0.25 g, 0.6 mmol) and *N*-hydroxy succinimide (0.71 g, 0.6 mmol) in THF (5 mL) at 0 °C was added DCC (0.13 g, 0.6 mmol). After 2 hours, the reaction mixture was filtered and the filtrate concentrated *in vacuo* to yield a white foam. The crude product was dissolved in DMF (5 mL) and a solution of H-Arg(Pmc)-OH (0.27 g, 0.6 mmol) and NEt_3 (86 µL, 0.6 mmol) in DMF (2 mL) was added. The reaction mixture was stirred overnight and concentrated *in vacuo*. The residue was taken into water (50 mL), extracted with EtOAc (4 x 50 mL), the organic extracts combined, dried ($MgSO_4$) and concentrated *in vacuo* to yield the title compound as a white solid (0.39 g, 77%).

Mpt 203-206 °C.

***R*$_f$** 0.37 (EtOAc/hexane, 1:1).

^{1}H NMR (400 MHz, CD_3OD): δ 8.05 (d, 1H, J = 7.5, ArC<u>H</u>), 7.59 (d, 1H, J = 7.5, ArC<u>H</u>), 7.47 (s, 1H, ArC<u>H</u>), 7.24 (t, 1H, J = 7.5, ArC<u>H</u>), 7.17 (t, 1H, J = 7.5, ArC<u>H</u>), 4.41-4.32 (m, 2H, Arg αC<u>H</u>, Trp αC<u>H</u>), 3.22-3.10 (m, 3H, Trp βCH<u>H</u>, Arg δC<u>H</u>$_2$), 2.92 (dd, 1H, J = 14.5, 9, Trp βCH<u>H</u>), 2.61 (t, 2H, J = 7, ArC<u>H</u>$_2$), 2.53 (s, 3H, ArC<u>H</u>$_3$), 2.51 (s, 3H, ArC<u>H</u>$_3$), 2.06 (s, 3H, ArC<u>H</u>$_3$), 1.90-1.73 (m, 3H, Arg βCH<u>H</u>, ArCH$_2$C<u>H</u>$_2$), 1.70-1.58 (m, 10H,

Arg βCHH, $CO_2C(CH_3)_3$), 1.55-1.45 (m, 2H, Arg γCH_2), 1.34-1.23 (m, 15H, $CO_2C(CH_3)_3$, $C(CH_3)_2$).

^{13}C NMR (100 MHz, CD_3OD): δ 174.7 (C), 174.3 (C), 157.6 (C), 154.7 (C), 151.0 (C), 136.8 (C), 136.5 (C), 136.1 (C), 134.7 (C),131.8 (C), 125.4 (CH), 125.0 (C), 123.6 (CH), 120.1 (CH), 119.3 (C), 117.5 (C), 116.0 (CH), 84.6 (C), 80.7 (C), 74.8 (C), 55.9 (CH), 53.2 (CH), 41.5 (CH_2), 34.7 (CH_2), 33.8 (CH_2), 30.1 (CH_2), 28.7 (CH_3), 28.4 (CH_3), 27.0 (CH_3), 22.3 (CH_2), 19.0 (CH_3), 17.9 (CH_3), 12.3 (CH_3).

IR ν (cm^{-1}): 3300, 1728, 1547, 1453, 1368, 1252, 1157.

LRMS (ESI): 827.5 $[M+H]^+$ (100%), 849.5 $[M+Na]^+$ (92%).

HRMS (ESI): Found 849.3797, $C_{41}H_{58}N_6O_{10}SNa$ requires 849.4008.

HPLC 12.0 min, 100% (λ = 220 nm, gradient 1).

<u>*L*-Tryptophanyl-*L*-arginine (145), *L*-Tryptophanyl-N^G-2,2,5,7,8-pentamethylchroman-6-sulfonamide-*L*-arginine (146)</u>

144 (0.10 g, 0.1 mmol) was treated with a solution of TFA/thioanisole/DCM/water (10:2:7:1, 5 mL) at room temperature for 30 min. The reaction mixture was concentrated *in vacuo*, the resulting oily residue dissolved in TFA, precipitated from ice-cold Et_2O and lyophilized. The desired compounds were purified as the TFA salts by semi-prep HPLC.

<u>*L*-Tryptophanyl-*L*-arginine (145)</u>

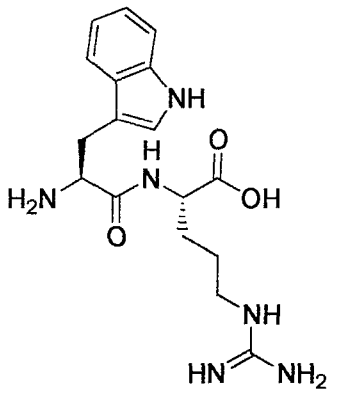

Semi-prep HPLC R_t = 22.0 min (gradient 4), yield = 12 mg, 33%.

^{1}H NMR (400 MHz, CD_3OD): δ 7.76 (d, 1H, J = 7.5, ArC<u>H</u>), 7.56 (d, 1H, J = 7.5, ArC<u>H</u>), 7.42 (s, 1H, ArC<u>H</u>), 7.30 (t, 1H, J = 7.5, ArC<u>H</u>), 7.21 (t, 1H, J = 7.5, ArC<u>H</u>), 4.37-4.52 (m, 2H, Arg αC<u>H</u>, Trp αC<u>H</u>), 3.60-3.42 (m, 2H, Trp βC<u>H_2</u>), 3.34-3.25 (m, 2H, Arg δC<u>H_2</u>), 2.16-1.64 (m, 4H, Arg βC<u>H_2</u>, Arg γC<u>H_2</u>).

^{13}C NMR (100 MHz, CD_3OD): δ 175.0 (C), 170.9 (C), 158.1 (C), 137.7 (C), 128.1 (C), 126.0 (CH), 122.9 (CH), 120.3 (CH), 119.0 (CH), 112.7 (CH), 107.4 (C), 54.7 (CH), 53.6 (CH), 41.7 (CH_2), 29.5 (CH_2), 28.1 (CH_2), 25.5 (CH_2).

LRMS (ESI): 361.1 $[M+H]^+$ (100).

HRMS (ESI): Found 361.1978, $C_{17}H_{25}N_6O_3$ requires 361.1982.

HPLC 11.6 min, 100% (λ = 220 nm, gradient 2).

<u>*L*-Tryptophanyl-N^G-2,2,5,7,8-pentamethylchroman-6-sulfonamide-*L*-arginine (146)</u>

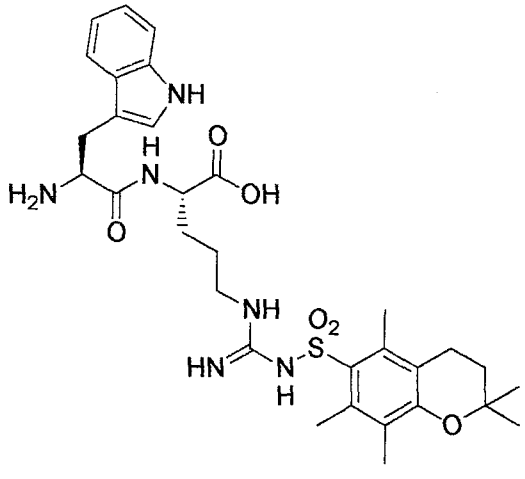

Semi-prep HPLC R_t = 42.6 min (gradient 4), yield = 15 mg, 24%.

^{1}H NMR (400 MHz, CD_3OD): δ 7.73 (d, 1H, J = 7.5, ArC<u>H</u>), 7.41 (d, 1H, J = 7.5, ArC<u>H</u>), 7.27 (s, 1H, ArC<u>H</u>), 7.17 (t, 1H, J = 7.5, ArC<u>H</u>), 7.09 (t, 1H, J = 7.5, ArC<u>H</u>), 4.46 (dd, 1H, J = 8.5, 4.5, Arg αC<u>H</u>), 4.24 (dd, 1H, J = 9, 5.5,

Trp αC<u>H</u>), 3.50 (dd, 1H, J = 15, 5.5, Trp βCH<u>H</u>), 3.29-3.15 (m, 3H, Trp βC<u>H</u><u>H</u>, Arg δC<u>H</u>$_2$), 2.70 (t, 2H, J = 7, ArC<u>H</u>$_2$), 2.59 (s, 3H, ArC<u>H</u>$_3$), 2.57 (s, 3H, ArC<u>H</u>$_3$), 2.13 (s, 3H, ArC<u>H</u>$_3$), 2.02-1.91 (m, 1H, Arg βCH<u>H</u>), 1.86 (t, 2H, J = 7.0, ArCH$_2$C<u>H</u>$_2$), 1.82-1.71 (m, 1H, Arg βCH<u>H</u>), 1.69-1.59 (m, 2H, Arg γC<u>H</u>$_2$), 1.34 (s, 6H, C(C<u>H</u>$_3$)$_2$).

^{13}C NMR (100 MHz, CD_3OD): δ 174.4 (C), 170.2 (C), 158.0 (C), 154.8 (C), 138.3 (C), 136.6 (C), 136.2 (C), 134.3 (C), 128.3 (C), 125.8 (CH), 125.1 (C), 122.9 (CH), 120.3 (CH), 119.5 (C), 119.1 (CH), 112.6 (CH), 107.8 (C), 75.0 (C), 54.8 (CH), 53.6 (CH), 41.5 (CH_2), 33.8 (CH_2), 29.9 (CH_2), 28.8 (CH_2), 26.9 (CH_3), 22.3 (CH_2), 18.9 (CH_3), 17.8 (CH_3), 12.2 (CH_3).

LRMS (ESI): 627.4 $[M+H]^+$ (100), 649.4 $[M+Na]^+$ (48).

HRMS (ESI): Found 627.2972, $C_{31}H_{43}N_6O_6S$ requires 627.2960.

HPLC 15.8 min, 100% (λ = 220 nm, gradient 2).

<u>Single Point Screening of Library at 100 μM</u>

Assays were performed using 1 mL total volume, containing ammonium acetate buffer (50 mM NH_4OAc, pH 7.5), EDTA (1 mM), NADPH (100 μM), nortrypanothione disulfide (30 μM), TR (2 nM) and inhibitor (100 μM). Initial rates were recorded at 340 nm at inhibitor concentrations of 100 μM. Data were collected in triplicate and compared to a control containing no inhibitor to determine the % inhibition. Initial rate data are displayed in Table 15.

Compound	v ($\Delta Asec^{-1} \times 10^3$)	v control ($\Delta Asec^{-1} \times 10^3$)	% Inhibition
110	0.613	4.526	86
125	4.852	5.119	5
126	4.979	5.119	3
127	4.890	5.119	4
128	5.124	5.119	0
129	4.992	5.119	2
130	5.008	5.119	2
131	3.558	4.526	21
132	2.382	4.526	47
133	0.544	4.526	88
134	3.204	4.526	29
135	2.951	4.526	35
136	2.276	4.526	50
137	0.232	4.526	95
138	0.507	4.526	89
139	0.174	4.526	96
140	0.641	5.222	74
141	0.896	5.222	88
142	1.348	5.222	83
145	5.167	5.222	1
146	4.476	5.222	14

Table 15: Initial rate data from 100 μM screening.

Single Point Screening of Library Hits at 10 μM

Assays were performed as described above at an inhibitor concentration of 10 μM. Initial rate data are displayed in Table 16.

Compound	v ($\Delta Asec^{-1} \times 10^3$)	v control ($\Delta Asec^{-1} \times 10^3$)	% Inhibition
110	3.019	4.792	37
131	4.850	4.792	-1
132	4.447	4.792	7
133	2.545	4.792	7
134	4.903	4.792	-2
135	4.692	4.792	2
136	4.515	4.792	6
137	1.754	4.792	63
138	3.225	4.792	33
139	2.267	4.792	53
140	3.648	4.792	24
141	1.990	4.792	58
142	0.718	4.792	85

Table 16: Initial rate data from 10 μM screening.

Enzymatic Assays with Nortrypanothione as Variable Substrate

Studies were performed as described in Section 4.2. Initial rate data are shown in Tables 17-28.

[Substrate] (μM)	v ($\Delta Asec^{-1}$ x 10^3) at specified [Inhibitor]			
	0	20 μM	50 μM	100 μM
5	1.074	0.921	0.786	0.586
10	1.917	1.449	1.195	1.029
15	2.533	2.091	1.608	1.266
20	2.762	2.365	2.043	1.581
25	2.962	2.654	2.246	1.727
30	3.352	2.796	2.452	2.039
V_{max}[a]	5.764	4.919	4.799	3.976

[a]value obtained from Grafit non-linear regression analysis

Table 17: Initial rate data for N^1-*L*-arginyl(2,2,5,7,8-pentamethylchroman-6-sulfonamide)-norspermidine (**131**).

[Substrate] (μM)	v ($\Delta Asec^{-1}$ x 10^3) at specified [Inhibitor]			
	0	30 μM	**60 μM**	120 μM
5	0.934	0.608	0.521	0.331
10	1.863	1.194	0.861	0.605
15	2.287	1.416	1.087	0.844
20	2.706	1.793	1.411	0.927
25	3.057	2.134	1.589	1.279
30	3.115	2.260	1.761	1.266
V_{max}	6.043	4.817	3.725	3.166

Table 18: Initial rate data for N^1-*L*-arginyl(2,2,5,7,8-pentamethylchroman-6-sulfonamide)-N^9-acetyl-norspermidine (**132**).

[Substrate] (μM)	v (ΔAsec^{-1} x 10^3) at specified [Inhibitor]			
	0	5 μM	10 μM	20 μM
5	1.192	0.645	0.418	0.235
10	1.967	1.034	0.754	0.363
15	2.456	1.314	0.936	0.524
20	2.797	1.575	1.058	0.642
25	3.076	1.880	1.234	0.777
30	3.199	1.948	1.367	0.747
V_{max}	5.227	3.595	2.369	1.596

Table 19: Initial rate data for N^1-*L*-arginyl(2,2,5,7,8-pentamethylchroman-6-sulfonamide)-N^9-hexanoyl-norspermidine (**133**).

[Substrate] (μM)	v (ΔAsec^{-1} x 10^3) at specified [Inhibitor]			
	0	40 μM	80 μM	160 μM
5	1.137	0.846	0.660	0.387
10	1.863	1.444	1.096	0.846
15	2.287	1.870	1.533	1.189
20	2.706	2.117	1.782	1.541
25	3.057	2.410	2.123	1.661
30	3.115	2.695	2.357	1.924
V_{max}	4.915	4.648	5.220	5.399

Table 20: Initial rate data for N^1-*L*-tryptophanyl-*L*-arginyl-norspermidine (**134**).

[Substrate] (μM)	v ($\Delta Asec^{-1}$ x 10^3) at specified [Inhibitor]			
	0	30 μM	60 μM	120 μM
5	1.502	1.091	0.896	0.599
10	1.894	1.580	1.334	1.097
15	2.576	2.192	1.846	1.438
20	2.864	2.479	2.087	1.820
25	3.104	2.890	2.325	1.924
30	3.374	2.960	2.623	2.151
V_{max}	4.711	4.974	4.441	4.193

Table 21: Initial rate data for N^1-*L*-tryptophanyl-*L*-arginyl-N^9-acetyl-norspermidine (**136**).

[Substrate] (μM)	v ($\Delta Asec^{-1}$ x 10^3) at specified [Inhibitor]			
	0	50 μM	100 μM	200 μM
5	1.152	0.518	0.287	0.177
10	1.894	0.879	0.539	0.323
15	2.576	1.189	0.829	0.498
20	2.864	1.537	0.951	0.571
25	3.104	1.870	1.238	0.743
30	3.374	2.237	1.432	0.922
V_{max}	4.895	10.499	4.938	5.270

Table 22: Initial rate data for N^1-*L*-tryptophanyl-*L*-arginyl-N^9-hexanoyl-norspermidine (**138**).

[Substrate] (μM)	v ($\Delta Asec^{-1}$ x 10^3) at specified [Inhibitor]			
	0	5 μM	10 μM	20 μM
5	1.140	0.781	0.481	0.230
10	1.703	1.432	0.886	0.342
15	2.414	1.752	1.097	0.496
20	2.551	2.119	1.459	0.522
25	2.923	2.110	1.777	0.597
30	3.378	2.555	1.571	0.694
V_{max}	5.811	4.081	3.300	1.176

Table 23: Initial rate data for N^1-*L*-tryptophanyl-*L*-arginyl(2,2,5,7,8-pentamethylchroman-6-sulfonamide)-norspermidine (**135**).

[Substrate] (μM)	v ($\Delta Asec^{-1}$ x 10^3) at specified [Inhibitor]			
	0	5 μM	10 μM	20 μM
5	1.733	1.166	0.917	0.552
10	2.534	1.652	1.216	0.751
15	2.933	1.895	1.587	0.983
20	3.068	2.083	1.664	1.001
25	3.282	2.330	1.721	1.314
30	3.416	2.612	1.916	1.318
35	3.434	2.450	1.852	1.466
V_{max}	4.339	3.201	2.328	2.114

Table 24: Initial rate data for N^1-*L*-tryptophanyl-*L*-arginyl(2,2,5,7,8-pentamethylchroman-6-sulfonamide)-N^9-acetyl-norspermidine (**137**).

[Substrate] (μM)	v ($\Delta Asec^{-1} \times 10^3$) at specified [Inhibitor]			
	0	5 μM	10 μM	20 μM
5	1.004	0.507	0.338	0.190
10	1.869	0.899	0.526	0.328
15	2.278	1.217	0.834	0.490
20	2.511	1.547	0.965	0.598
25	2.971	1.710	1.107	0.651
30	3.320	1.839	1.222	0.720
V_{max}	6.088	3.910	2.798	1.592

Table 25: Initial rate data for N^1-*L*-tryptophanyl-*L*-arginyl(2,2,5,7,8-pentamethylchroman-6-sulfonamide)-N^9-hexanoyl-norspermidine (**139**).

[Substrate] (μM)	v ($\Delta Asec^{-1} \times 10^3$) at specified [Inhibitor]			
	0	15 μM	30 μM	60 μM
5	1.355	0.824	0.556	0.368
10	1.954	1.088	0.844	0.677
15	2.630	1.792	1.481	0.883
20	2.891	2.122	1.656	1.198
25	3.115	2.523	2.051	1.437
30	3.463	2.657	2.221	1.690
V_{max}	5.366	6.334	6.661	8.323

Table 26: Initial rate data for N^1,N^9-*bis*-(*L*-tryptophanyl)-norspermidine (**140**).

[Substrate] (μM)	v ($\Delta Asec^{-1} \times 10^3$) at specified [Inhibitor]			
	0	5 μM	10 μM	20 μM
5	1.041	0.628	0.463	0.289
10	1.896	1.234	0.822	0.491
15	2.482	1.676	1.214	0.815
20	2.977	2.054	1.589	0.911
25	3.298	2.359	1.810	1.135
30	3.458	2.448	1.810	1.315
V_{max}	7.118	5.283	4.518	4.996

Table 27: Initial rate data for N^1-*L*-arginyl(2,2,5,7,8-pentamethylchroman-6-sulfonamide)-N^9-*L*-arginyl-norspermidine (**141**).

[Substrate] (μM)	v ($\Delta Asec^{-1} \times 10^3$) at specified [Inhibitor]			
	0	1 μM	2 μM	4 μM
5	1.101	1.082	0.692	0.343
10	2.186	1.704	1.017	0.723
15	2.630	2.213	1.534	0.843
20	2.739	2.571	1.673	1.037
25	3.017	2.714	1.878	1.250
30	3.303	2.946	2.076	1.257
V_{max}	5.323	4.508	3.629	2.460

Table 28: Initial rate data for N^1,N^9-*bis*-(*L*-arginyl(2,2,5,7,8-pentamethylchroman-6-sulfonamide))-norspermidine (**142**).

REFERENCES

(1) Barrett, M. *Lancet* **1999**, *353*, 1113-1114.

(2) Anene, B. M.; Onah, D. N.; Nawa, Y. *Vet. Parasitol.* **2001**, *96*, 83-100.

(3) Guerrant, R.; Walker, D.; Weller, P.; *Tropical Infectious Diseases: Principals, Pathogens and Practice,* Churchill Livingstone:Philadelphia, **1999.**

(4) World Health Organisation *http://www.who.int/index.html*

(5) Imlay, J. A.; Linn, S. In *Science*, 1988; Vol. 240, pp 1302-1309.

(6) Aust, S. D.; Morehouse, L. A.; Thomas, C. E. *J. Free Radic. Biol. Med.* **1985**, *1*, 3-25.

(7) Bannister, J. V.; Bannister, W. H.; Rotillo, G. *Crit. Rev. Biochem.* **1987**, *22*, 111-180.

(8) Le Trang, N.; Meshnick, S. R.; Kitchener, K.; Eaton, J. W.; Cerami, A. *J. Biol. Chem.* **1983**, *258*, 125-130.

(9) Henderson, G. B.; Fairlamb, A. H.; Cerami, A. *Mol. Biochem. Parasitol.* **1987**, *24*, 39-45.

(10) Akerboom, T. P. M.; Bilzer, M.; Sies, H. *J. Biol. Chem.* **1982**, *257*, 4248-4252.

(11) Krohne-Ehrich, G.; Schirmer, R. H.; Untucht-Grau, R. *Eur. J. Biochem.* **1977**, *80*, 65-71.

(12) Schiltz, E.; Blatterspiel, R.; Untucht-Grau, R. *Eur. J. Biochem.* **1979**, 269-278.

(13) Untucht-Grau, R.; Schirmer, R. H.; Schirmer, I.; Krauth-Siegel, R. *Eur. J. Biochem.* **1981**, *120*, 407-419.

(14) Krauth-Siegel, R.; Blatterspiel, R.; Saleh, M.; Schiltz, E.; Schirmer, R. H.; Untucht-Grau, R. *Eur. J. Biochem.* **1982**, *121*, 259-267.

(15) Fairlamb, A. H.; Blackburn, P.; Ulrich, P.; Chait, B. T.; Cerami, A. *Science* **1985**, *227*, 1485-1487.

(16) Shames, S. L.; Fairlamb, A. H.; Cerami, A.; Walsh, C. T. *Biochemistry* **1986**, *25*, 3519-3526.

(17) Krauthsiegel, R. L.; Enders, B.; Henderson, G. B.; Fairlamb, A. H.; Schirmer, R. H. *Eur. J. Biochem.* **1987**, *164*, 123-128.

(18) Fairlamb, A. H.; Carter, N. S.; Cunningham, M.; Smith, K. *Mol. Biochem. Parasitol.* **1992**, *53*, 213-222.

(19) Sullivan, F. X.; Shames, S. L.; Walsh, C. T. *Biochemistry* **1989**, *28*, 4986-4992.

(20) Ghisla, S.; Massey, V. *Eur. J. Biochem.* **1989**, *181*, 1-17.

(21) Henderson, G. B.; Fairlamb, A. H. *Parasitol. Today* **1987**, *3*, 312-315.

(22) Krauth-Siegel, R.; Jockersscherubl, M. C.; Becker, K.; Schirmer, R. H. *Biochem. Soc. Trans.* **1989**, *17*, 315-317.

(23) Walsh, C, T.; Bradley, M.; Nadeau, K. *Trends Biochem.Sci.* **1991**, *16*, 305-309.

(24) Henderson, G. B.; Fairlamb, A. H.; Ulrich, P.; Cerami, A. *Biochemistry* **1987**, *26*, 3023-3027.

(25) Karplus, P. A.; Pai, E. F.; Schulz, G. E. *Eur. J. Biochem.* **1989**, *178*, 693-703.

(26) Pai, E. F.; Schulz, G. E. *J. Biol. Chem.* **1983**, *258*, 1752-1757.

(27) Pai, E. F.; Karplus, P. A.; Schulz, G. E. *Biochemistry* **1988**, *27*, 4465-4474.

(28) Bilzer, M.; Krauth-Siegel, R. L.; Schirmer, R. H.; Akerboom, T. P. M.; Sies, H.; Schulz, G. E. *Eur. J. Biochem.* **1984**, *138*, 373-378.

(29) Karplus, P. A.; Schulz, G. E. *J. Mol. Biol.* **1987**, *195*, 701-729.

(30) Karplus, P. A.; Schulz, G. E. *J. Mol. Biol.* **1989**, *210*, 163-180.

(31) Kuriyan, J.; Kong, X. P.; Krishna, T. S. R.; Sweet, R. M.; Murgolo, N. J.; Field, H.; Cerami, A.; Henderson, G. B. *Proc. Natl. Acad. Sci. U. S. A.* **1991**, *88*, 8764-8768.

(32) Field, H.; Cerami, A.; Henderson, G. B. *Mol. Biochem. Parasitol.* **1992**, *50*, 47-56.

(33) Shames, S. L.; Kimmel, B. E.; Peoples, O. P.; Agabian, N.; Walsh, C. T. *Biochemistry* **1988**, *27*, 5014-5019.

(34) Sullivan, F. X.; Walsh, C. T. *Mol. Biochem. Parasitol.* **1991**, *44*, 145-147.

(35) Taylor, M. C. *PhD thesis. Univ. London, London* **1992**.

(36) Bradley, M.; Bucheler, U. S.; Walsh, C. T. *Biochemistry* **1991**, *30*, 6124-6127.

(37) Sullivan, F. X.; Sobolov, S. B.; Bradley, M.; Walsh, C. T. *Biochemistry* **1991**, *30*, 2761-2767.

(38) Henderson, G. B.; Murgolo, N. J.; Kuriyan, J.; Osapay, K.; Kominos, D.; Berry, A.; Scrutton, N. S.; Hinchliffe, N. W.; Perham, R. N.; Cerami, A. *Proc. Natl. Acad. Sci. U. S. A.* **1991**, *88*, 8769-8773.

(39) Elwaer, A.; Douglas, K. T.; Smith, K.; Fairlamb, A. H. *Anal. Biochem.* **1991**, *198*, 212-216.

(40) Benson, T. J.; McKie, J. H.; Garforth, J.; Borges, A.; Fairlamb, A. H.; Douglas, K. T. *Biochem. J.* **1992**, *286*, 9-11.

(41) Garforth, J.; Yin, H.; McKie, J. H.; Douglas, K. T.; Fairlamb, A. H. *J. Enzym. Inhib.* **1997**, *12*, 161-173.

(42) Chan, C.; Yin, H.; Garforth, J.; McKie, J. H.; Jaouhari, R.; Speers, P.; Douglas, K. T.; Rock, P. J.; Yardley, V.; Croft, S. L.; Fairlamb, A. H. *J. Med. Chem.* **1998**, *41*, 148-156.

(43) Khan, M. O. F.; Austin, S. E.; Chan, C.; Yin, H.; Marks, D.; Vaghjiani, S. N.; Kendrick, H.; Yardley, V.; Croft, S. L.; Douglas, K. T. *J. Med. Chem.* **2000**, *43*, 3148-3156.

(44) Fernandezgomez, R.; Moutiez, M.; Aumercier, M.; Bethegnies, G.; Luyckx, M.; Ouaissi, A.; Tartar, A.; Sergheraert, C. *Int. J. Antimicrob. Agents* **1995**, *6*, 111-118.

(45) Baillet, S.; Buisine, E.; Horvath, D.; Maes, L.; Bonnet, B.; Sergheraert, C. *Bioorg. Med. Chem.* **1996**, *4*, 891-899.

(46) Girault, S.; Baillet, S.; Horvath, D.; Lucas, V.; Davioud-Charvet, E.; Tartar, A.; Sergheraert, C. *Eur. J. Med. Chem.* **1997**, *32*, 39-52.

(47) McGovern, S. L.; Caselli, E.; Grigorieff, N.; Shoichet, B. K. *J. Med. Chem.* **2002**, *45*, 1712-1722.

(48) Girault, S.; Davioud-Charvet, E.; Maes, L.; Dubremetz, J. F.; Debreu, M. A.; Landry, V.; Sergheraert, C. *Bioorg. Med. Chem.* **2001**, *9*, 837-846.

(49) Jacoby, E. M.; Schlichting, I.; Lantwin, C. B.; Kabsch, W.; Krauth-Siegel, R. L. *Proteins* **1996**, *24*, 73-80.

(50) Bonse, S.; Santelli-Rouvier, C.; Barbe, J.; Krauth-Siegel, R. L. *J. Med. Chem.* **1999**, *42*, 5448-5454.

(51) Girault, S.; Grellier, P.; Berecibar, A.; Maes, L.; Mouray, E.; Lemiere, P.; Debreu, M. A.; Davioud-Charvet, E.; Sergheraert, C. *J. Med. Chem.* **2000**, *43*, 2646-2654.

(52) Chibale, K.; Haupt, H.; Kendrick, H.; Yardley, V.; Saravanamuthu, A.; Fairlamb, A. H.; Croft, S. L. *Bioorg. Med. Chem. Lett.* **2001**, *11*, 2655-2657.

(53) Chibale, K.; Visser, M.; Yardley, V.; Croft, S. L.; Fairlamb, A. H. *Bioorg. Med. Chem. Lett.* **2000**, *10*, 1147-1150.

(54) Chibale, K.; Visser, M.; van Schalkwyk, D.; Smith, P. J.; Saravanamuthu, A.; Fairlamb, A. H. *Tetrahedron* **2003**, *59*, 2289-2296.

(55) Faerman, C. H.; Savvides, S. N.; Strickland, C.; Breidenbach, M. A.; Ponasik, J. A.; Ganem, B.; Ripoll, D.; Krauth-Siegel, R. L.; Karplus, P. A. *Bioorg. Med. Chem.* **1996**, *4*, 1247-1253.

(56) Stoll, V. S.; Simpson, S. J.; Krauth-Siegel, R. L.; Walsh, C. T.; Pai, E. F. *Biochemistry* **1997**, *36*, 6437-6447.

(57) Fournet, A.; Inchausti, A.; Yaluff, G.; De Arias, A. R.; Guinaudeau, H.; Bruneton, J.; Breidenbach, M. A.; Karplus, P. A.; Faerman, C. H. *J. Enzym. Inhib.* **1998**, *13*, 1-9.

(58) Ponasik, J. A.; Strickland, C.; Faerman, C.; Savvides, S.; Karplus, P. A.; Ganem, B. *Biochem. J.* **1995**, *311*, 371-375.

(59) O'Sullivan, M. C.; Zhou, Q. B. *Bioorg. Med. Chem. Lett.* **1995**, *5*, 1957-1960.

(60) O'Sullivan, M. C.; Dalrymple, D. M.; Zhou, Q. B. *J. Enzym. Inhib.* **1996**, *11*, 97-114.

(61) O'Sullivan, M. C.; Zhou, Q. B.; Li, Z. L.; Durham, T. B.; Rattendi, D.; Lane, S.; Bacchi, C. J. *Bioorg. Med. Chem.* **1997**, *5*, 2145-2155.

(62) Li, Z. L.; Fennie, M. W.; Ganem, B.; Hancock, M. T.; Kobaslija, M.; Rattendi, D.; Bacchi, C. J.; O'Sullivan, M. C. *Bioorg. Med. Chem. Lett.* **2001**, *11*, 251-254.

(63) Bonnet, B.; Soullez, D.; Davioud-Charvet, E.; Landry, V.; Horvath, D.; Sergheraert, C. *Bioorg. Med. Chem.* **1997**, *5*, 1249-1256.

(64) Bonnet, B.; Soullez, D.; Girault, S.; Maes, L.; Landry, V.; Davioud-Charvet, E.; Sergheraert, C. *Bioorg. Med. Chem.* **2000**, *8*, 95-103.

(65) Chitkul, B.; Bradley, M. *Bioorg. Med. Chem. Lett.* **2000**, *10*, 2367-2369.

(66) Tromelin, A.; Moutiez, M.; Mezianecherif, D.; Aumercier, M.; Tartar, A.; Sergheraert, C. *Bioorg. Med. Chem. Lett.* **1993**, *3*, 1971-1976.

(67) Garrard, E. A.; Borman, E. C.; Cook, B. N.; Pike, E. J.; Alberg, D. G. *Org. Lett.* **2000**, *2*, 3639-3642.

(68) Cenas, N.; Bironaite, D.; Dickancaite, E.; Anusevicius, Z.; Sarlauskas, J.; Blanchard, J. S. *Biochem. Biophys. Res. Commun.* **1994**, *204*, 224-229.

(69) Blumenstiel, K.; Schoneck, R.; Yardley, V.; Croft, S. L.; Krauth-Siegel, R. L. *Biochem. Pharmacol.* **1999**, *58*, 1791-1799.

(70) Zani, C. L.; Chiari, E.; Krettli, A. U.; Murta, S. M. F.; Cunningham, M. L.; Fairlamb, A. H.; Romanha, A. J. *Bioorg. Med. Chem.* **1997**, *5*, 2185-2192.

(71) Henderson, G. B.; Ulrich, P.; Fairlamb, A. H.; Rosenberg, I.; Pereira, M.; Sela, M.; Cerami, A. *Proc. Natl. Acad. Sci. U. S. A.* **1988**, *85*, 5374-5378.

(72) Salmon-Chemin, L.; Buisine, E.; Yardley, V.; Kohler, S.; Debreu, M. A.; Landry, V.; Sergheraert, C.; Croft, S. L.; Krauth-Siegel, R. L.; Davioud-Charvet, E. *J. Med. Chem.* **2001**, *44*, 548-565.

(73) Gallwitz, H.; Bonse, S.; Martinez-Cruz, A.; Schlichting, I.; Schumacher, K.; Krauth-Siegel, R. L. *J. Med. Chem.* **1999**, *42*, 364-372.

(74) Bonse, S.; Richards, J. M.; Ross, S. A.; Lowe, G.; Krauth-Siegel, R. L. *J. Med. Chem.* **2000**, *43*, 4812-4821.

(75) Inhoff, O.; Richards, J. M.; Briet, J. W.; Lowe, G.; Krauth-Siegel, R. L. *J. Med. Chem.* **2002**, *45*, 4524-4530.

(76) McKie, J. H.; Garforth, J.; Jaouhari, R.; Chan, C.; Yin, H.; Besheya, T.; Fairlamb, A. H.; Douglas, K. T. *Amino Acids* **2001**, *20*, 145-153.

(77) Chan, C.; Yin, H.; McKie, J. H.; Fairlamb, A. H.; Douglas, K. T. *Amino Acids* **2002**, *22*, 297-308.

(78) Smith, H. K.; Bradley, M. *J. Comb. Chem.* **1999**, *1*, 326-332.

(79) Bycroft, B. W.; Chan, W. C.; Chhabra, S. R.; Hone, N. D. *J. Chem. Soc.-Chem. Commun.* **1993**, 778-779.

(80) Nash, I. A.; Bycroft, B. W.; Chan, W. C. *Tetrahedron Lett.* **1996**, *37*, 2625-2628.

(81) Kellam, B.; Chan, W. C.; Chhabra, S. R.; Bycroft, B. W. *Tetrahedron Lett.* **1997**, *38*, 5391-5394.

(82) Kellam, B.; Bycroft, B. W.; Chhabra, S. R. *Tetrahedron Lett.* **1997**, *38*, 4849-4852.

(83) Chhabra, S. R.; Khan, A. N.; Bycroft, B. W. *Tetrahedron Lett.* **2000**, *41*, 1099-1102.

(84) Chhabra, S. R.; Khan, A. N.; Bycroft, B. W. *Tetrahedron Lett.* **2000**, *41*, 1095-1098.

(85) Chhabra, S. R.; Hothi, B.; Evans, D. J.; White, P. D.; Bycroft, B. W.; Chan, W. C. *Tetrahedron Lett.* **1998**, *39*, 1603-1606.

(86) Davies, M.; Bradley, M. *Tetrahedron* **1999**, *55*, 4733-4746.

(87) Marsh, I. R.; Bradley, M. *Eur. J. Biochem.* **1997**, *243*, 690-694.

(88) Jockersscherubl, M. C.; Schirmer, R. H.; Krauth-Siegel, R. L. *Eur. J. Biochem.* **1989**, *180*, 267-272.

(89) Baker, P. J.; Britton, K. L.; Engel, P. C.; Farrants, G. W.; Lilley, K. S.; Rice, D. W.; Stillman, T. J. *Proteins* **1992**, *12*, 75-86.

(90) Shoichet, B. K.; Stroud, R. M.; Santi, D. V.; Kuntz, I. D.; Perry, K. M. *Science* **1993**, *259*, 1445-1450.

(91) Desjarlais, R. L.; Seibel, G. L.; Kuntz, I. D.; Furth, P. S.; Alvarez, J. C.; Demontellano, P. R. O.; Decamp, D. L.; Babe, L. M.; Craik, C. S. *Proc. Natl. Acad. Sci. U. S. A.* **1990**, *87*, 6644-6648.

(92) Dunten, P.; Kammlott, U.; Crowther, R.; Levin, W.; Foley, L. H.; Wang, P.; Palermo, R. *Protein Sci.* **2001**, *10*, 923-926.

(93) Sun, L.; Tran, N.; Tang, F.; App, H.; Hirth, P.; McMahon, G.; Tang, C. *J. Med. Chem.* **1998**, *41*, 2588-2603.

(94) Boehm, H. J.; Boehringer, M.; Bur, D.; Gmuender, H.; Huber, W.; Klaus, W.; Kostrewa, D.; Kuehne, H.; Luebbers, T.; Meunier-Keller, N. *J. Med. Chem.* **2000**, *43*, 2664-2674.

(95) Breccia, P.; Boggetto, N.; Perez-Fernandez, R.; Van Gool, M.; Takahashi, M.; Rene, L.; Prados, P.; Badet, B.; Reboud-Ravaux, M.; de Mendoza, J. *J. Med. Chem.* **2003**, *46*, 5196-5207.

(96) Boggetto, N.; Reboud-Ravaux, M. *Biol. Chem.* **2002**, *383*, 1321-1324.

(97) Blasko, E.; Glaser, C. B.; Devlin, J. J.; Xia, W.; Feldman, R. I.; Polokoff, M. A.; Phillips, G. B.; Whitlow, M.; Auld, D. S.; McMillan, K.; Ghosh, S.; Stuehr, D. J.; Parkinson, J. F. *J. Biol. Chem.* **2002**, *277*, 295-302.

(98) McMillan, K.; Adler, M.; Auld, D. S.; Baldwin, J. J.; Blasko, E.; Browne, L. J.; Chelsky, D.; Davey, D.; Dolle, R. E.; Eagen, K. A.; Erickson, S.; Feldman, R. I.; Glaser, C. B.; Mallari, C.; Morrissey, M. M.; Ohlmeyer, M. H. J.; Pan, C. H.; Parkinson, J. F.; Phillips, G. B.; Polokoff, M. A.; Sigal, N. H.; Vergona, R.; Whitlow, M.; Young, T. A.; Devlin, J. J. *Proc. Natl. Acad. Sci. U. S. A.* **2000**, *97*, 1506-1511.

(99) Bowman, M. J.; Chmielewski, J. *Bioorg. Med. Chem. Lett.* **2004**, *14*, 1395-1398.

(100) Fairlamb, A. H.; Cerami, A. *Annu. Rev. Microbiol.* **1992**, *46*, 695-729.

(101) Winzor, D. J. *J. Biochem. Biophys. Methods* **2003**, *56*, 15-52.

(102) Matthews, B. W. *J. Mol. Biol.* **1968**, *33*, 491-497.

(103) Yingyongnarongkul, B.; Howarth, M.; Elliott, T.; Bradley, M. *Chem.-Eur. J.* **2004**, *10*, 463-473.

(104) Xu, D. Q.; Prasad, K.; Repic, O.; Blacklock, T. J. *Tetrahedron Lett.* **1995**, *36*, 7357-7360.

(105) Kaiser, E. C., R. L.; Bossinger, C. D.; Cook, P. I. *Anal. Biochem.* **1970**, *34*, 595-598.

(106) Atherton, E.; Logan, C. J.; Sheppard, R. C. *J. Chem. Soc.-Perkin Trans. 1* **1981**, 538-546.

(107) Bradford, M. M. In *Analytical Biochemistry*, 1976; Vol. 72, p 248.

(108) Marsh, I. R.; Bradley, M. *Tetrahedron* **1997**, *53*, 17317-17334.

(109) Bailey, S. *Acta Crystallogr. Sect. D-Biol. Crystallogr.* **1994**, *50*, 760-763.

(110) Vagin, A.; Teplyakov, A. *J. Appl. Crystallogr.* **1997**, *30*, 1022-1025.

(111) Zhang, Y. H.; Bond, C. S.; Bailey, S.; Cunningham, M. L.; Fairlamb, A. H.; Hunter, W. N. *Protein Sci.* **1996**, *5*, 52-61.

(112) Brunger, A. T.; Adams, P. D.; Clore, G. M.; DeLano, W. L.; Gros, P.; Grosse-Kunstleve, R. W.; Jiang, J. S.; Kuszewski, J.; Nilges, M.; Pannu, N. S.; Read, R. J.; Rice, L. M.; Simonson, T.; Warren, G. L. *Acta Crystallogr. Sect. D-Biol. Crystallogr.* **1998**, *54*, 905-921.